RESPONSE TO REQUEST FOR ADDITIONAL INFORMATION

APR1400 Design Certification

Korea Electric Power Corporation / Korea Hydro & Nuclear Power Co., LTD

Docket No. 52-046

RAI No.: **183-8197**

SRP Section: **03.07.02 – Seismic System Analysis**

Application Section: **3.7.2**

Date of RAI Issue: **08/31/2015**

Question No. 03.07.02-1

10 CFR 50 Appendix S requires that safety-related structures, systems, and components (SSCs) remain functional and within applicable stress, strain, and deformation limits for safe shutdown earthquake (SSE) ground motions. The seismic analysis and design of the APR1400 standard plant are based on the certified seismic design response spectra (CSDRS) described in DCD Subsection 3.7.1.1.1 which, per DCD Section 3.7.1 is the SSE for the APR 1400 standard plant. Additionally, the APR1400 standard plant is evaluated for the potential effects of hard rock high frequency (HRHF) spectra. DCD Appendix 3.7B and technical report APR1400-E-S-NR-14004-P, Rev 1, summarize the methodology and results of the evaluation of the effects of hard rock high frequency (HRHF) input ground motion on SSCs of the APR1400 standard plant. To assist the staff in assessing whether the acceptance criteria in SRP Section 3.7.2 II.4 have been adequately addressed, the applicant is requested to provide additional information related to the following aspects of the HRHF evaluation.

a) In-structure Response Spectra (ISRS) Reduction Limits

In Figures 5-5 through 5-23 in APR1400-E-S-NR-14004-P, Rev 1, the applicant provided comparisons of HRHF-based ISRS with and without consideration of spatial incoherence of seismic ground motion (i.e., incoherent ISRS and coherent ISRS, respectively). Staff review of these ISRS comparisons finds that while the HRHF-based incoherent ISRS generally show the expected outcome of reduced spectral accelerations in high frequencies, the magnitude of the reductions exceed the reduction limits set forth in SRP Section 3.7.2.II.4. Per the guidance in SRP Section 3.7.2.II.4, larger ISRS reductions may be acceptable subject to the applicant providing sufficient technical information supporting the larger reductions. As such the staff requests the applicant to provide justification for implementing ISRS reduction levels in excess of those provided in SRP Section 3.7.2.II.4.

b) SSI Analysis Results using 7 and 12 Modes

DCD Section 3.7B.4 and Section 5.4 in APR1400-E-S-NR-14004-P, Rev 1, describe the use of 7 modes for capturing the incoherent- motion SSI response based on a comparison with the response obtained by using 12 modes. Staff review of such comparisons as provided in Appendix B of APR1400-E-S-NR-14004-P finds that the use of 7 modes generally results in greater reductions in the ISRS, above 10 Hz, than the reductions presented in SRP Section 3.7.2.II.4 as indicated in item (a) above. Further, the staff notes that a 15 mode solution was also calculated; however, the 15 mode results were not presented in the aforementioned comparison. Based on staff experience, the staff finds that the use of 7, 12, or 15 modes may not be sufficient to adequately capture the incoherent- motion and structural responses. Therefore, the staff requests the applicant to provide the technical justification for the selection of the appropriate number of modes to be used to capture the incoherent-motion and structural responses.

c) Seismic Response Demands of the HRHF Spectra

In DCD Section 3.7B.7.1 and Section 6.1 of APR1400-E-S-NR-14004-P, Rev 1, the applicant states that the NI structures are considered qualified for high frequency input if the seismic loads and equivalent acceleration from the CSDRS envelope those from the high frequency input. The staff's review of the results provided in Tables 6-1 through 6-3, and Table 6-6 of APR1400-E-S-NR-14004-P, Rev. 1, for the containment internal structures (CIS) and the emergency diesel generator building (EDGB)/diesel fuel oil tank (DFOT) room, respectively, finds that generally the HRHF-based results exceed the CSDRS-based results. Furthermore, the staff notes that while the applicant documented these exceedances in Section 6.1 of APR1400-E-S-NR-14004-P, Rev 1, the applicant did not provide the basis for their acceptance. Based on the current results and lack of justification, the staff does not have sufficient basis to conclude that the APR1400 standard plant structures are qualified for the applicant's HRHF input motions. Therefore, the staff requests the applicant to provide additional information including analysis results that demonstrate that the APR1400 standard plant is qualified for the HRHF input motions. After addressing items (a) and (b) above, the staff requests the applicant to provide revised results for ISRS comparisons and seismic loads, between the CSDRS and the HRHF, and to provide a detailed justification for the acceptability of all HRHF exceedances. Additionally, in accordance with the guidance in SRP Section 3.7.2.II.4, the staff requests the applicant to confirm that (1) all reductions in structural loads based on consideration of incoherency will be limited to 10%; and (2) all increases in structural loads based on consideration of incoherency will be used in the structural evaluation.

Response

a) In-structure Response Spectra (ISRS) Reduction Limits

The magnitude of ISRS amplitude reductions due to incoherence of hard-rock high-frequency (HRHF) seismic input motion is justifiable since the ISRS results obtained from incoherence SSI analyses for additional coherency modes (13 to 16) as described in the response b) (below) demonstrate that a converged solution still exceeds the reduction limits set forth in SRP Section 3.7.2.II.4.

To further confirm that the cumulated effect of principal coherency modes higher than the 16 modes is insignificant and, thus, can be neglected, a supplementary study has been performed. For this study, a simplified basemat model extracted from the full SSI FE model of APR1400 NI for the S09 hard-rock soil profile case is created. The basemat foundation in this model is modeled with solid elements - the element shape and mesh being exactly the same as the NI full model, as shown in Figure 1. The concrete material property is assigned to the entire basemat (elements in blue in Figure 1). The elements surrounding the basemat (elements in red in Figure 1) are assigned with backfill properties between El. 45' to 55'. Additional rigid beams are installed in the locations of the major shear walls to properly simulate the stiffening effect of the walls to the foundation basemat stiffness, as shown in Figure 2.

Incoherence SSI analyses for the vertical direction input for principal coherency modes (up to 50 modes) are performed on this model using ACS SASSI V3.0 (Reference 1). The frequency points selected for the analysis are the same as those documented in Technical Report APR1400-E-S-NR-14004. The amplitudes of vertical Acceleration Response Spectra (ARS) obtained for the vertical response motions, with different number of cumulated spatial coherency modes, are compared with each other at the locations of the corners, the center of the basemat, and selected locations between walls. The selected different numbers of spatial coherency modes cumulated are as follows: 1-7 modes, 1-16 modes, and 1-50 modes. The locations for the selected shear wall and floor slab nodes are shown in Figure 3 and Figure 4, respectively. The comparisons shown in Figures 5 through 33 is intended to demonstrate that the additional thirty plus coherency modes beyond the first 16 modes have an insignificant effect on the basemat vertical response due to the HRHF incoherent vertical input motion considered in the study.

Based on the results shown in Figures 5 through 33, the accumulative effect of spatial coherency modes higher than 16 on the ISRS for the vertical response motions of the basemat are insignificant and the16-mode-combined results achieve a converged solution.

b) SSI Analysis Results Using 7 and 12 Principal Spatial Coherency Modes

In order to provide the technical justification for the selection of the appropriate number of modes to be used in the SSI analysis to capture the incoherent-motion structural response, SSI analyses are performed for the additional coherency modes 13 through 16. This is in addition to the 7 and 12 modes considered in the previous analysis using the same methodology as documented in Technical Report APR1400-E-S-NR-14004.

The responses of the structures are obtained for the combination of modes 1 through 16 using the square-root-of-the-sum-of-squares (SRSS) combination rule. The adequacy of 16 modes for considering the APR1400 NI HRHF incoherent motion effect is confirmed from the comparisons of responses developed from the study outlined as follows (i.e. convergence criteria):

b-1. Compare the 12-modes-combined and 16-modes-combined, 5%-damped in structure response spectra (ISRS) at selected key locations. The convergence

acceptance criterion is set as the differences from the two sets of results being within 5%.

b-2. Compare the amplitudes of vertical response acceleration transfer function (ATF) due to the vertical input at the key locations as defined in item a) at the foundation level mode by mode from modes 12 to 16, based on the consideration that the vertical response due to vertical input at the foundation level. This may be most sensitive by the addition of higher coherency modes.

The incoherent-motion SSI analysis models and the coherency functions used are identical to the models used in Technical Report APR1400-E-S-NR-14004. Both uncracked and cracked concrete stiffness conditions are considered. All other conditions such as the input site properties and input ground motion for HRHF are the same as those documented in Technical Report APR1400-E-S-NR-14004.

The INCOH program module, as used in Technical Report APR1400-E-S-NR-14004, is developed and used to perform the modal decomposition for coherency matrices based on the NRC approved Abrahamson 2007 hard-rock spatial coherency functions. The SASSI seismic input motion load vectors for each of the principal coherency modes considered in the analysis are developed. The resulting seismic load vectors for the coherency modes considered are incorporated into ACS SASSI and the responses of the system to the modal seismic load vectors are then obtained using the ACS SASSI module ANALYS. The modal responses are then combined using the SRSS combination rule and the combined responses are considered as the system response to the incoherent ground motions. The INCOH program module developed and used in these analyses is validated and verified by comparing the results computed with the corresponding results, as documented in Technical Report APR1400-E-S-NR-14004.

For the incoherent-input-motion SSI analyses for the additional coherency modes 13 through 16, SSI response transfer functions are calculated at 86 frequencies ranging from 0 to 71 Hz that are consistent with the frequencies documented in Technical Report APR1400-E-S-NR-14004. For comparative purposes, the coherent-input-motion SSI analysis is also performed for the same frequency points as those considered for in the incoherent-motion SSI analysis.

The same procedure, as documented in Technical Report APR1400-E-S-NR-14004, is employed to develop the ISRS at selected locations considering ground motion incoherency, which is summarized as follows:

Step 1 Perform SSI analyses for the principal coherency modes to be considered and three directional seismic excitations.

Step 2 For one particular mode and node, obtain the directional responses in terms of ARS.

Step 3 Combine the co-directional nodal ARS using SRSS rule.

Step 4 Repeat Steps 2 and 3 for other principal coherency modes.

Step 5 Combine the modal responses obtained in Step 4 using the SRSS rule.

Step 6 Repeat Steps 2 to Steps 5 for other nodes in the group and envelop the ISRS for the responses in the same group and broaden the resulting enveloped ISRS to obtain the design ISRS for the group.

Per the convergence criterion as discussed in b-2 above, the vertical response ATF at representative nodes of the foundation basemat due to vertical input at the foundation level is computed to show the relatively low amplitude of higher modes 13 through 16, compared to the SRSS-combined modes 1 through 12. Figures 35 through 49 show the ATF for the nodes shown in Figure 34.

For each plot in these figures, the black data line named “Mode 1-12” is computed using a function of the MOTION module of ACS SASSI to combine the modal transfer function results using the rule of SRSS (ATF-SRSS). The results show that the vertical response amplitude of the higher modes 13 through 16 is small compared to the amplitude of the SRSS-combined modes 1 through 12.

However, for the 1-F slab locations, the results generally do not show a decaying pattern from mode to mode, per Figure 49 (node 9501), as mode 15 has the highest amplitude of the 4 higher modes. This is also apparent in other locations throughout the NI model. Figures 50 and 51 show ATF results for nodes 12875 (2-F Wall, Uncracked) and 18165 (3-F Wall, Cracked), respectively. The results show that there is no clear decaying pattern from mode to mode up to mode 16 for these locations, as the ATF amplitudes of some modes from 2 through 16 are of the same magnitude or greater than mode 1.

In-structure response spectra (ISRS) are developed using the procedure described above (Step 1 ~ Step 6) to demonstrate the convergence of SSI analysis results considering 12 principal coherency modes, by comparing the 12-mode-combined to the 16-mode-combined results (criterion b-1). The selected nodal points on each of the designated structure locations used in these response comparisons are the same as those documented in Technical Report APR1400-E-S-NR-14003. The ISRS for all locations are calculated for 5% damping ratio.

Figures 52 through 81 show the ISRS comparison of results between SRSS-combined modes 1 to 7, SRSS-combined modes 1 to 12, SRSS-combined modes 1 to 16, and the coherent-input-motion SSI analysis results at the same selected key elevations as those documented in Technical Report APR1400-E-S-NR-14004. As shown in the comparisons, the ISRS results for the most locations satisfy the convergence criteria.

However, there are some locations below grade, such as the AB shear walls located below grade, as shown in Figures 82 through 84, where the criterion is not satisfied. In addition, two locations, AB shear wall 2-F for the uncracked case, and AB shear wall 3-F for the cracked case, do not satisfy the convergence criteria and have questionable responses, especially in the NS direction, as shown in Figures 85 and 86. The figures show a large difference between the combined 1-16 modes and the combined 1-12 modes, and between the combined 1-12 modes and the combined 1-7 modes. Figures 87 and 88 show the individual modes 13, 14, 15, and 16, for the 2-F uncracked NS response and the 3-F cracked NS response, respectively. The results show that mode 13 is the largest contributor for the 2-F uncracked case, and mode 14 is the largest

contributor for the 3-F cracked case. For these locations, the major contributions to the ISRS are due to the response contribution of a specific mode. The response combinations up to the specific modes have converged to the 16-mode-combined results.

Based on the ISRS comparison, the overall results satisfy the convergence criterion, b-1, for most of the locations in the NI, as the difference in the 12-mode-combined and 16-mode-combined results are within 5%. The comparisons of ISRS results show in general the incoherent-motion ISRS results have converged up to 12 modes, except for a few locations such as AB shear walls 2-F and 3-F where spatial incoherence modes 13 through 16 show non-convergent (i.e., more than 5%) contributions to the ISRS. The limited case study indicates that such questionable responses observed may be due to the adopted special modeling technique in the connection between the backfill element and the excavated soil element.

c) Seismic Response Demands of the HRHF Spectra

The HRHF responses exceed corresponding CSDRS responses in the containment internal structures (CIS), EDGB and DFOT only. These exceedances have been evaluated and the results show the HRHF response demands for these structures still meet the design criteria.

Although the comparisons of forces and moments from high frequency input motion are greater than the CSDRS, the design results of the CIS are not affected by the seismic responses from the HRHF seismic input. Since the design margin of the CIS for CSDRS input motion covers the exceeded forces and moments, the arrangements of rebar are not changed due to seismic responses from the HRHF seismic input. The maximum stress of the rebar in the CIS occurs at the SSW. The value at this location is 51.49 ksi, which is less than the allowable stress of 54 ksi.

In addition, although some of the equivalent accelerations from HRHF input motion are greater than those from the CSDRS, the design results of the EDGB are not affected by the seismic responses from the HRHF seismic input. Since the provided reinforcement of the EDGB for the CSDRS is greater than the required reinforcement for the HRHF, the rebar arrangements are not changed. The design critical section which has the lowest provided/required rebar ratio of 1.10 occurs at EL. 100'-0'' to 135'-0'' center wall of the EDGB due to the CSDRS seismic input. The critical section location is maintained for the HRHF seismic input and the provided/required rebar ratio is 1.02 which is still greater than the design limit of 1.00.

The structural loads due to incoherency are not compared with the structural loads resulting from coherent input motion, as recommended by SRP 3.7.2.II.4, for the following reasons:

1. For CIS: Since the incoherent-motion SSI response spectra are greater than the coherent-motion SSI response spectra below 10 Hz (See Figures 5-8 to 5-13 in Technical Report APR1400-E-S-NR-14004), the incoherent-motion SSI response member forces may increase as compared to the corresponding coherent-motion SSI response member forces.

2. For EDGB and DFOT: Although the incoherent-motion SSI response spectra are less than the coherent-motion SSI response spectra below 10 Hz, the differences are less than 10%.

References

1. ACS SASSI NQA Version 3.0 R2 Including Options A and FS, “An Advanced Computational Software for 3D Dynamic Analysis Including Soil-Structure Interaction,” User Manuals Revision 3, Ghiocel Predictive Technologies, Inc., March 31, 2015.

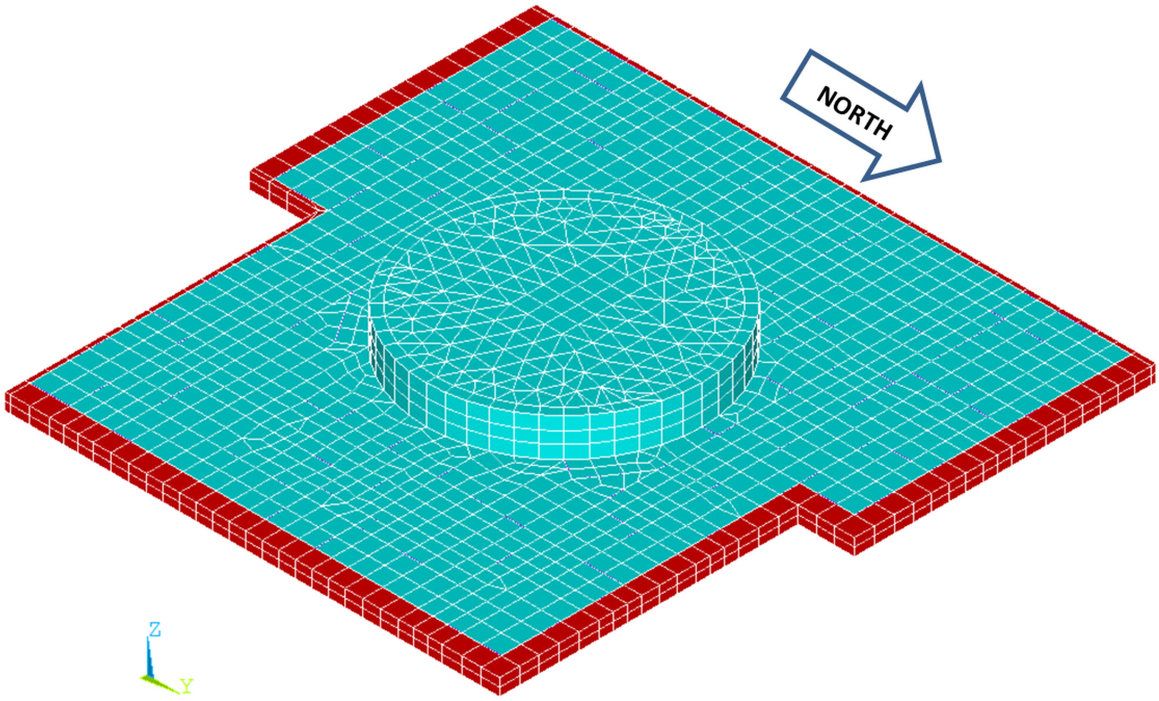

Figure 1 Simplified Basemat Model for APR1400 NI

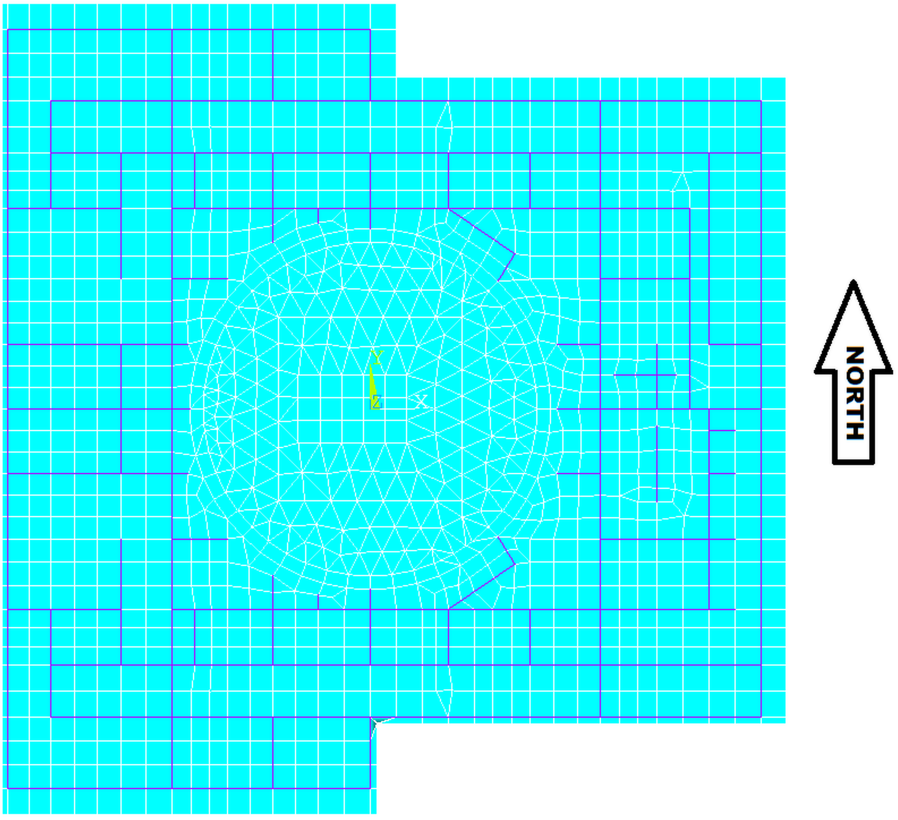

Figure 2 Rigid Beam Locations in Simplified Basemat Model

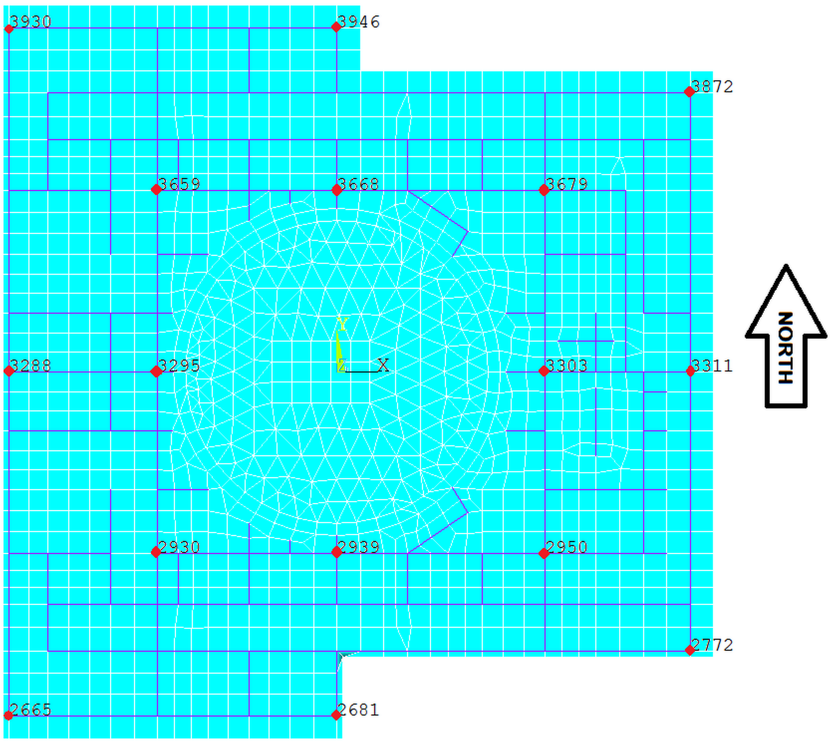

Figure 3 Locations for Selected Shear Wall Nodes at Basemat

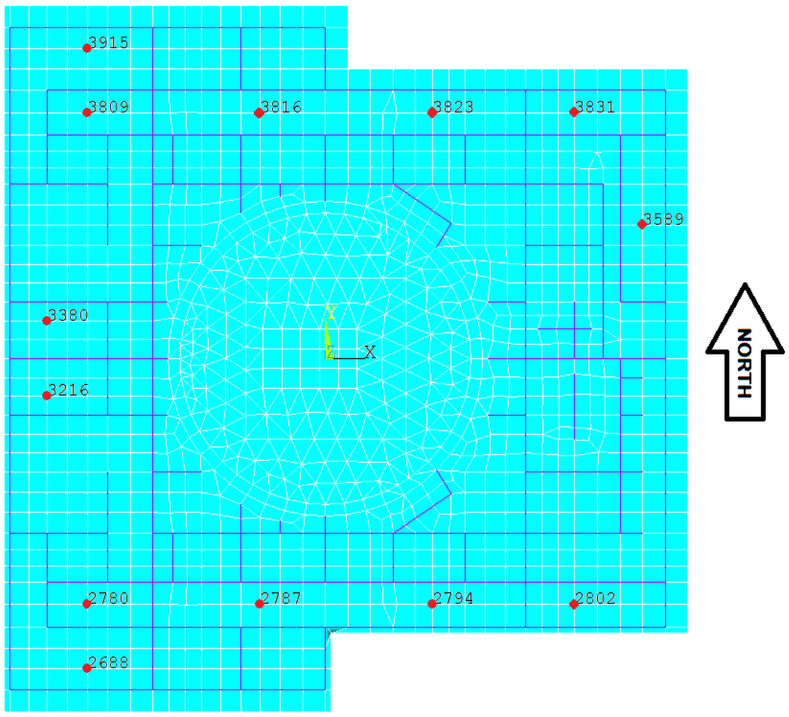

Figure 4 Locations for Selected Slab Nodes at Basemat

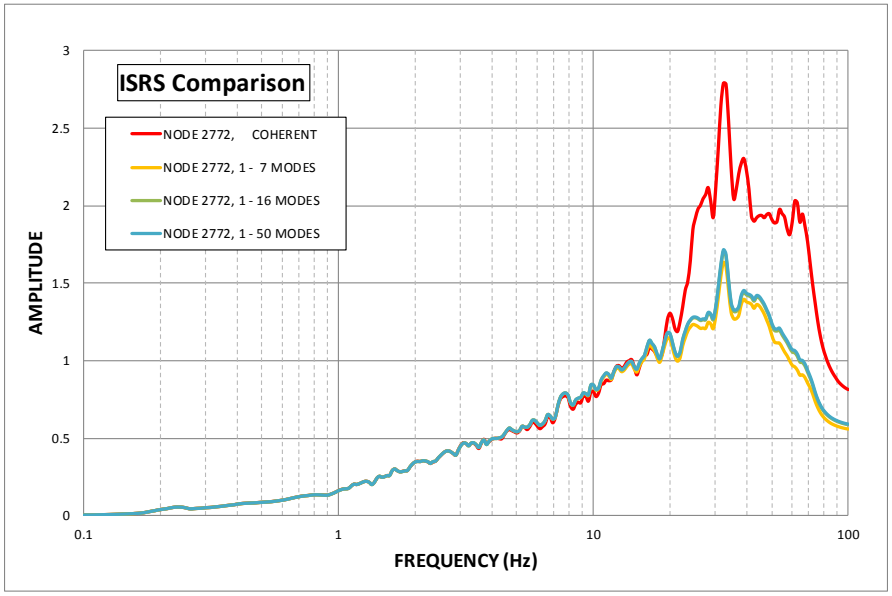

Figure 5 ARS – Shear Wall Node 2772 – Response in Vert. Direction

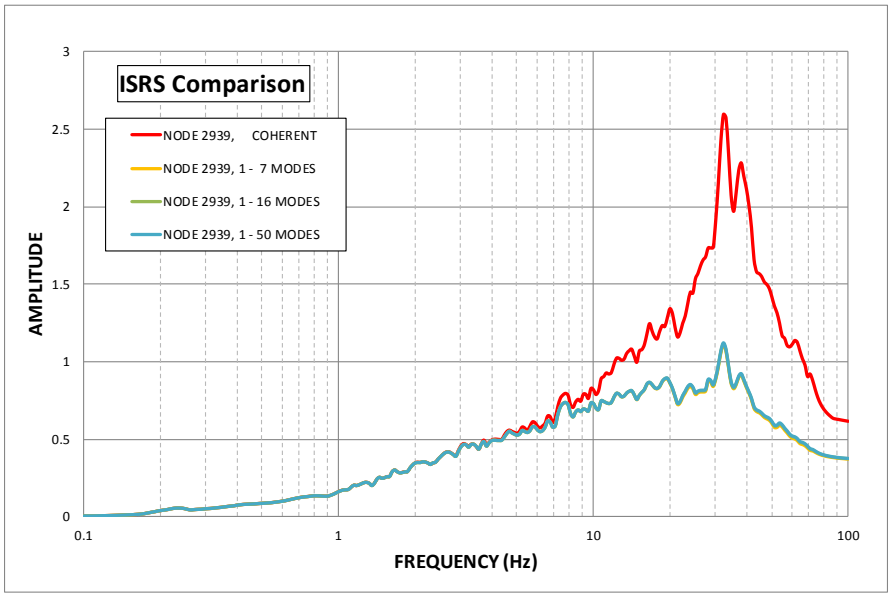

Figure 6 ARS – Shear Wall Node 2939 – Response in Vert. Direction

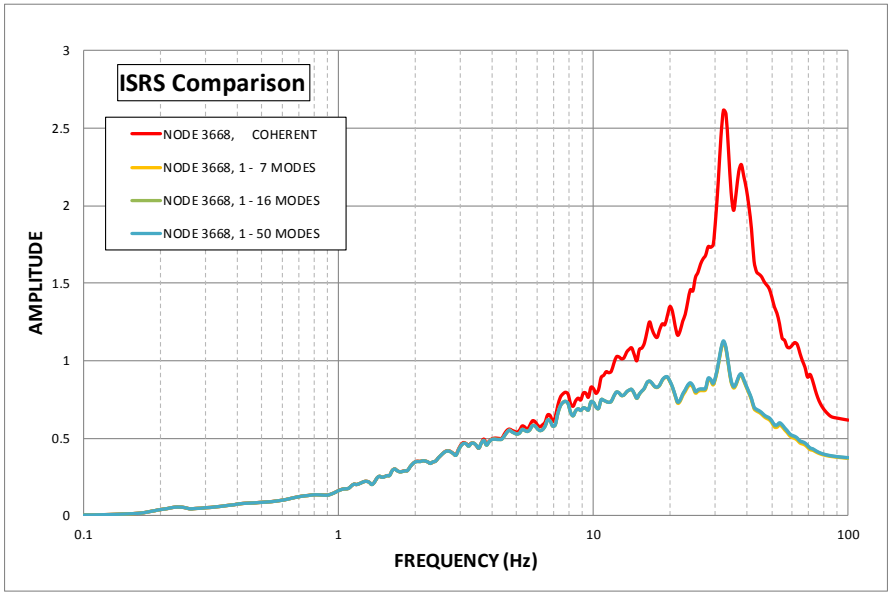

Figure 7 ARS – Shear Wall Node 3668 – Response in Vert. Direction

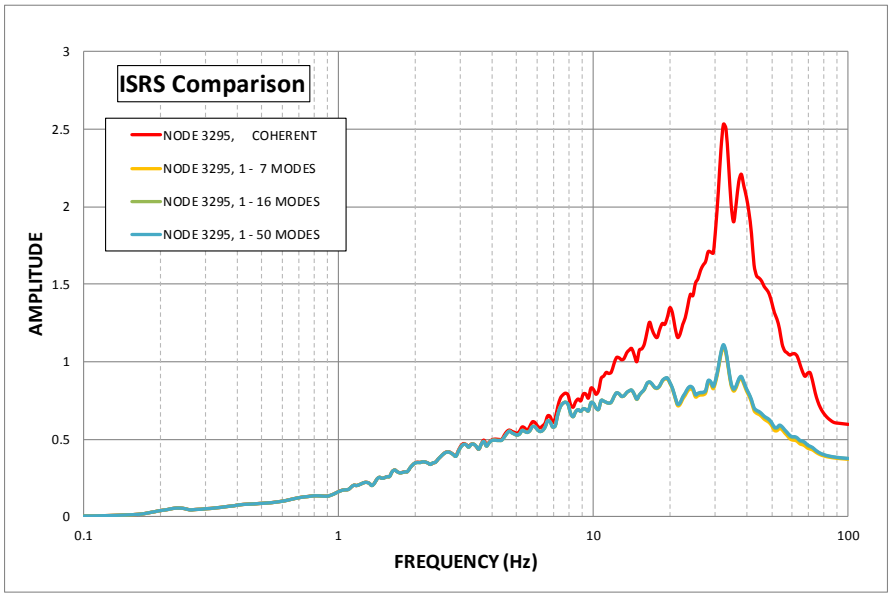

Figure 8 ARS – Shear Wall Node 3295 – Response in Vert. Direction

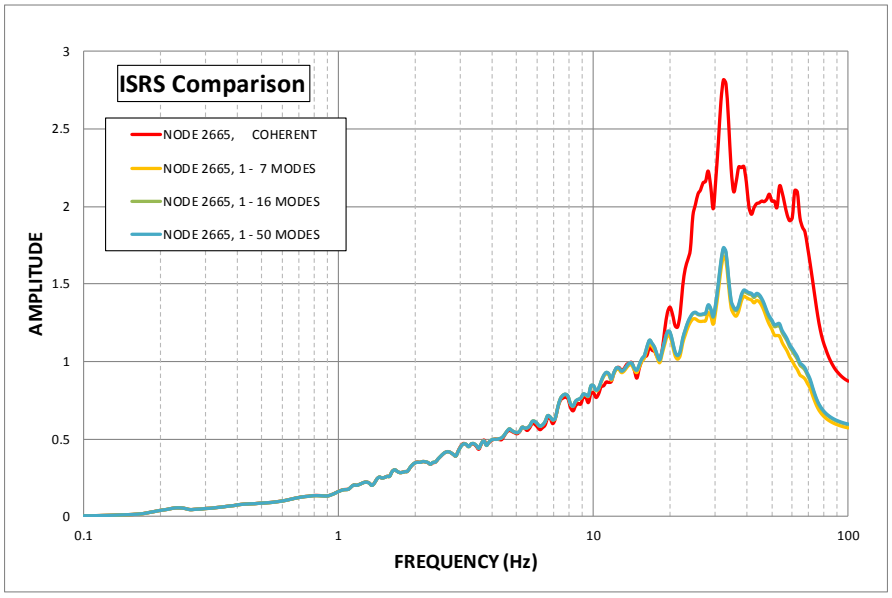

Figure 9 ARS – Shear Wall Node 2665 – Response in Vert. Direction

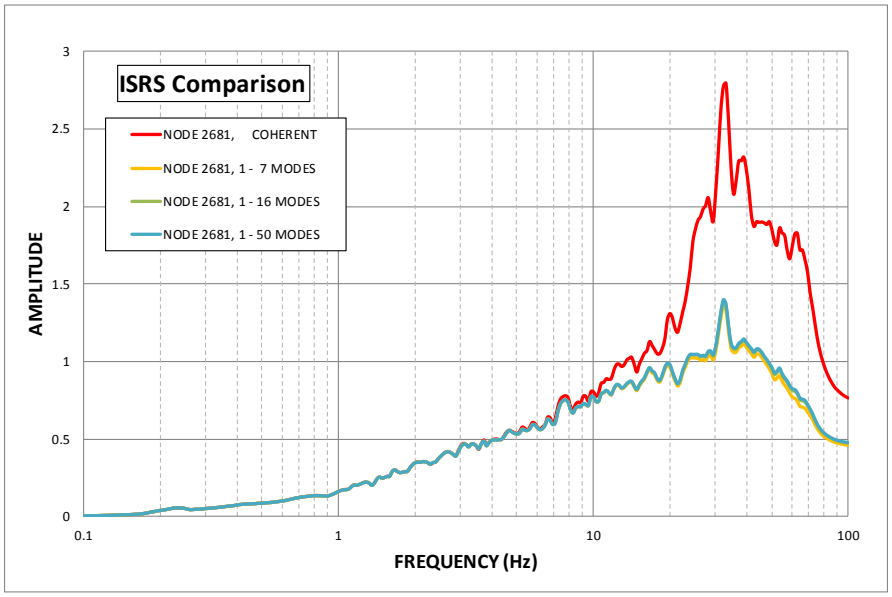

Figure 10 ARS – Shear Wall Node 2681 – Response in Vert. Direction

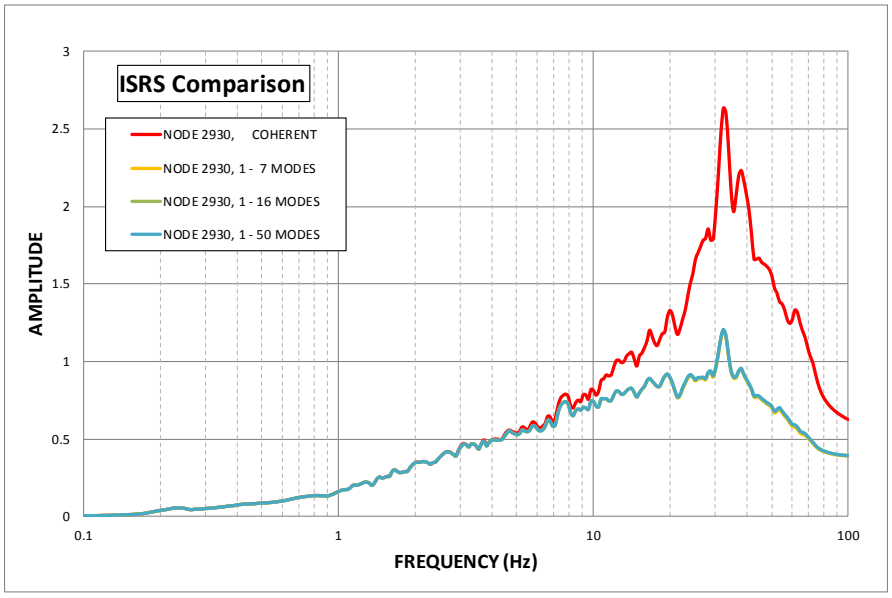

Figure 11 ARS – Shear Wall Node 2930 – Response in Vert. Direction

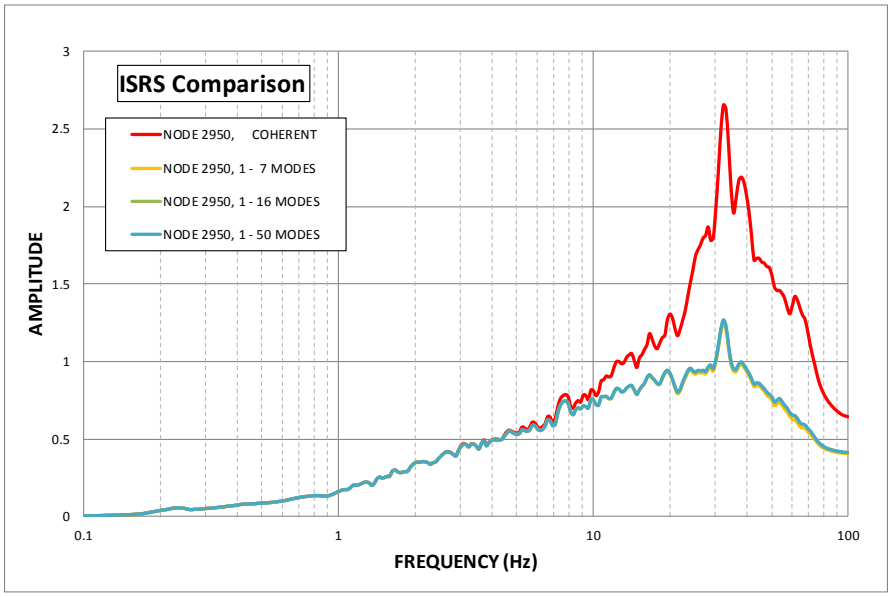

Figure 12 ARS – Shear Wall Node 2950 – Response in Vert. Direction

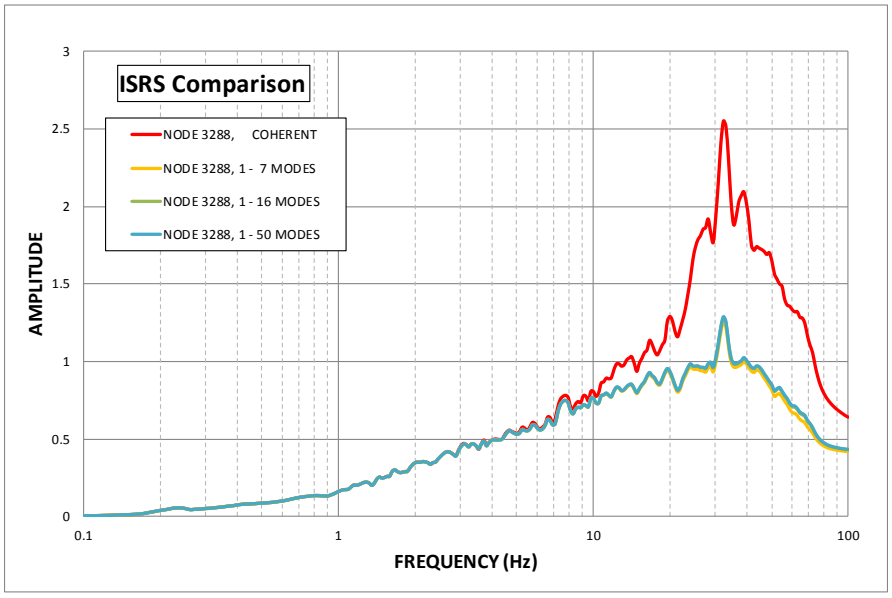

Figure 13 ARS – Shear Wall Node 3288 – Response in Vert. Direction

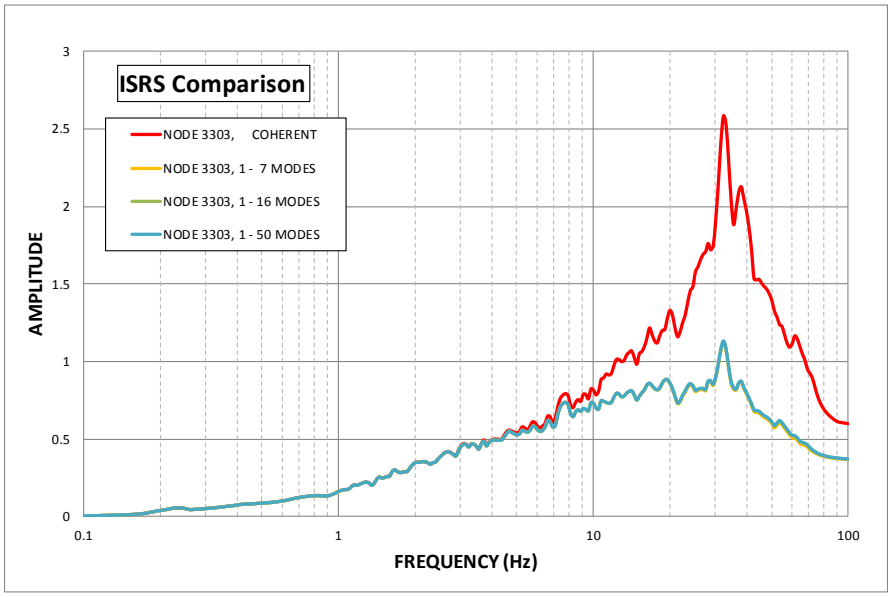

Figure 14 ARS – Shear Wall Node 3303 – Response in Vert. Direction

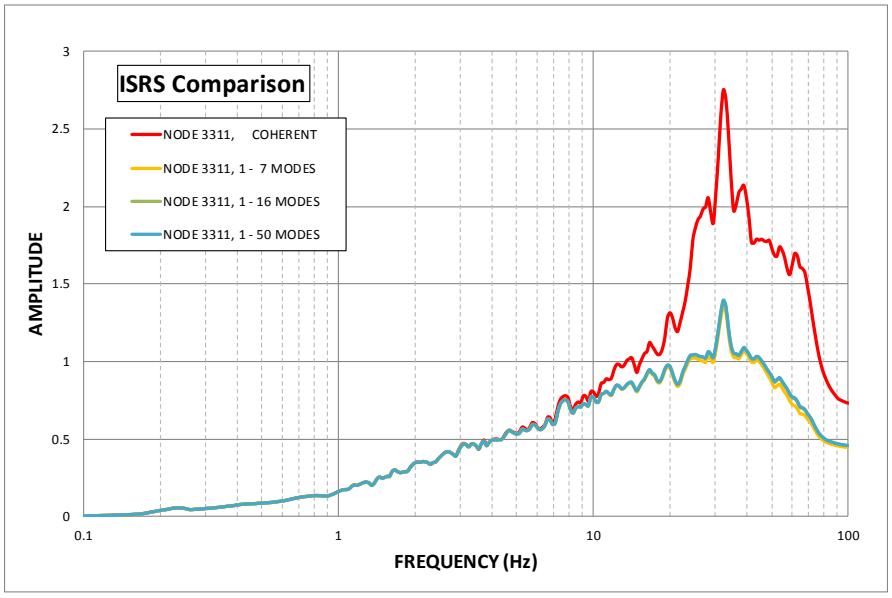

Figure 15 ARS – Shear Wall Node 3311 – Response in Vert. Direction

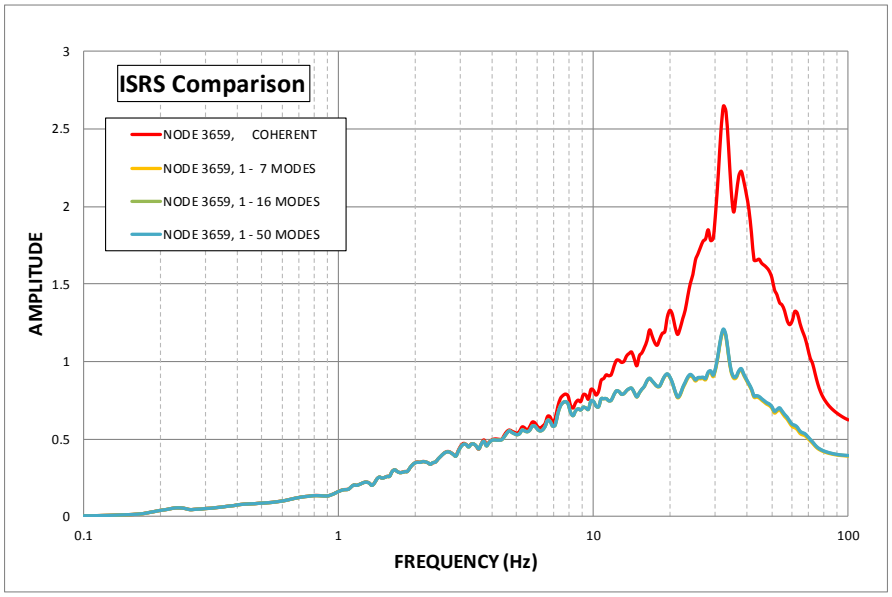

Figure 16 ARS – Shear Wall Node 3659 – Response in Vert. Direction

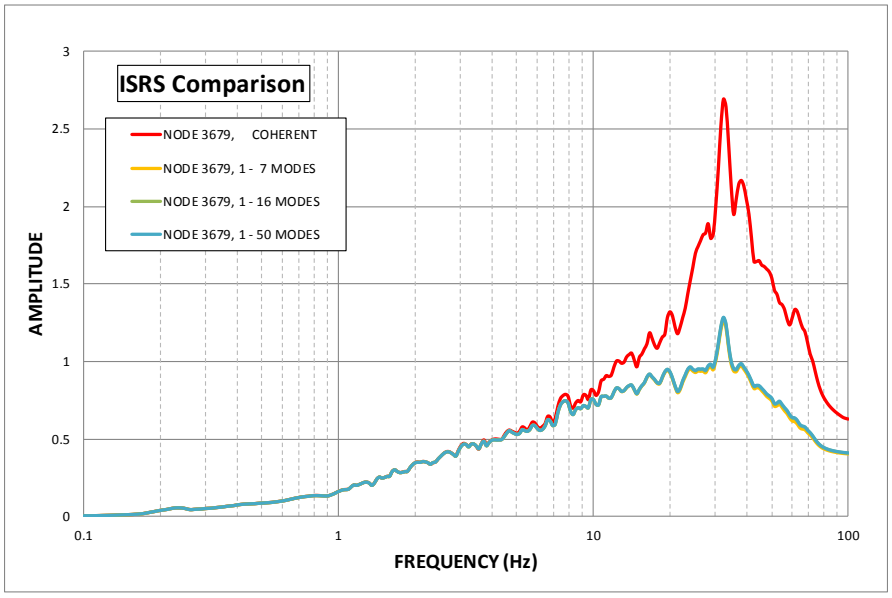

Figure 17 ARS – Shear Wall Node 3679 – Response in Vert. Direction

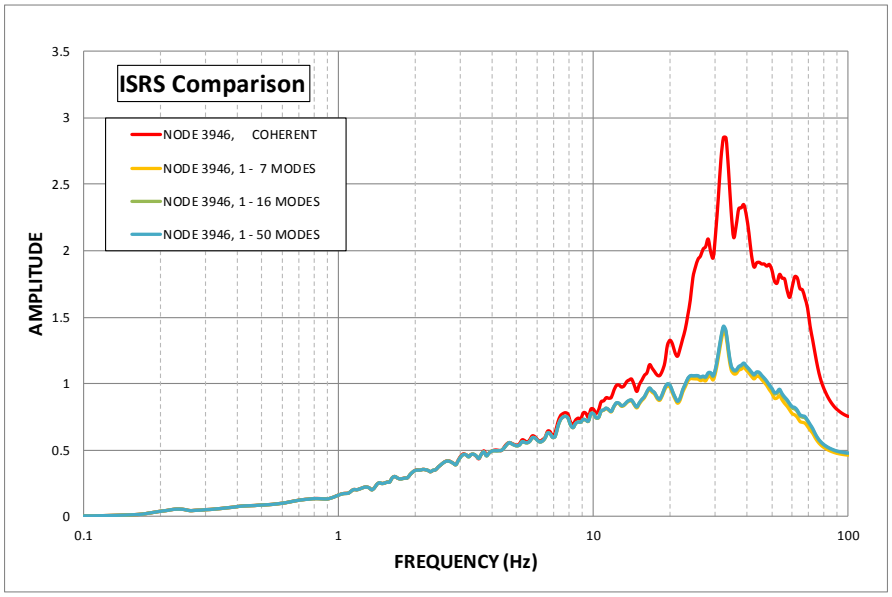

Figure 18 ARS – Shear Wall Node 3946 – Response in Vert. Direction

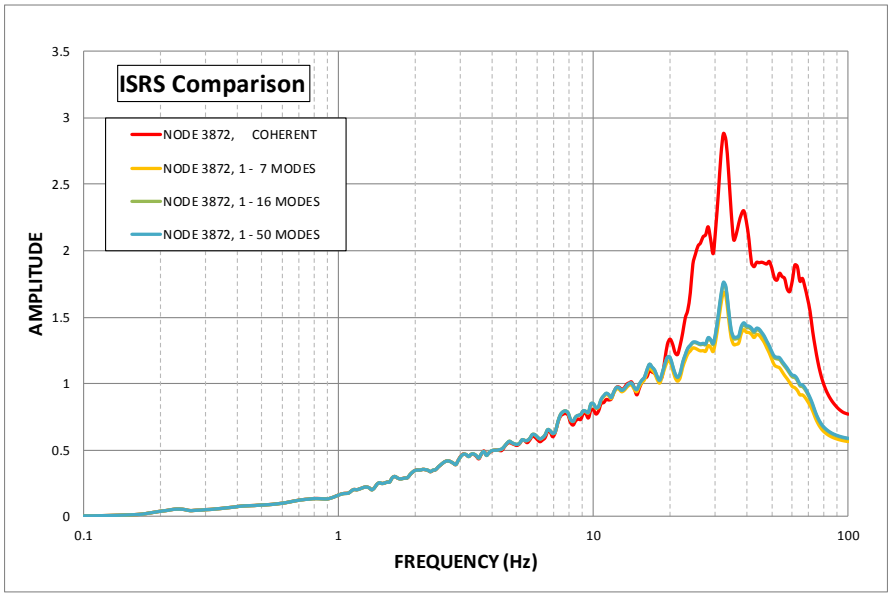

Figure 19 ARS – Shear Wall Node 3872 – Response in Vert. Direction

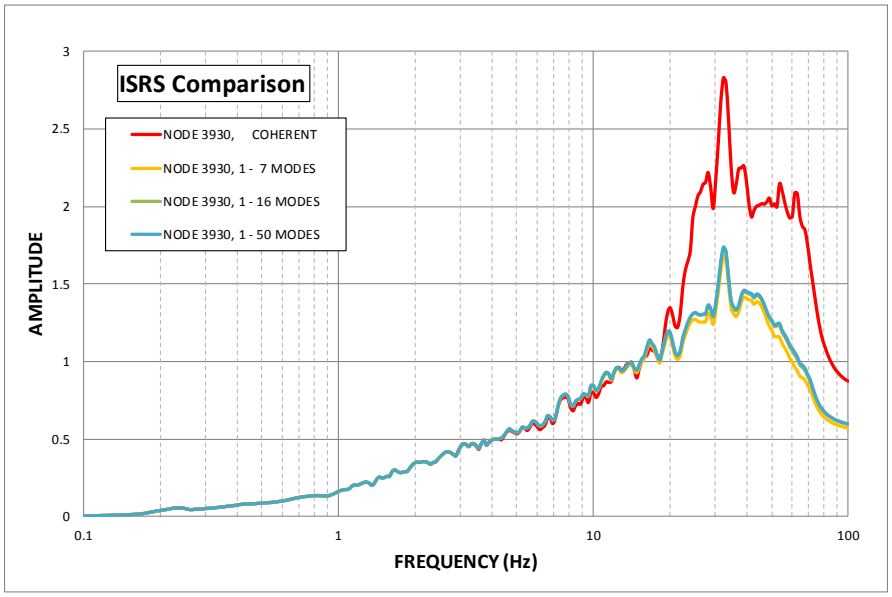

Figure 20 ARS – Shear Wall Node 3930 – Response in Vert. Direction

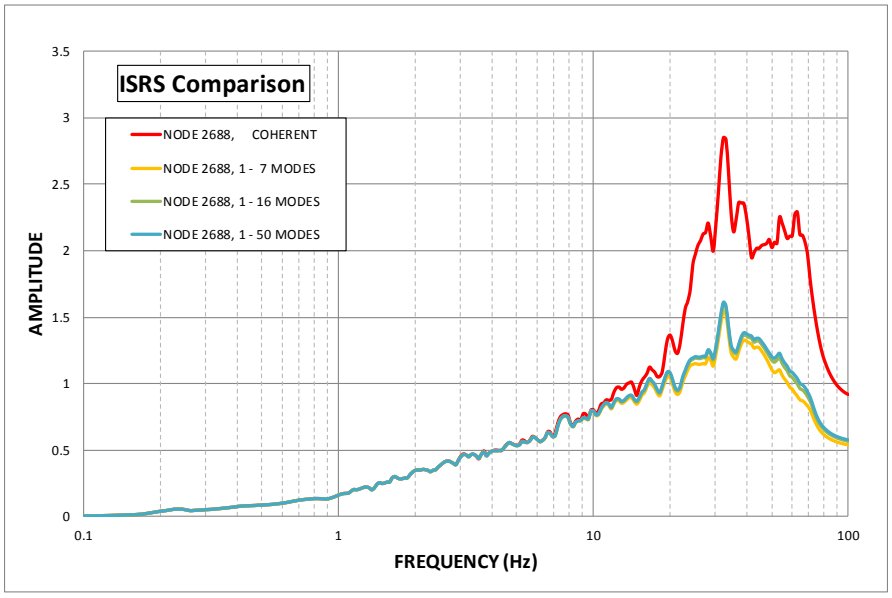

Figure 21 ARS – Floor Slab Node 2688 – Response in Vert. Direction

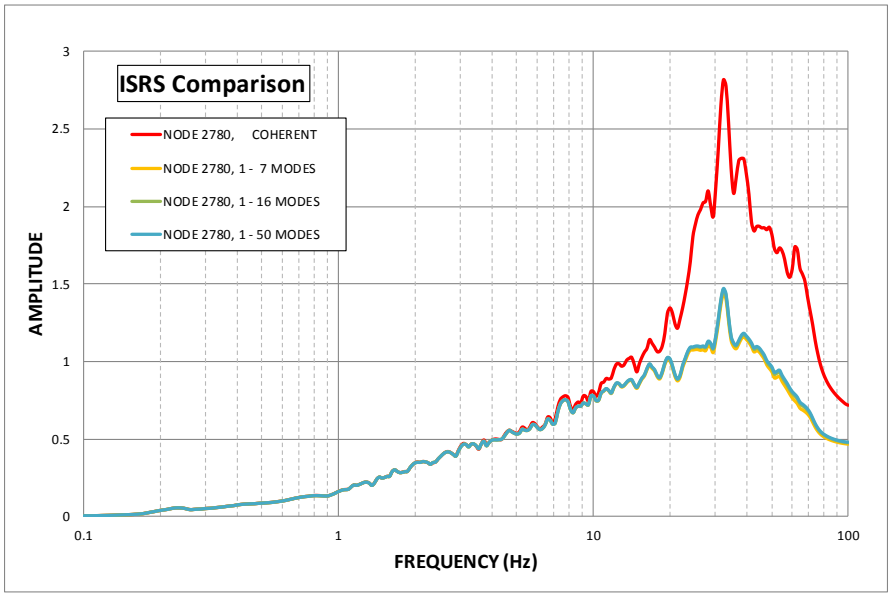

Figure 22 ARS – Floor Slab Node 2780 – Response in Vert. Direction

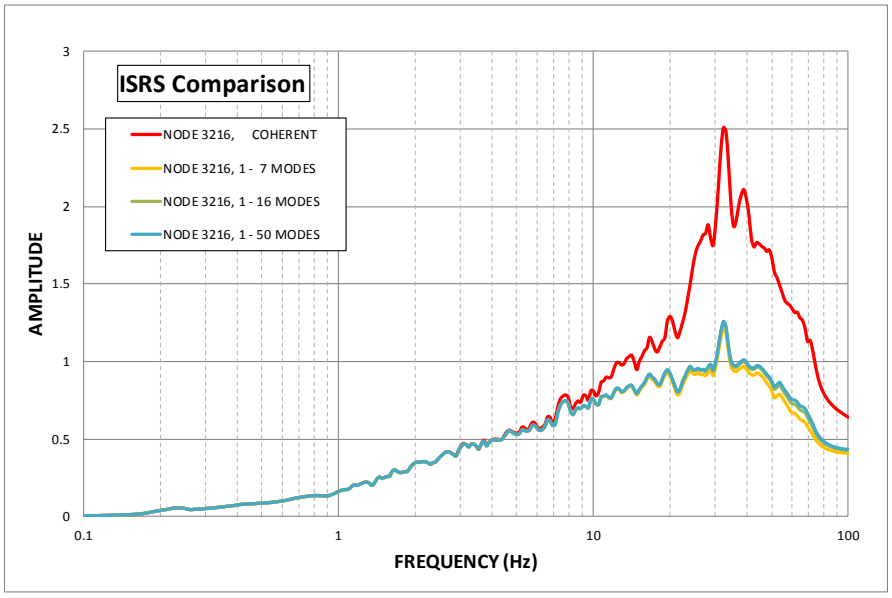

Figure 23 ARS – Floor Slab Node 3216 – Response in Vert. Direction

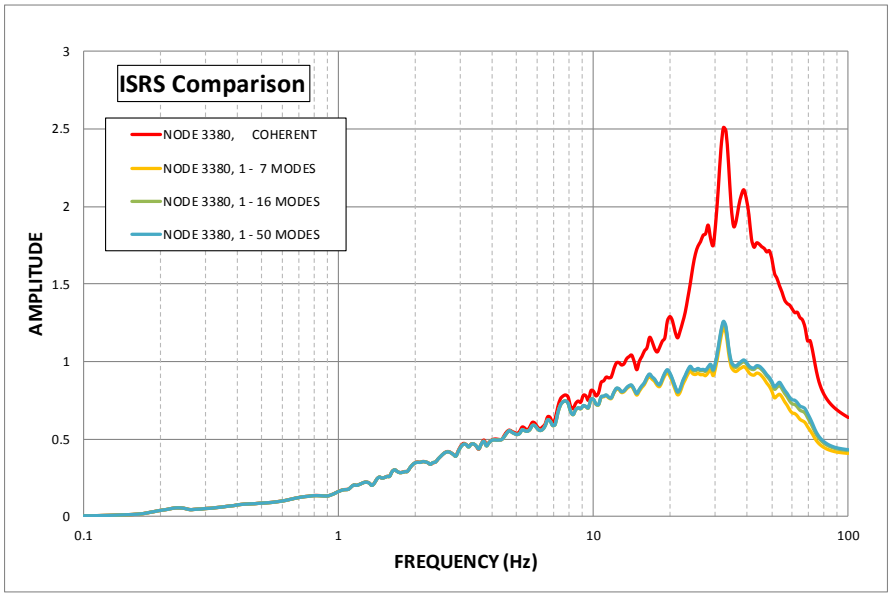

Figure 24 ARS – Floor Slab Node 3380 – Response in Vert. Direction

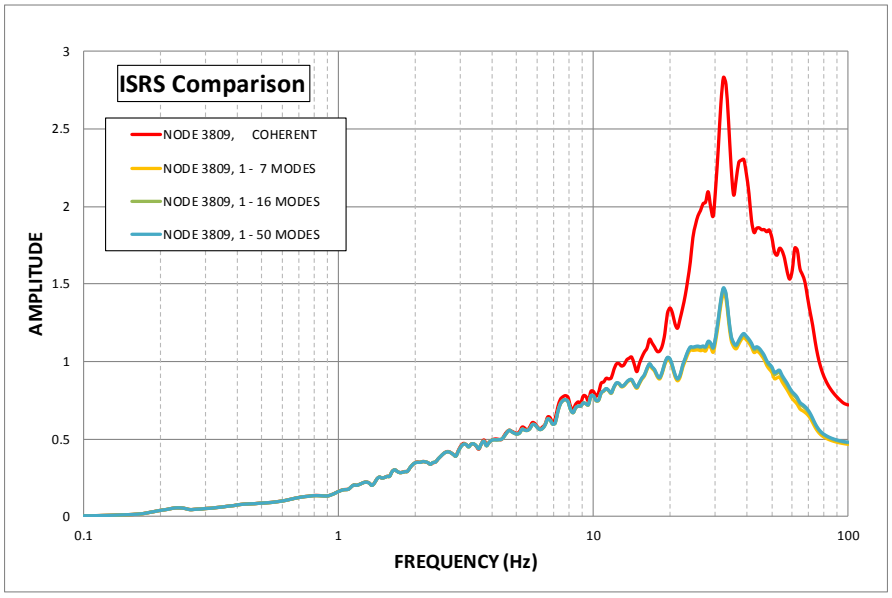

Figure 25 ARS – Floor Slab Node 3809 – Response in Vert. Direction

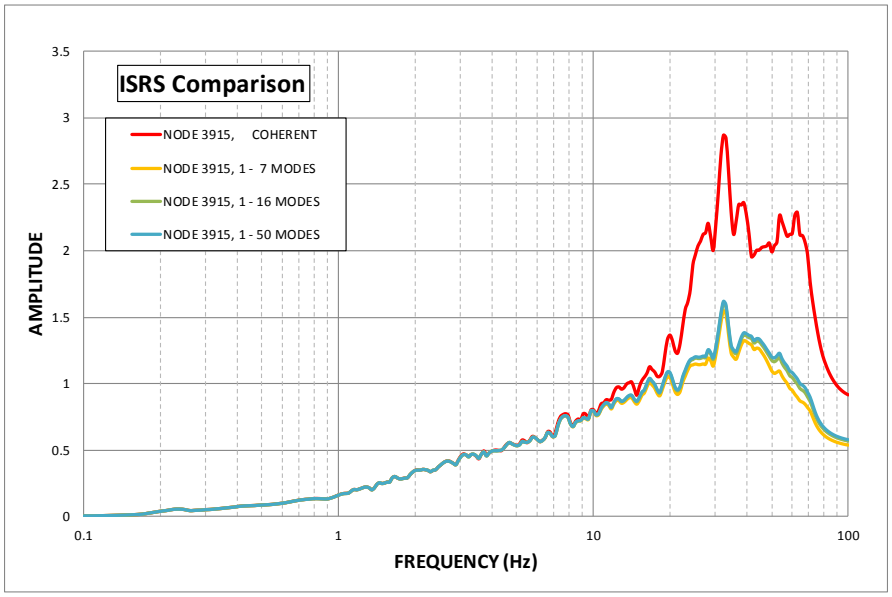

Figure 26 ARS – Floor Slab Node 3915 – Response in Vert. Direction

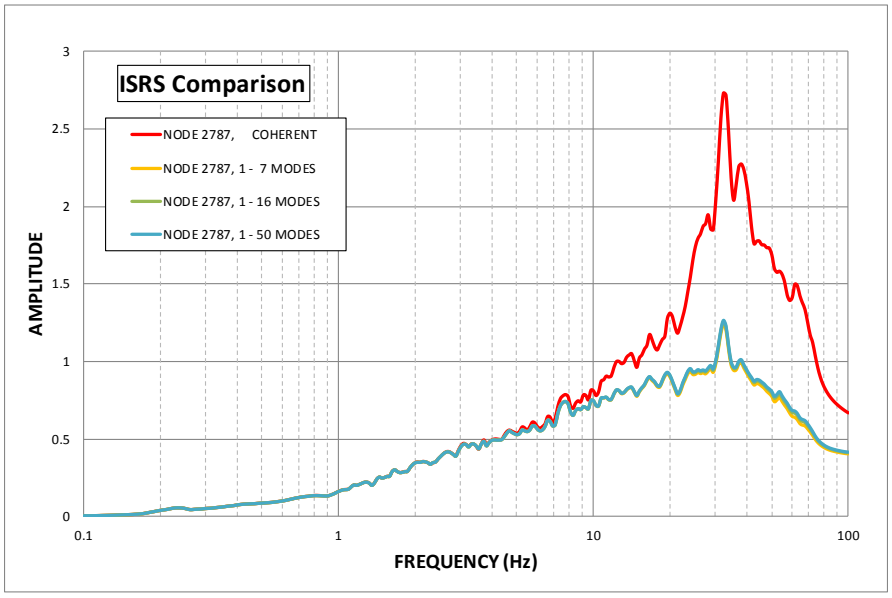

Figure 27 ARS – Floor Slab Node 2787 – Response in Vert. Direction

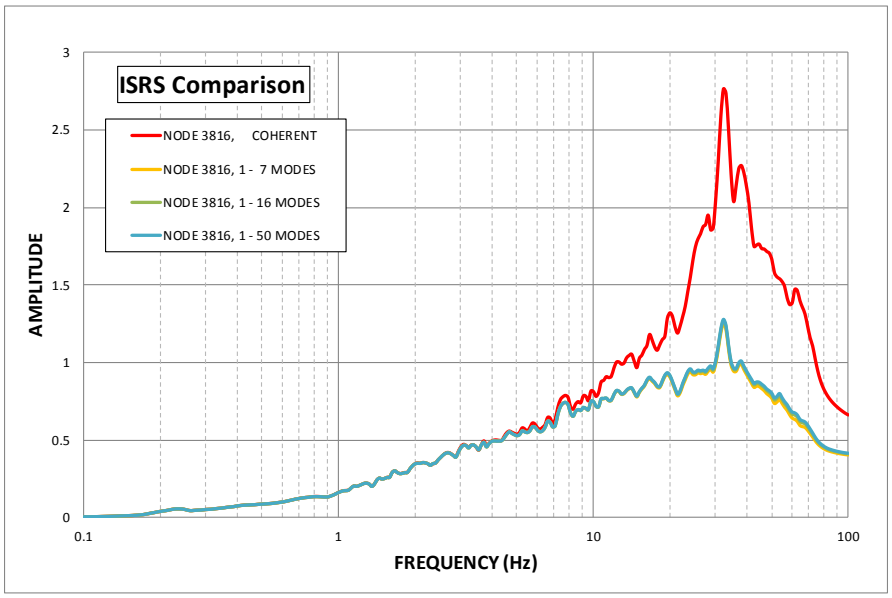

Figure 28 ARS – Floor Slab Node 3816 – Response in Vert. Direction

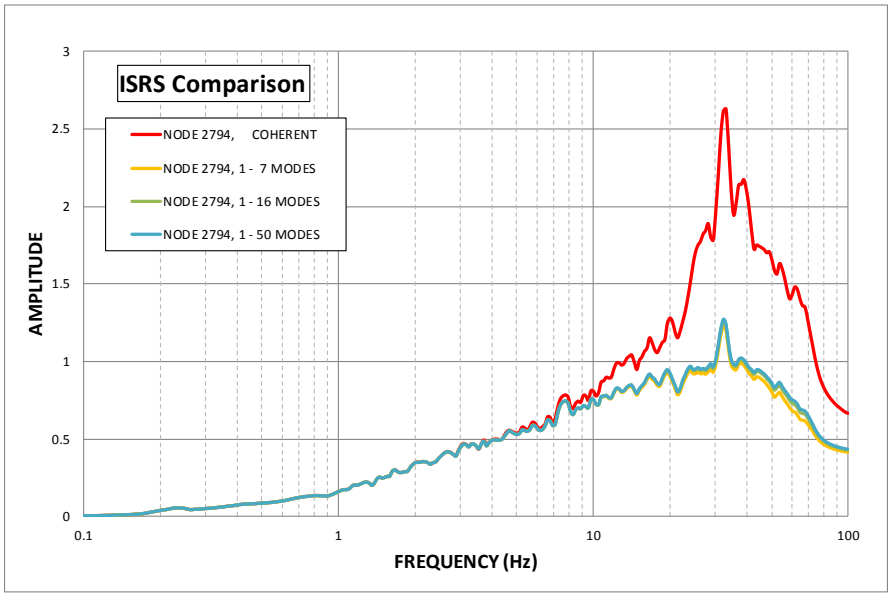

Figure 29 ARS – Floor Slab Node 2794 – Response in Vert. Direction

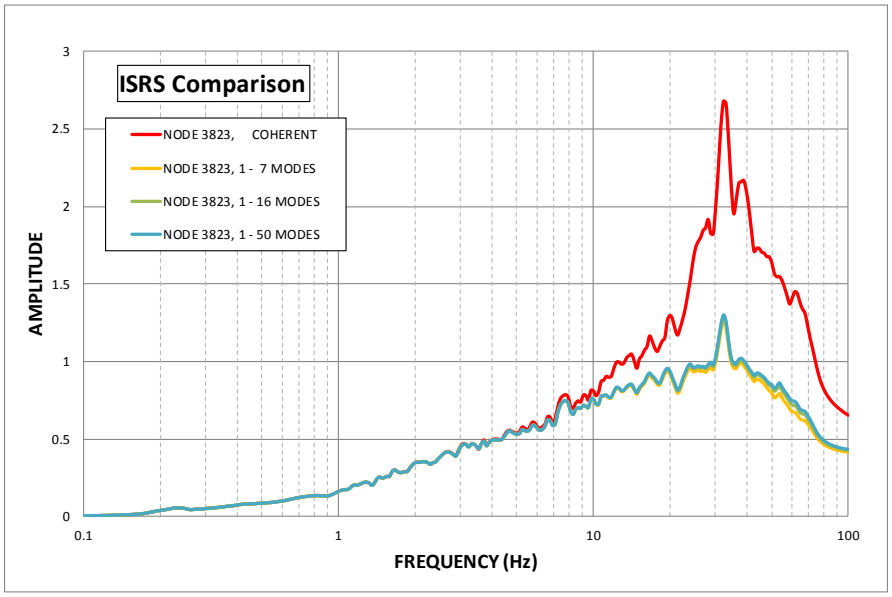

Figure 30 ARS – Floor Slab Node 3823 – Response in Vert. Direction

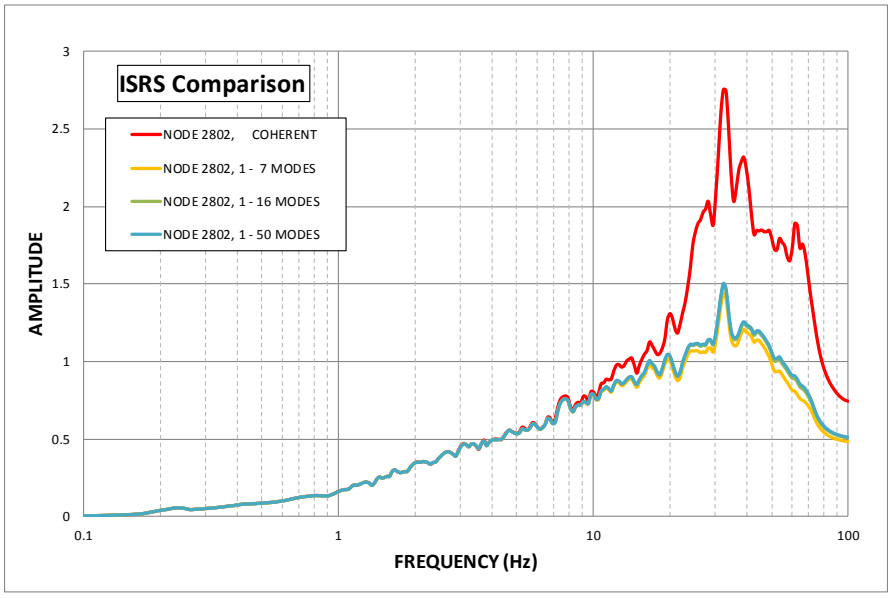

Figure 31 ARS – Floor Slab Node 2802 – Response in Vert. Direction

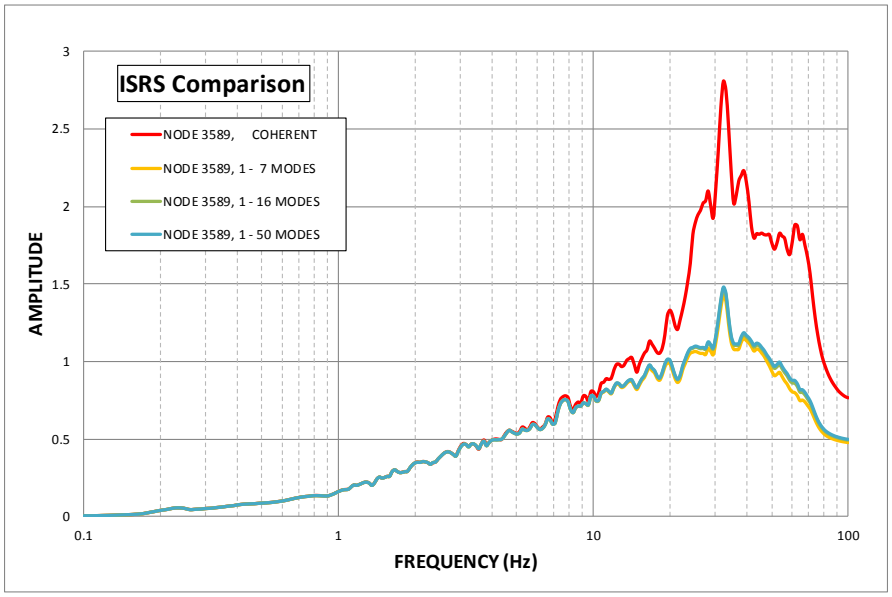

Figure 32 ARS – Floor Slab Node 3589 – Response in Vert. Direction

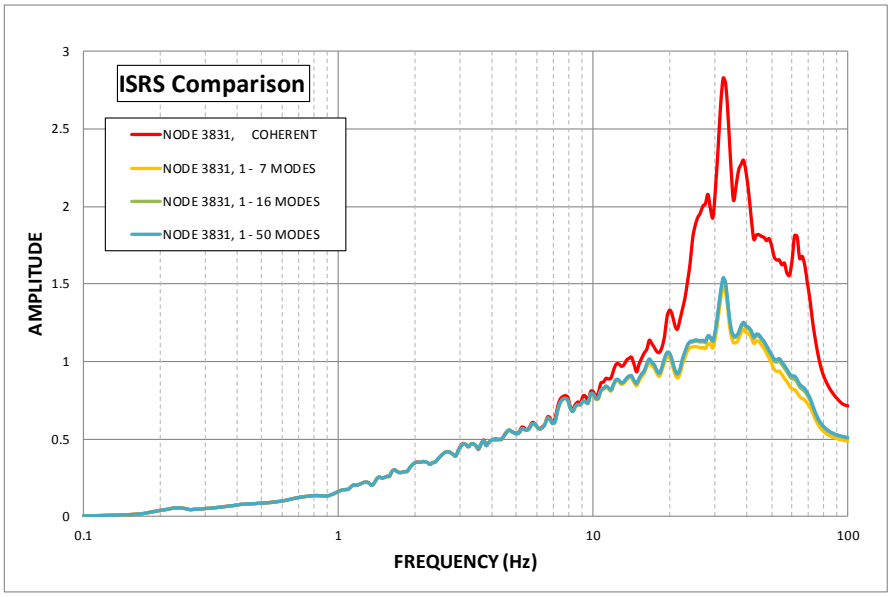

Figure 33 ARS – Floor Slab Node 3831 – Response in Vert. Direction

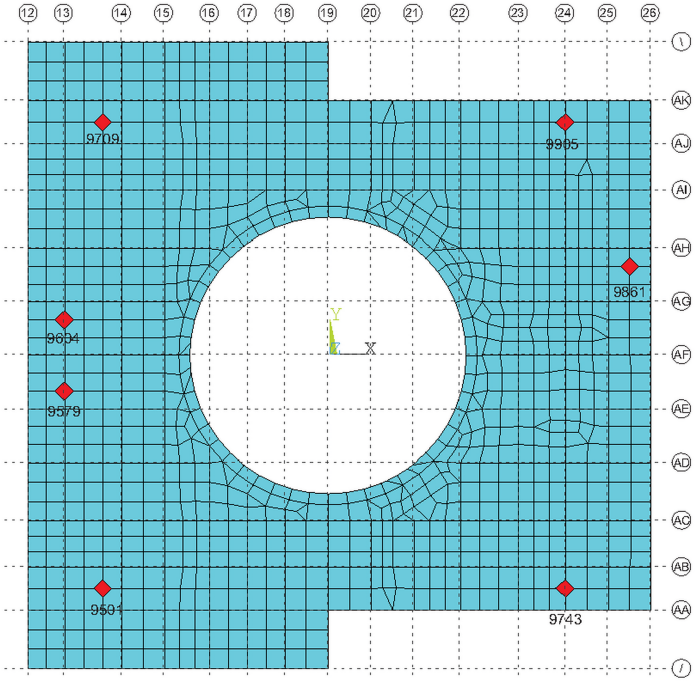

Figure 34 Selected Nodes for AB Floor Slab at El. 55’ (1-F)

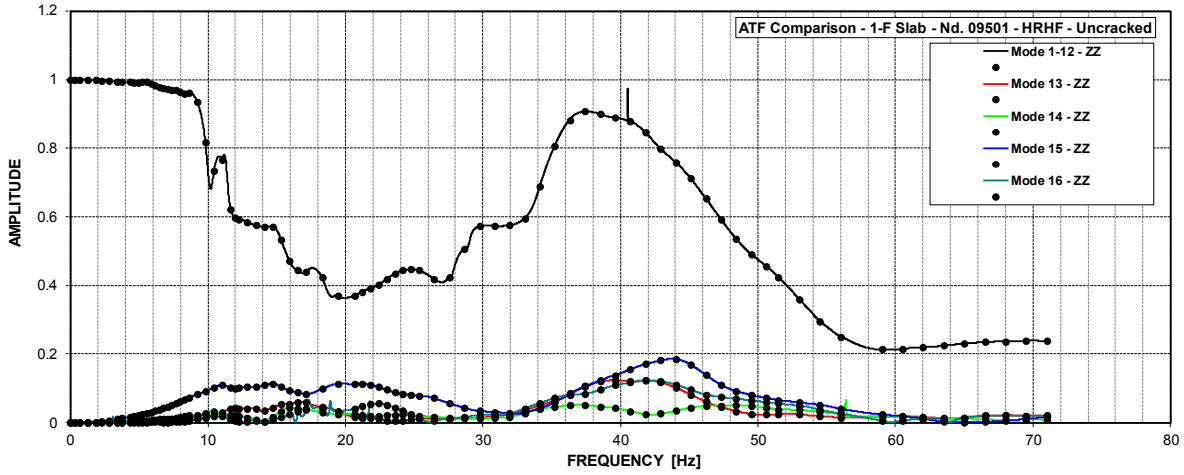

Figure 35 ATF – AB Slabs (1-F) at El. 55’ – Node 9501 – Z Resp. due to Z Input – Uncracked

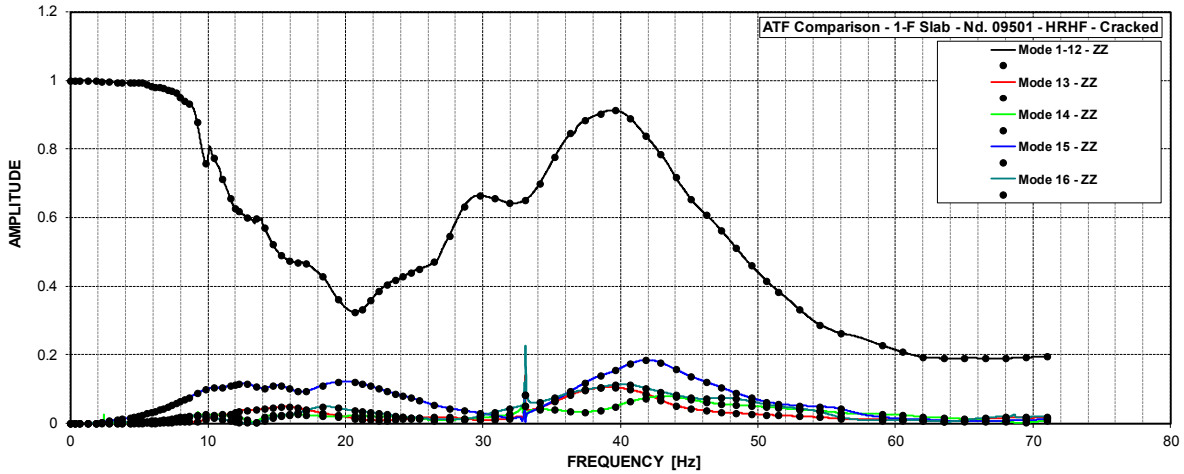

Figure 36 ATF – AB Slabs (1-F) at El. 55’ – Node 9501 – Z Resp. due to Z Input - Cracked

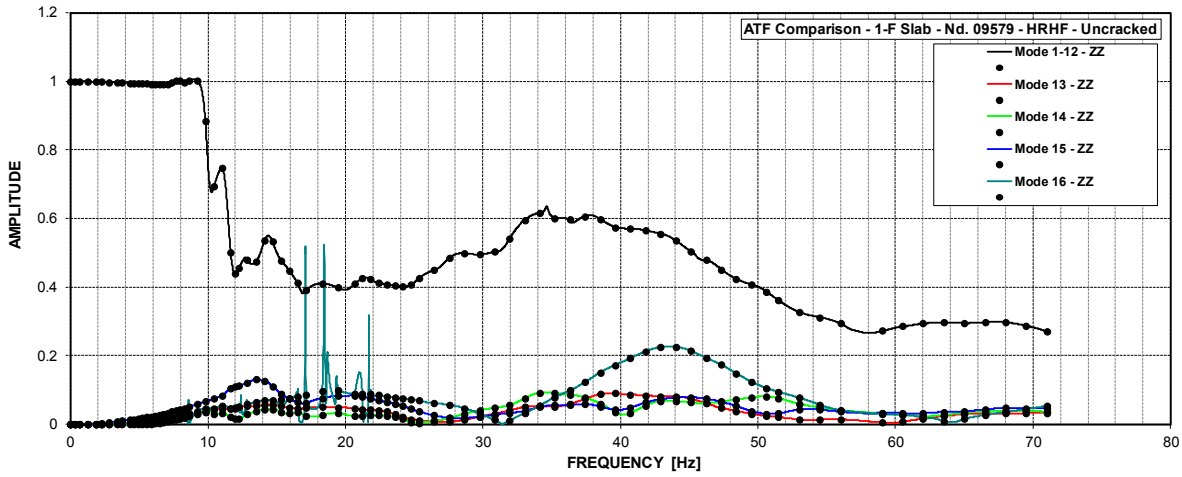

Figure 37 ATF – AB Slabs (1-F) at El. 55’ – Node 9579 – Z Resp. due to Z Input - Uncracked

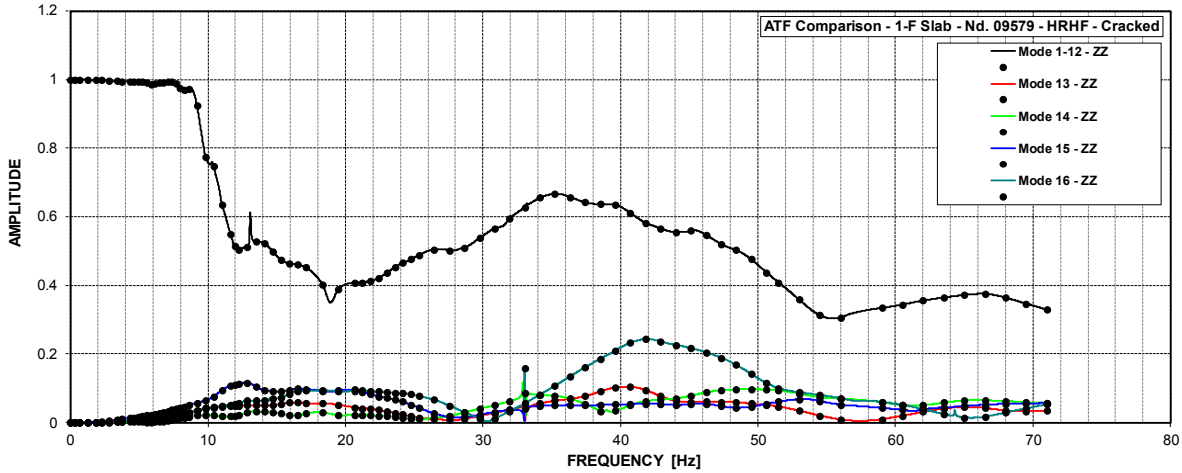

Figure 38 ATF – AB Slabs (1-F) at El. 55’ – Node 9579 – Z Resp. due to Z Input - Cracked

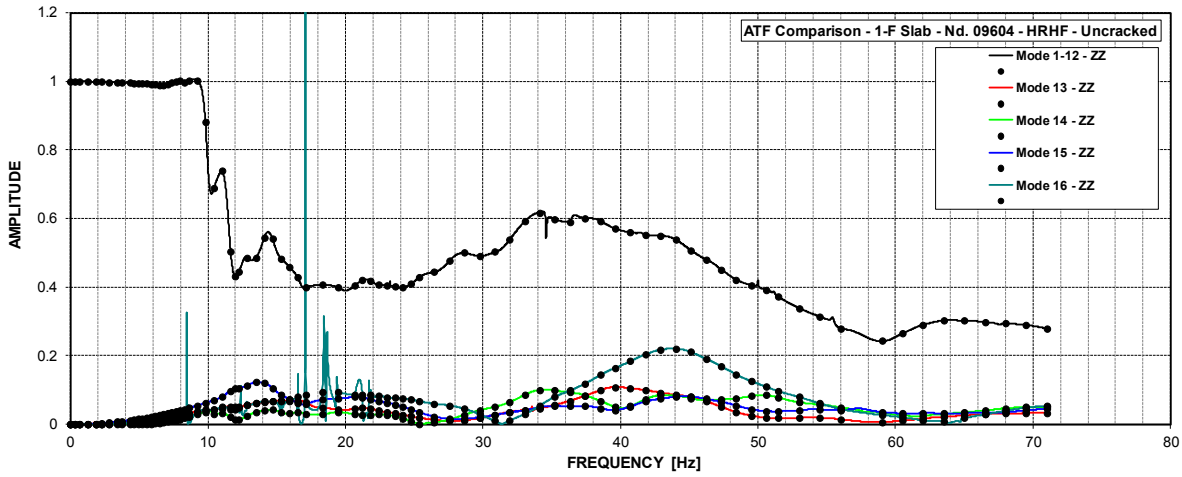

Figure 39 ATF – AB Slabs (1-F) at El. 55’ – Node 9604 – Z Resp. due to Z Input - Uncracked

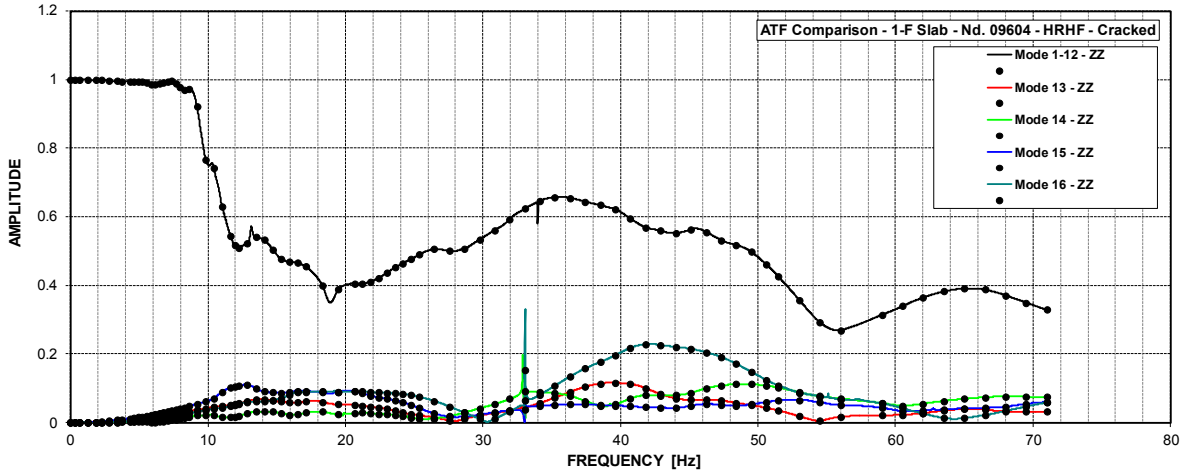

Figure 40 ATF – AB Slabs (1-F) at El. 55’ – Node 9604 – Z Resp. due to Z Input - Cracked

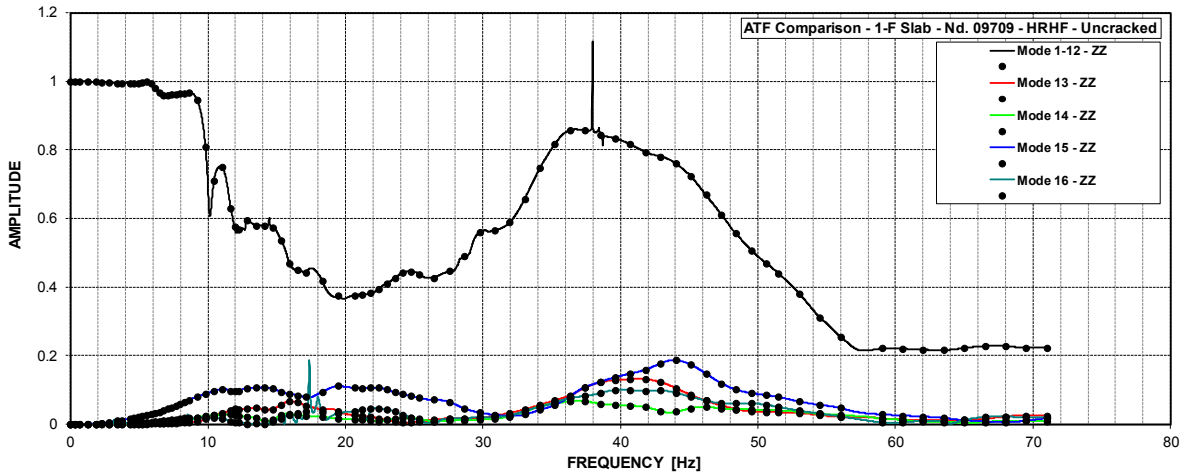

Figure 41 ATF – AB Slabs (1-F) at El. 55’ – Node 9709 – Z Resp. due to Z Input - Uncracked

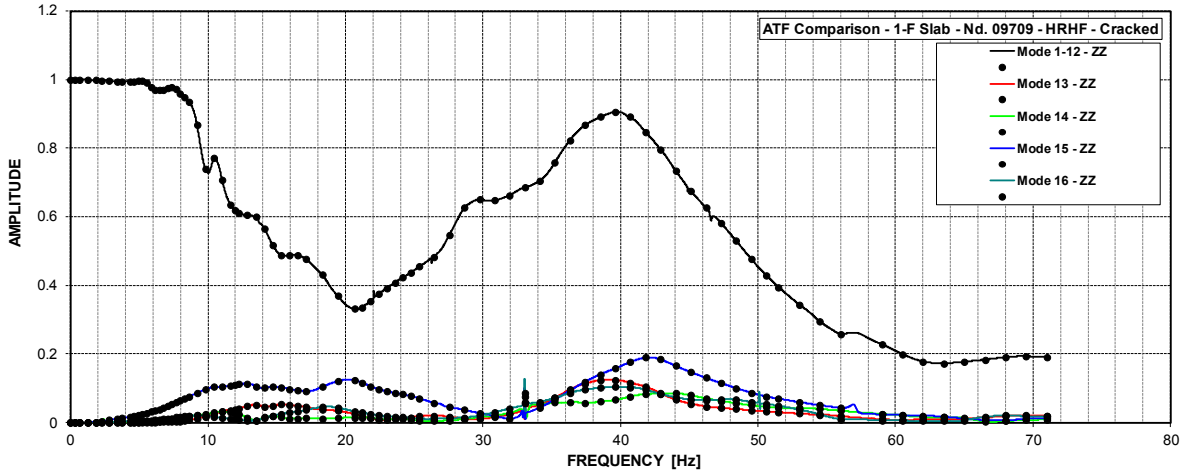

Figure 42 ATF – AB Slabs (1-F) at El. 55’ – Node 9709 – Z Resp. due to Z Input - Cracked

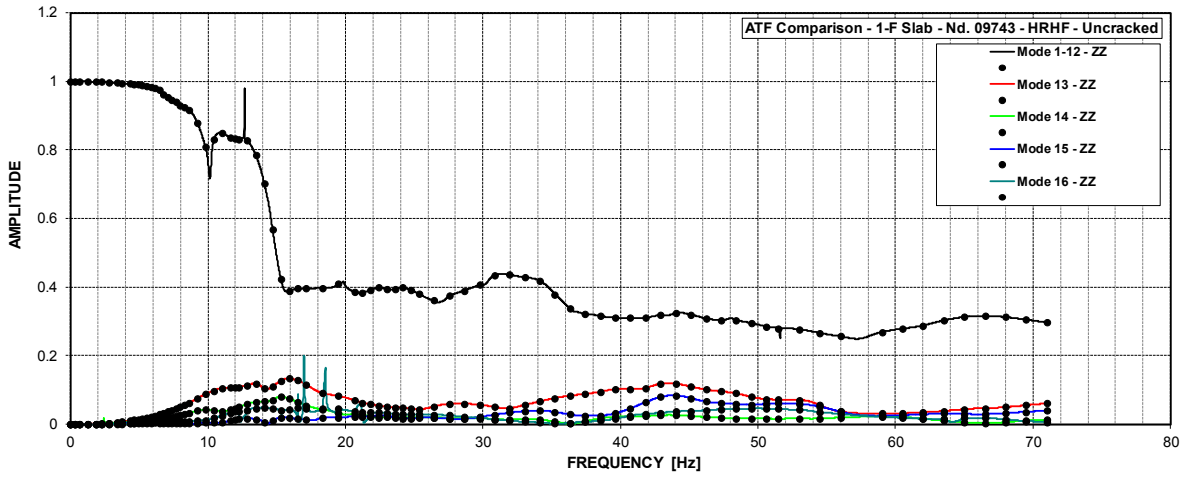

Figure 43 ATF – AB Slabs (1-F) at El. 55’ – Node 9743 – Z Resp. due to Z Input - Uncracked

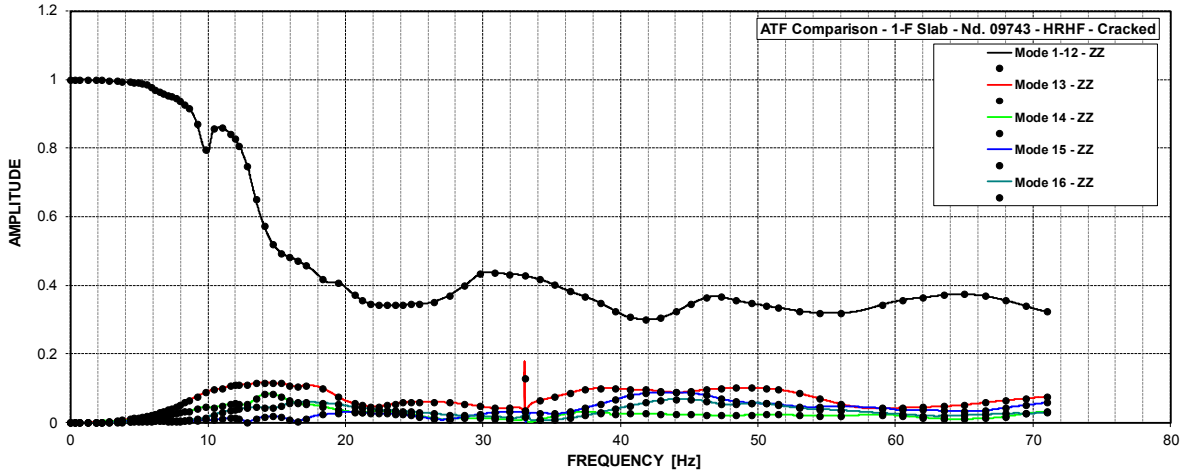

Figure 44 ATF – AB Slabs (1-F) at El. 55’ – Node 9743 – Z Resp. due to Z Input - Cracked

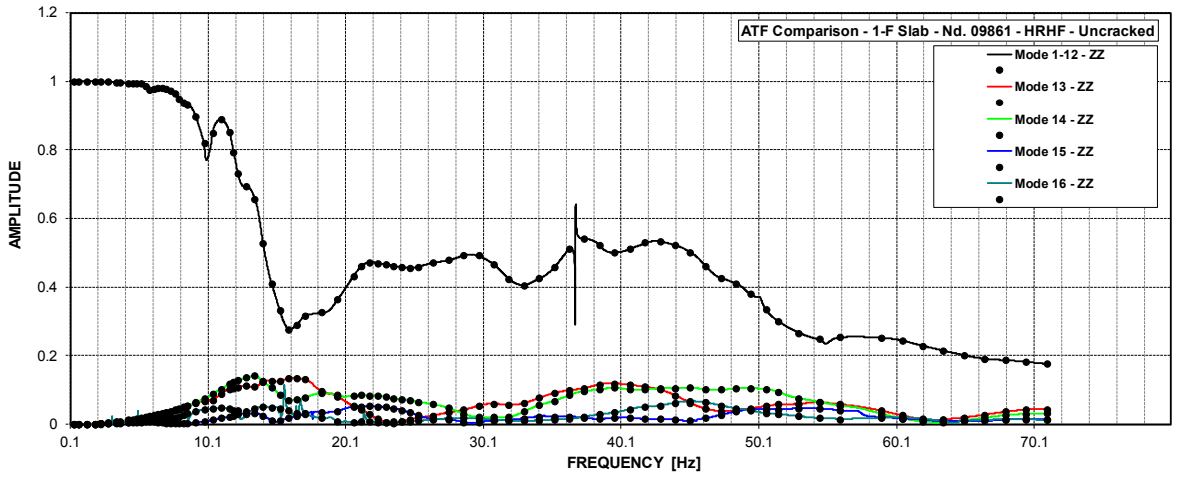

Figure 45 ATF – AB Slabs (1-F) at El. 55’ – Node 9861 – Z Resp. due to Z Input - Uncracked

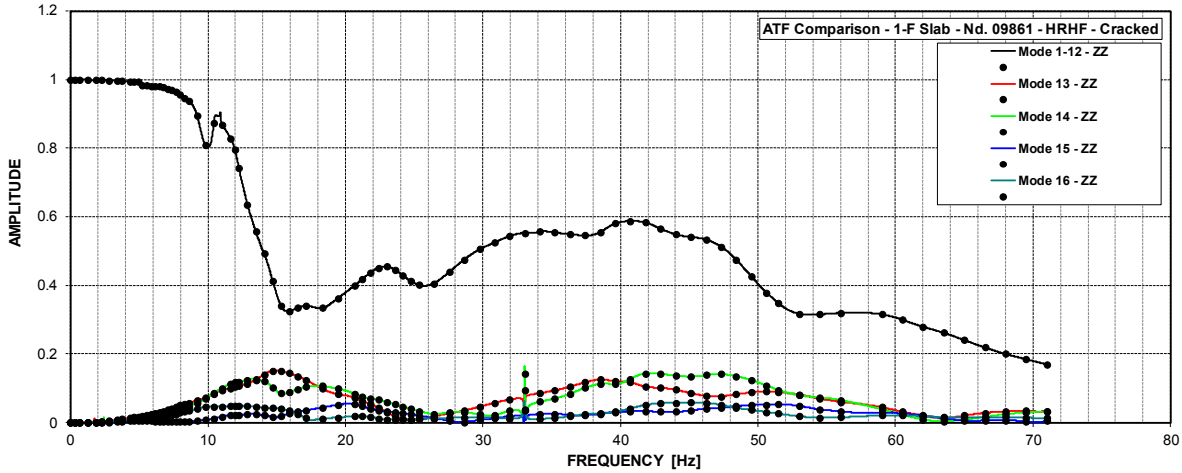

Figure 46 ATF – AB Slabs (1-F) at El. 55’ – Node 9861 – Z Resp. due to Z Input - Cracked

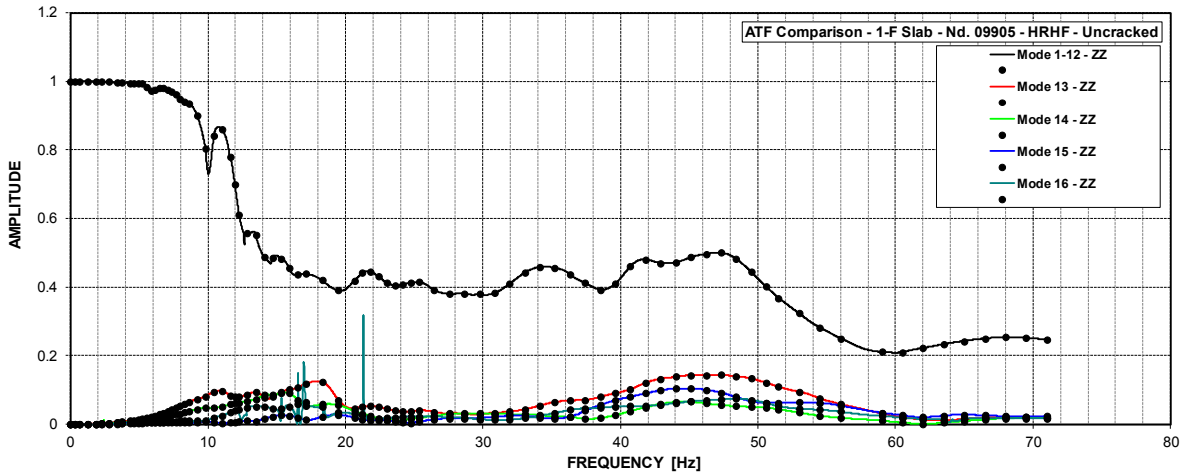

Figure 47 ATF – AB Slabs (1-F) at El. 55’ – Node 9905 – Z Resp. due to Z Input - Uncracked

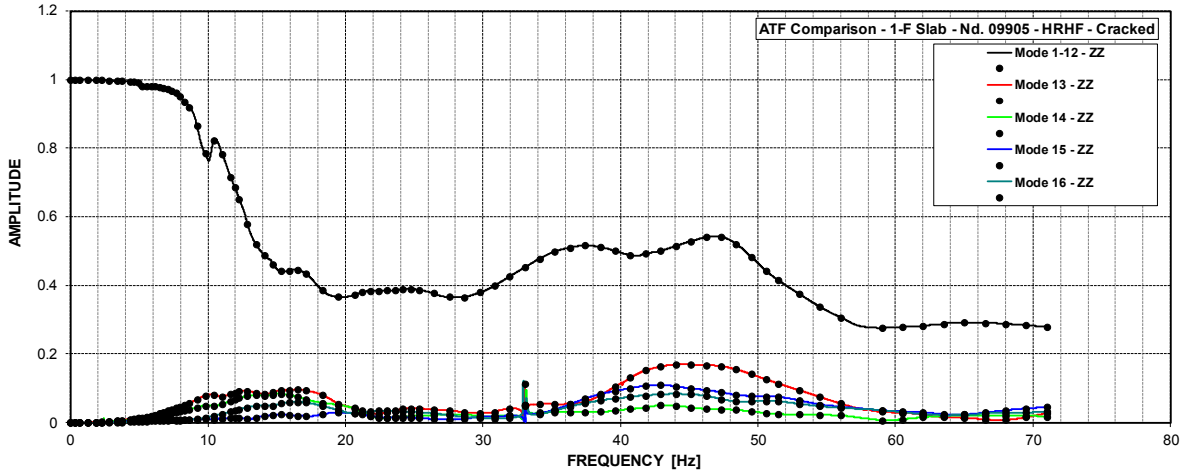

Figure 48 ATF – AB Slabs (1-F) at El. 55’ – Node 9905 – Z Resp. due to Z Input – Cracked

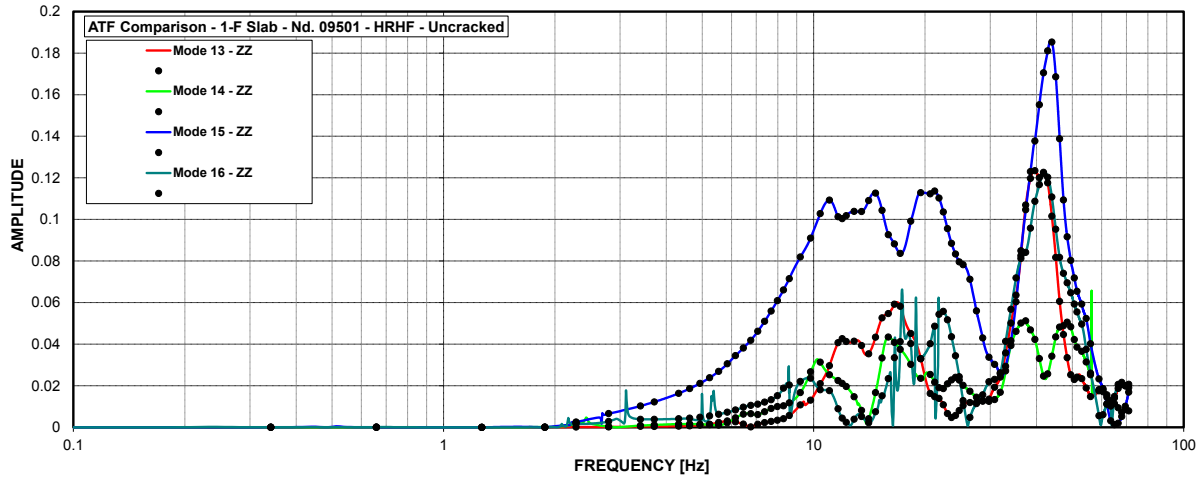

Figure 49 ATF – AB Slabs (1-F) at El. 55’ – Node 9501 – Z Resp. due to Z Input – Uncracked – Modes 13 through 16

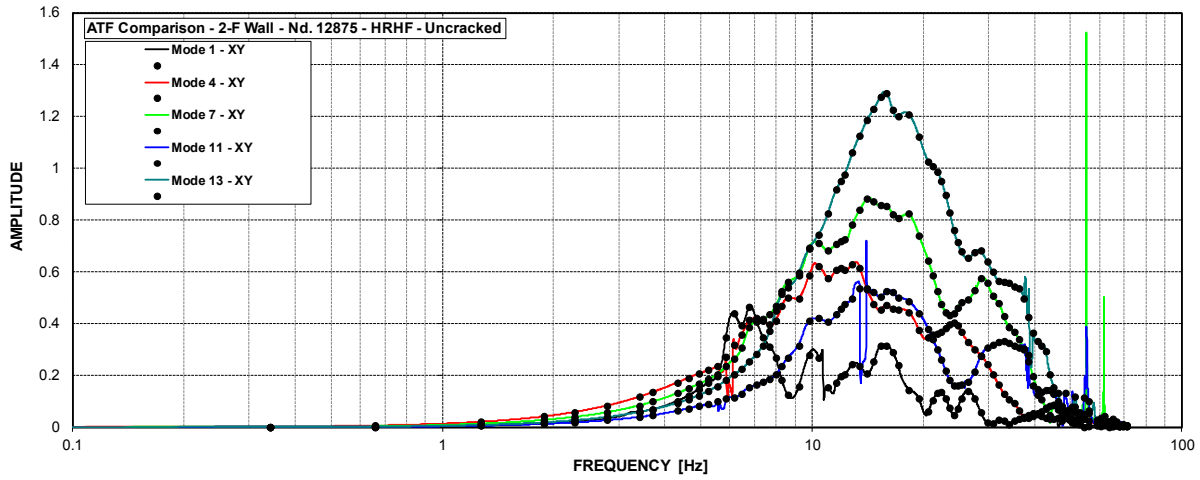

Figure 50 ATF – AB Walls (2-F) at El. 78’ – Node 12875 – Y Resp. due to X Input – Uncracked – Modes 1, 4, 7, 11, 13

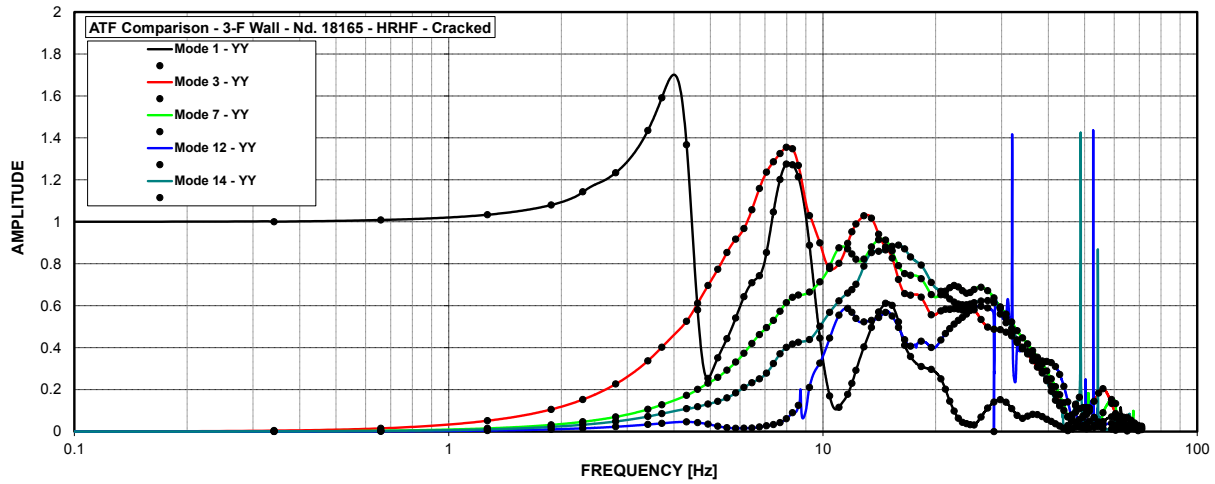

Figure 51 ATF – AB Walls (3-F) at El. 100’ – Node 18165 – Y Resp. due to Y Input – Cracked – Modes 1, 3, 7, 12, 14

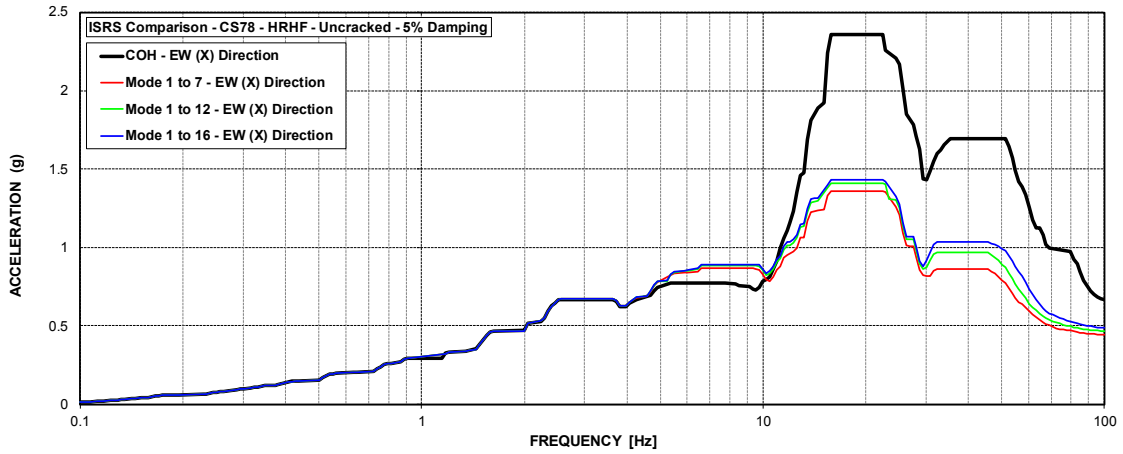

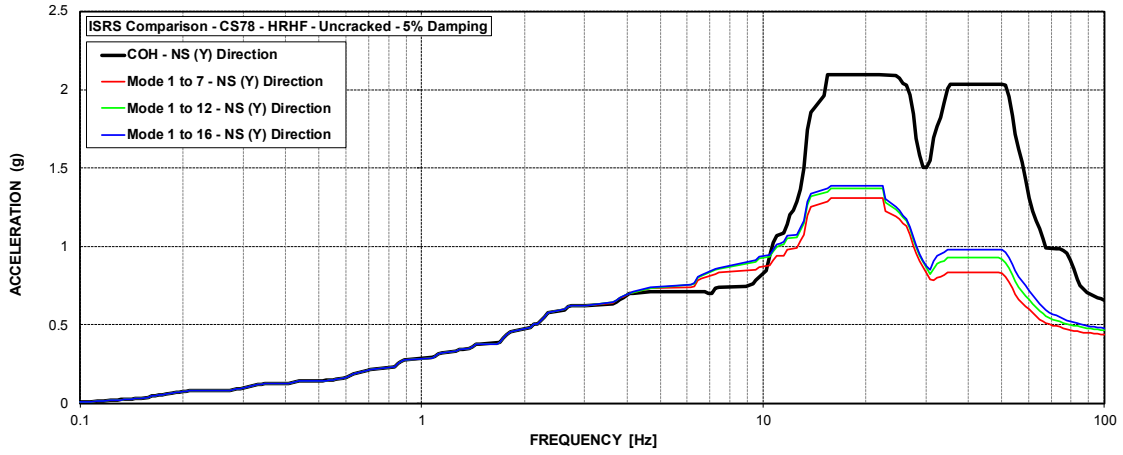

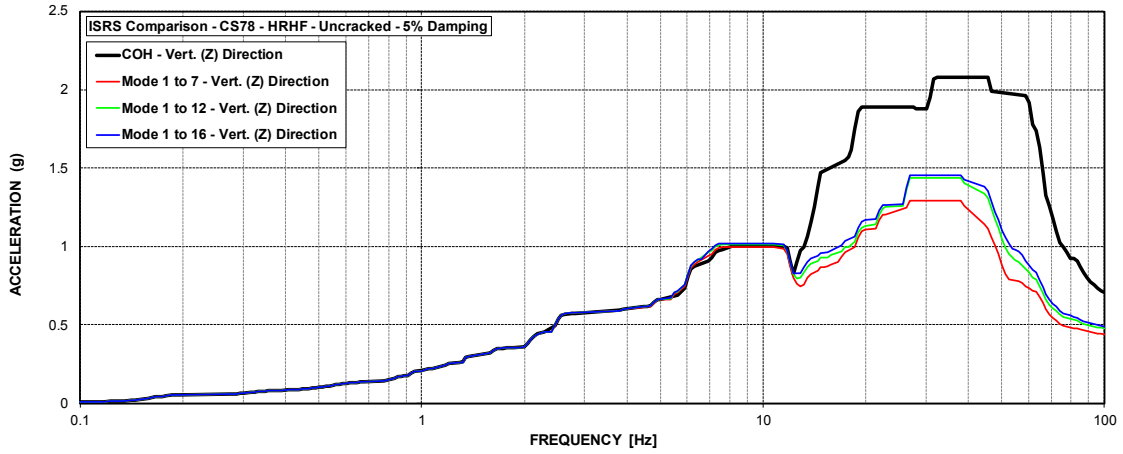

Figure 52 ISRS – Containment Structure (CS78) at El. 78’ – HRHF – Uncracked

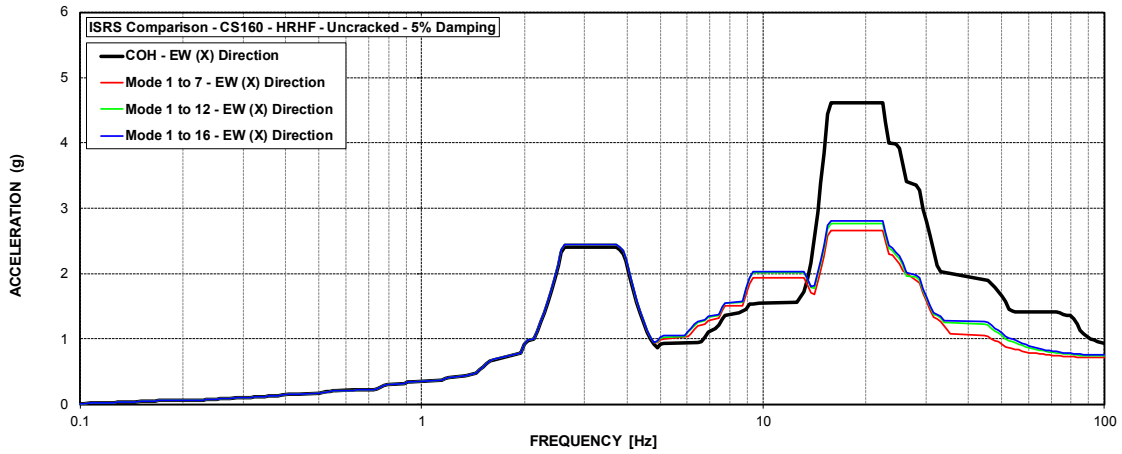

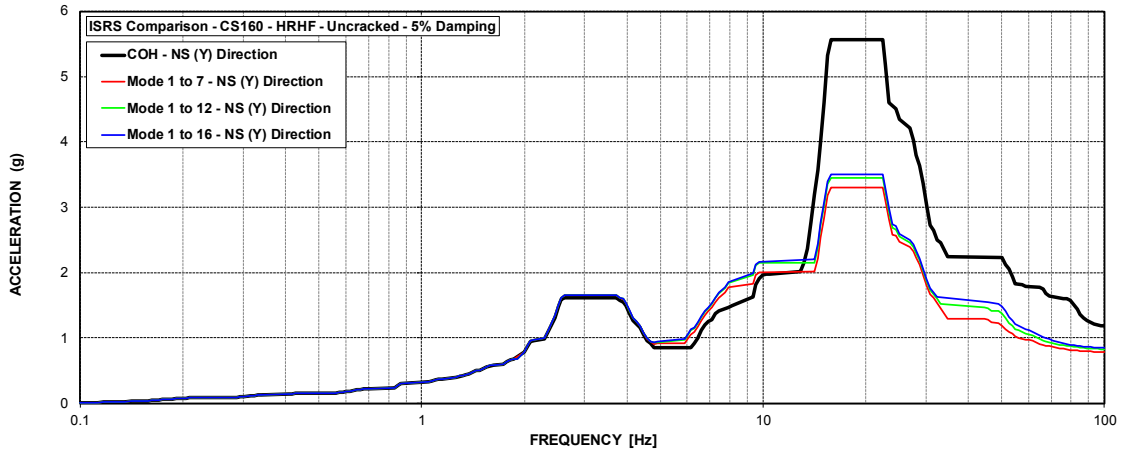

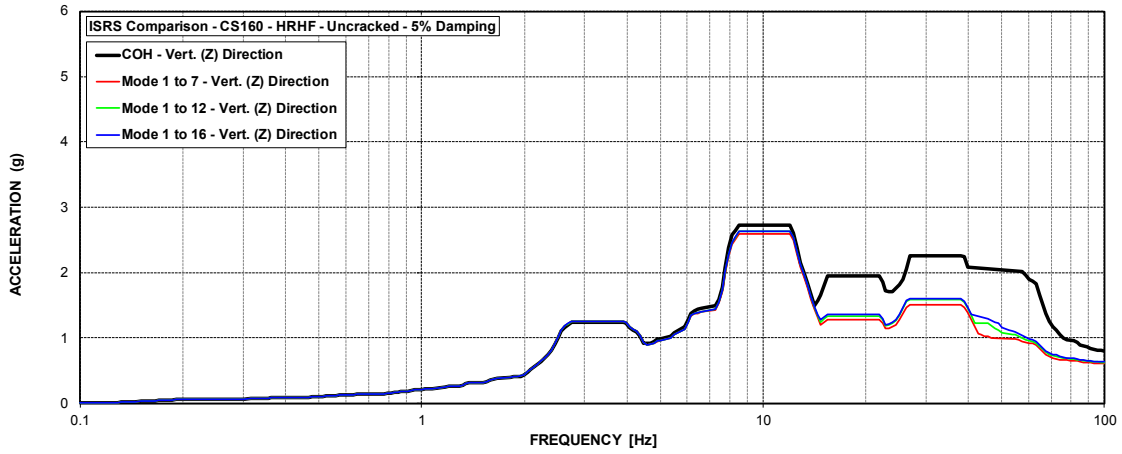

Figure 53 ISRS – Containment Structure (CS160) at El. 160’ – HRHF – Uncracked

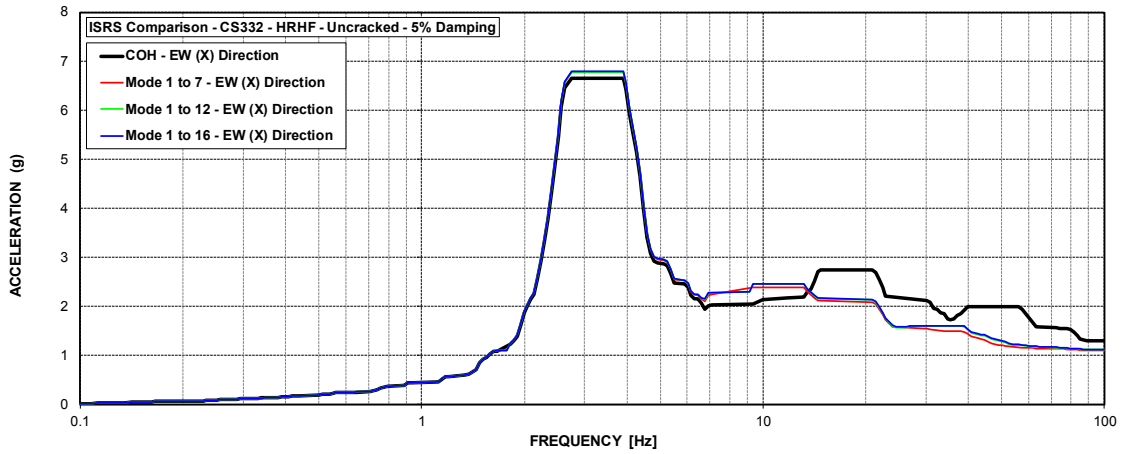

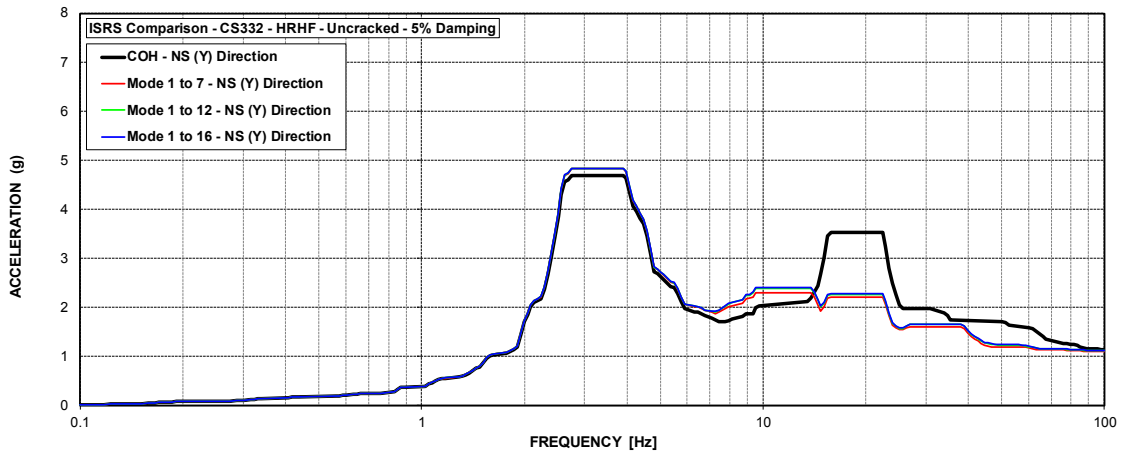

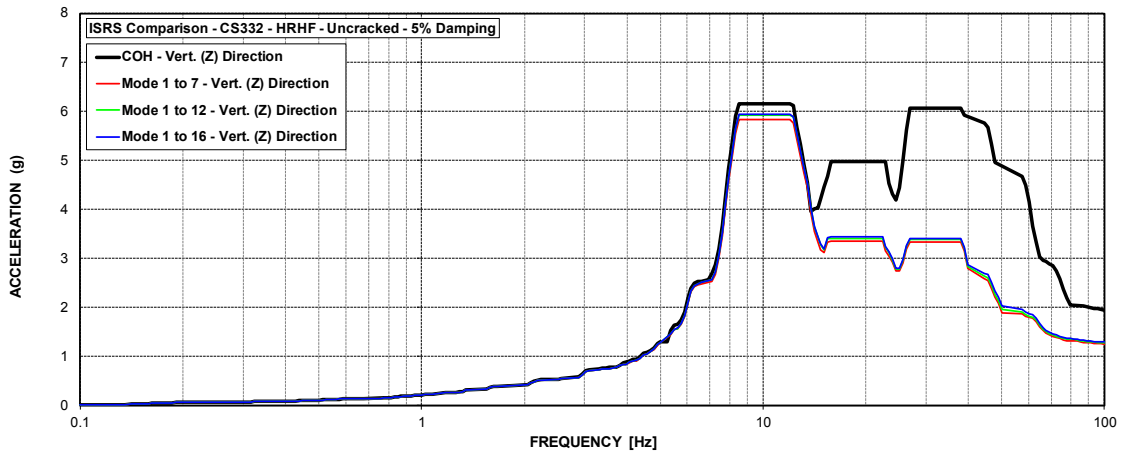

Figure 54 ISRS – Containment Structure (CS332) at El. 332’ – HRHF – Uncracked

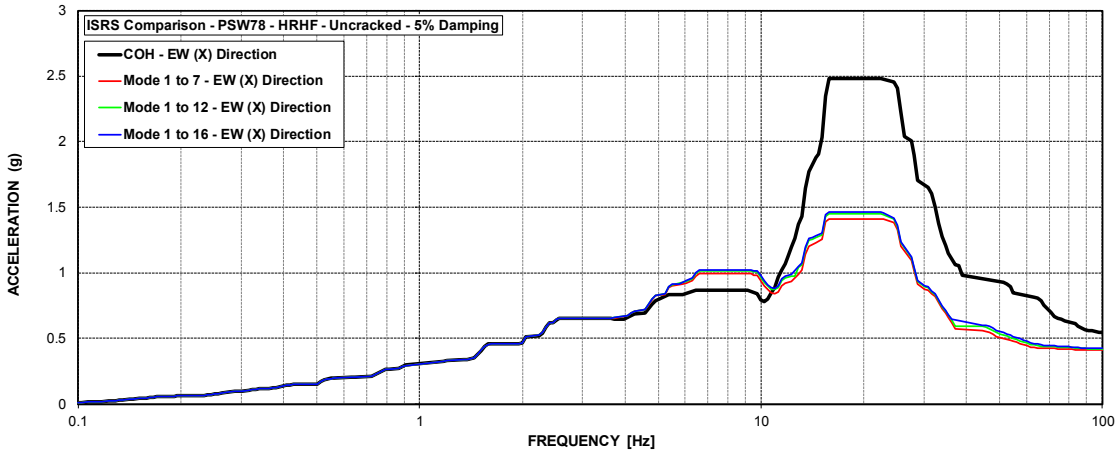

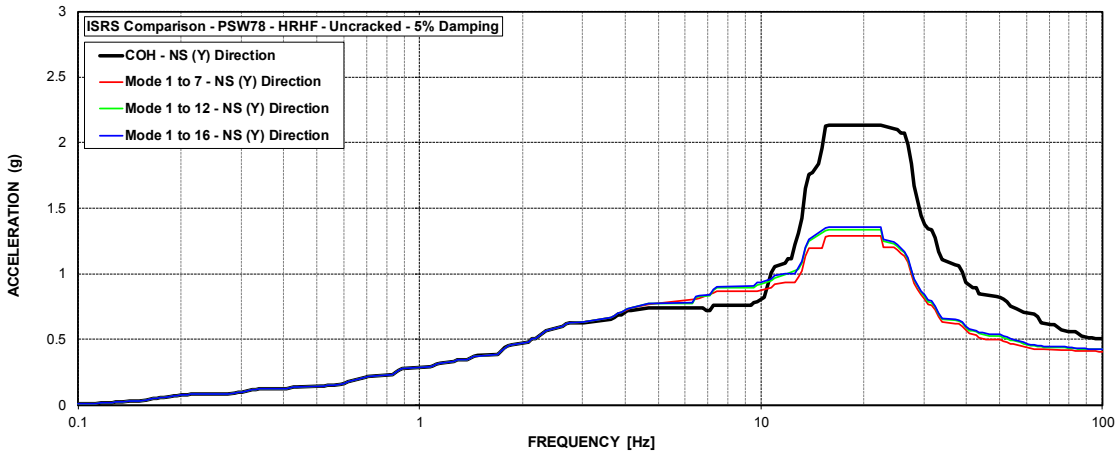

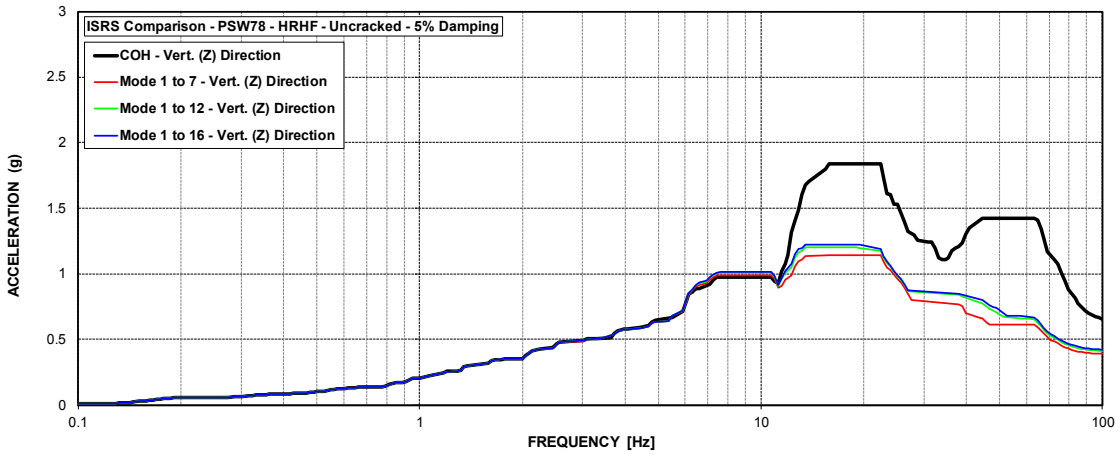

Figure 55 ISRS – Primary Shield Wall (PSW78) at El. 78’ – HRHF – Uncracked

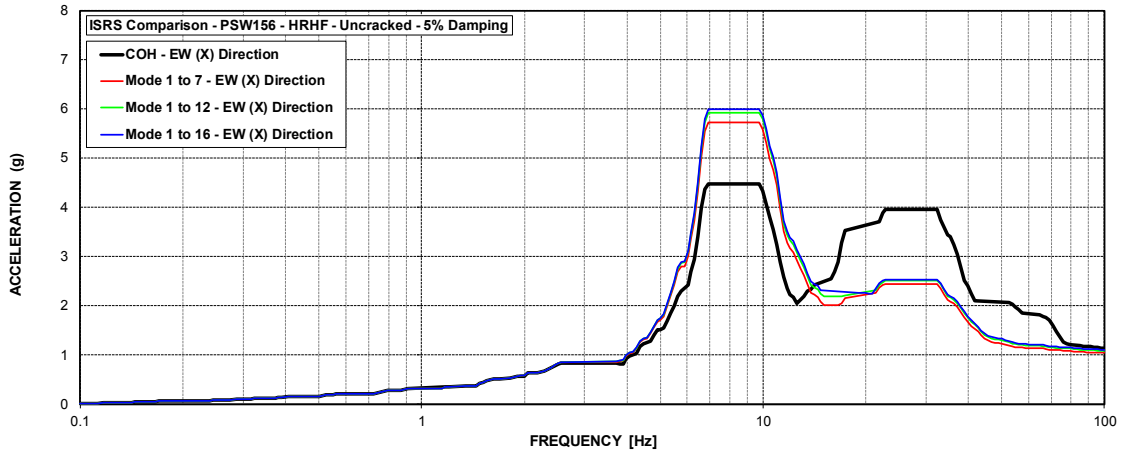

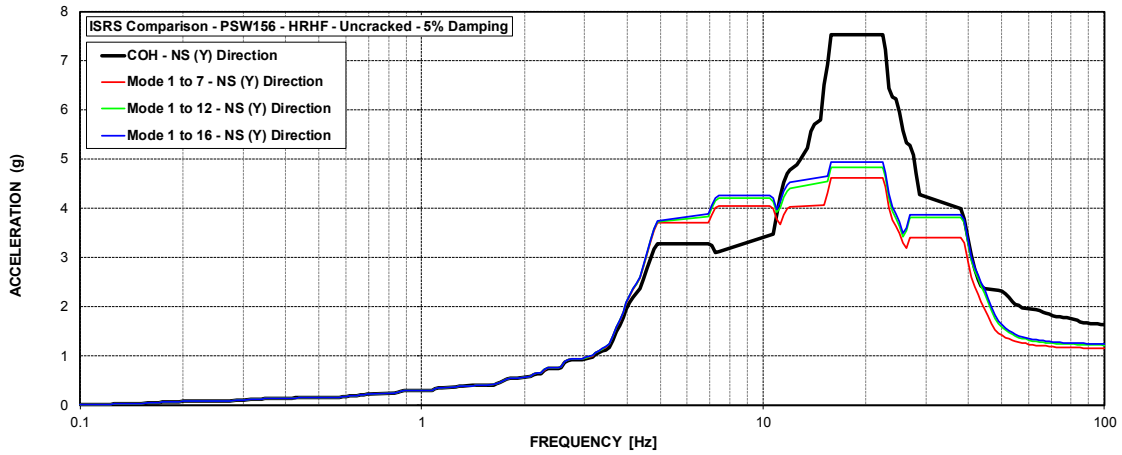

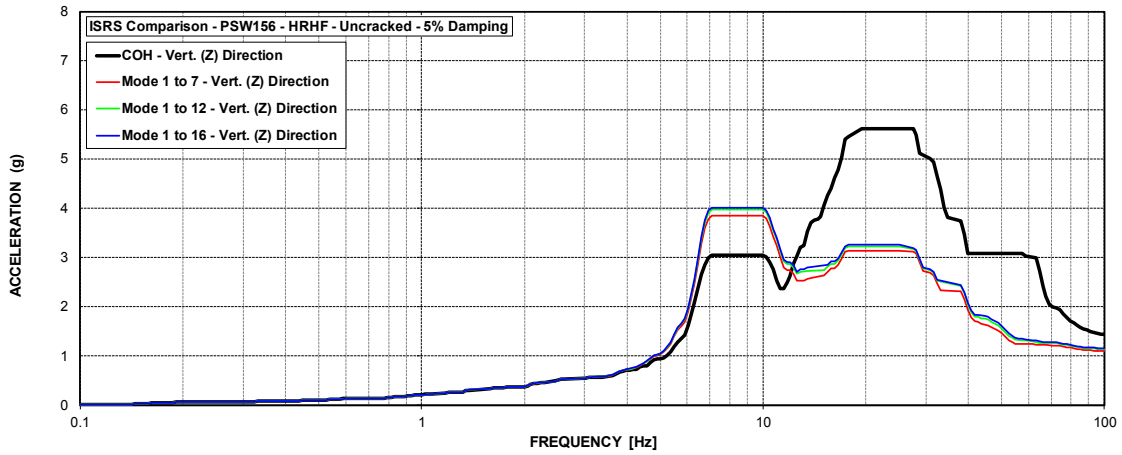

Figure 56 ISRS – Primary Shield Wall (PSW156) at El. 156’ – HRHF – Uncracked

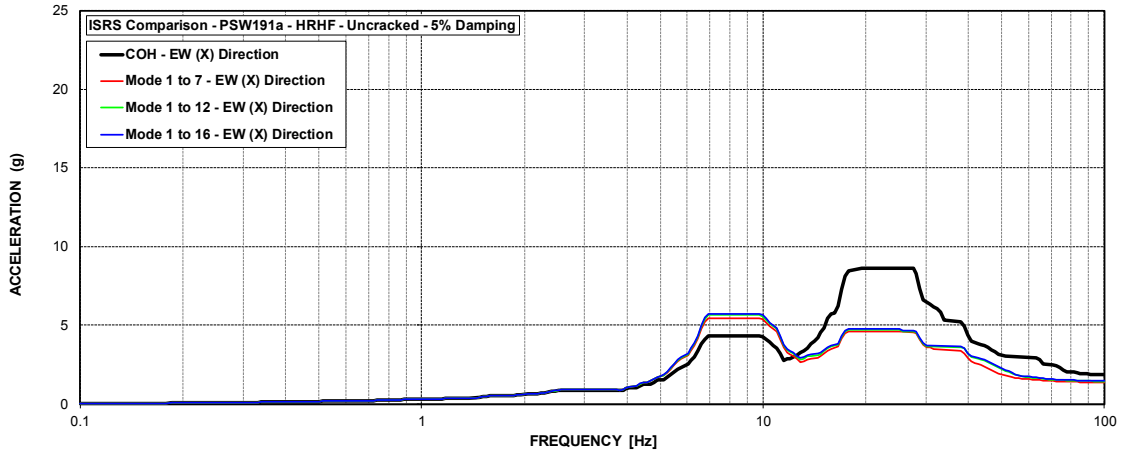

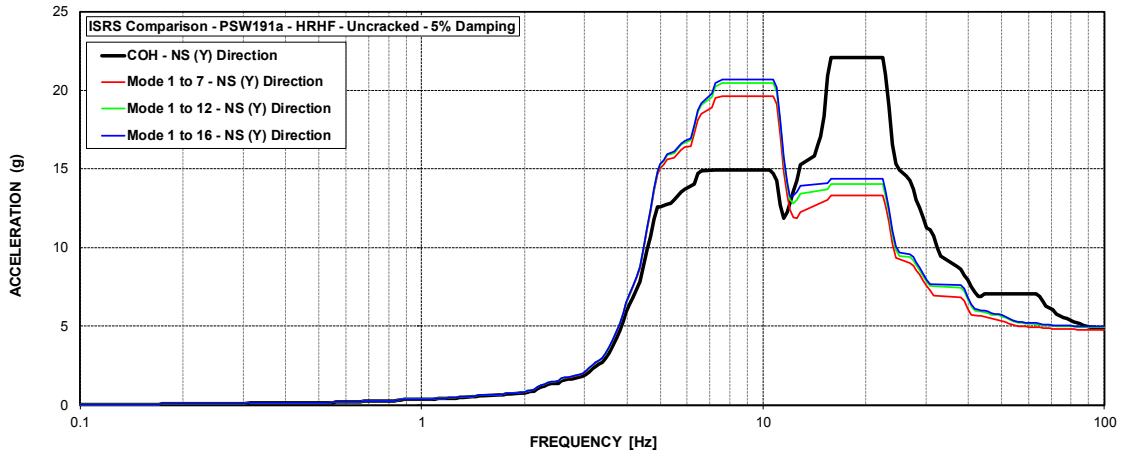

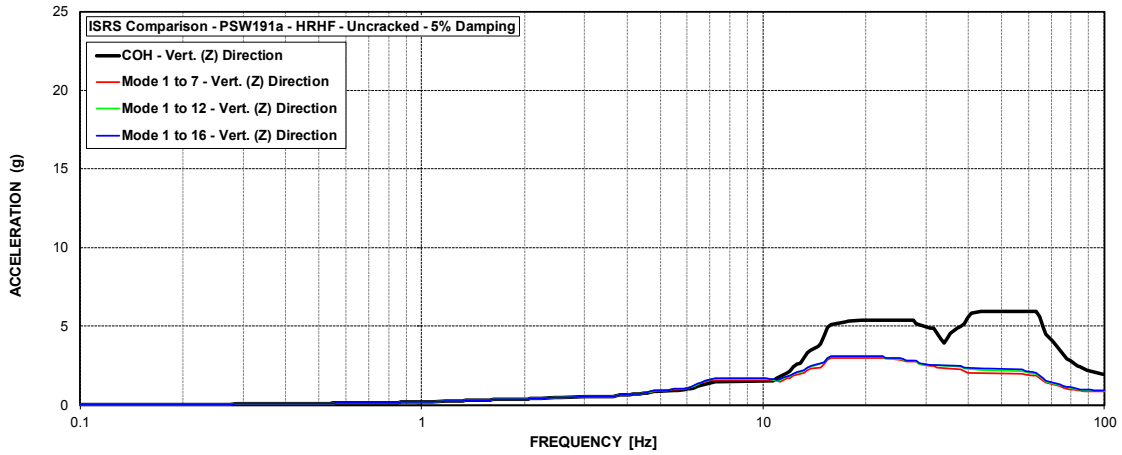

Figure 57 ISRS – Primary Shield Wall (PSW191a) at El. 191’ – HRHF – Uncracked

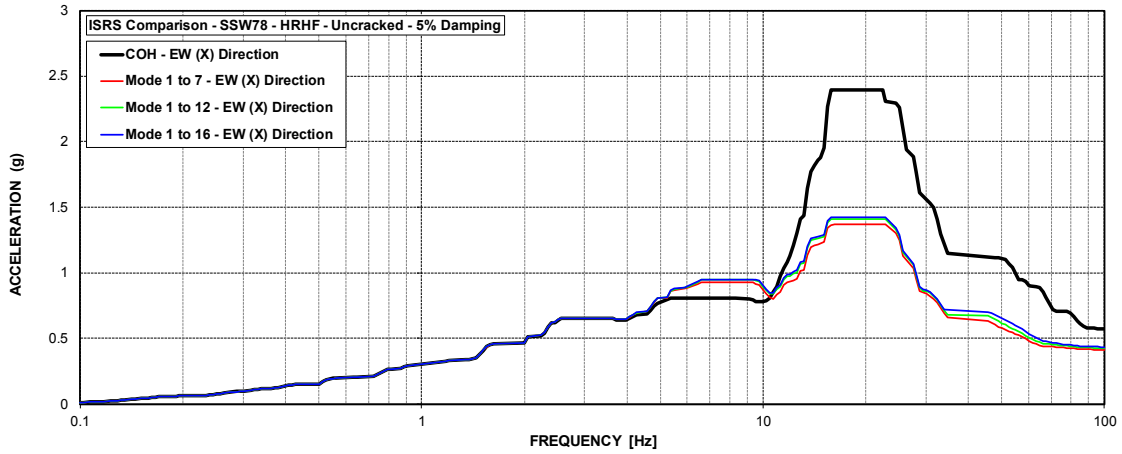

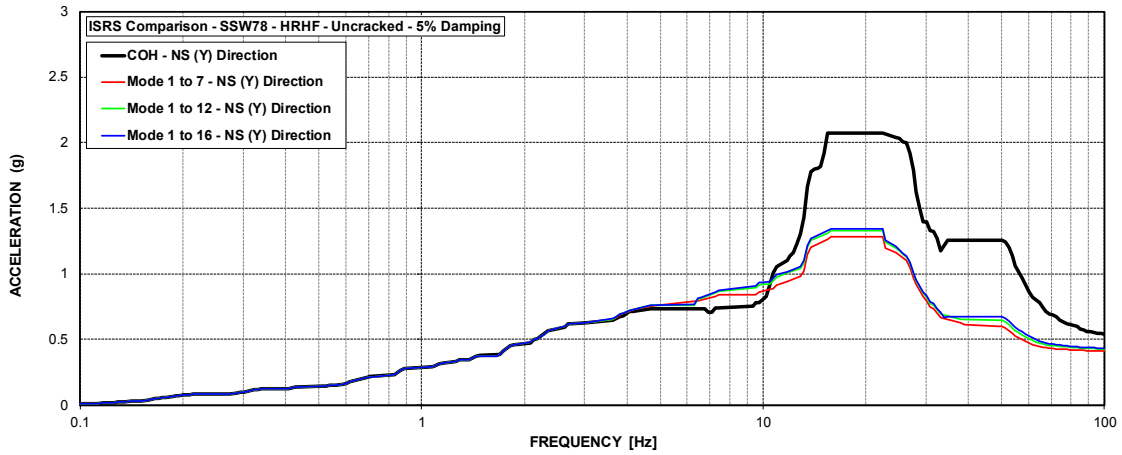

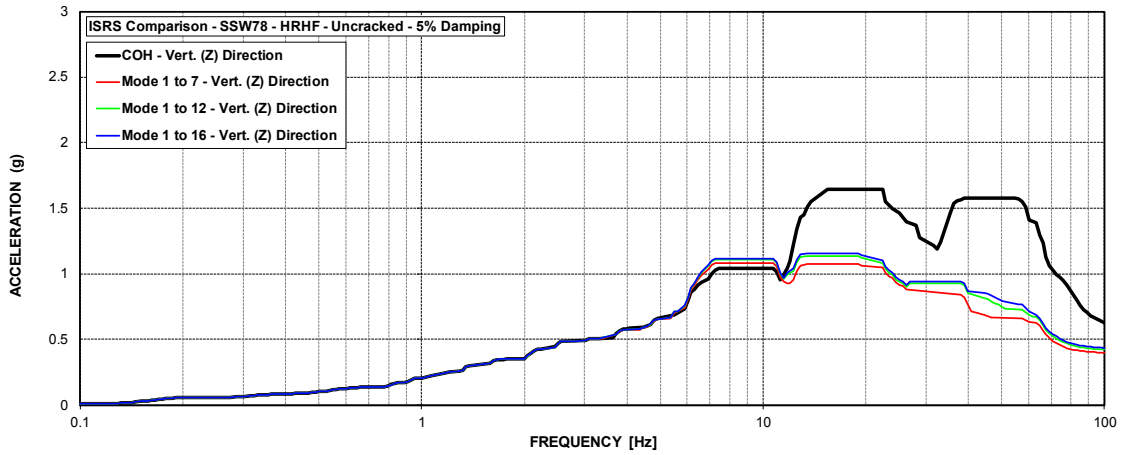

Figure 58 ISRS – Secondary Shield Wall (SSW78) at El. 78’ – HRHF – Uncracked

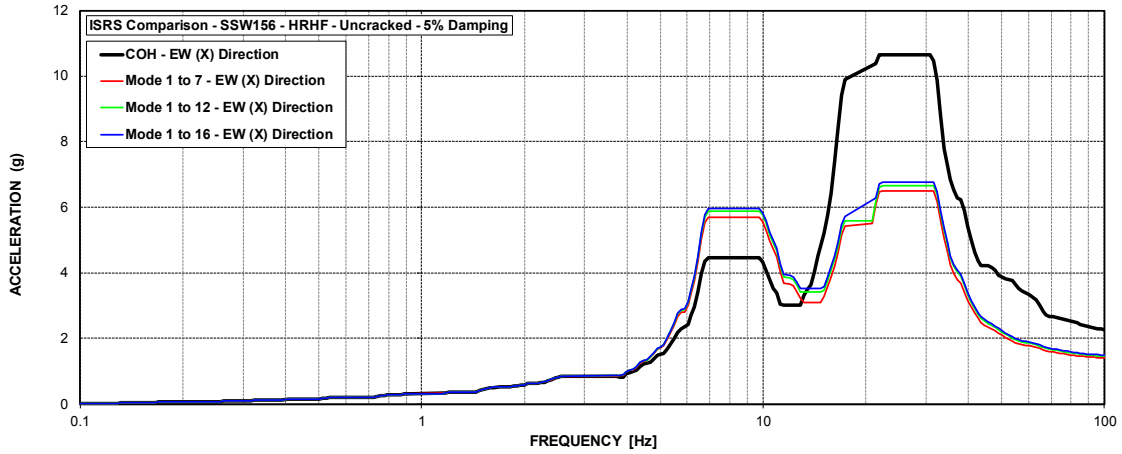

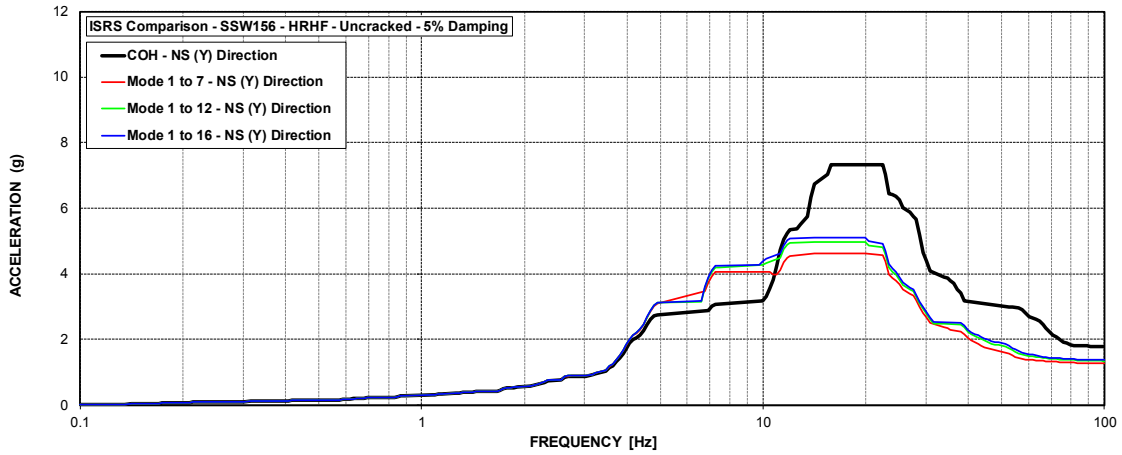

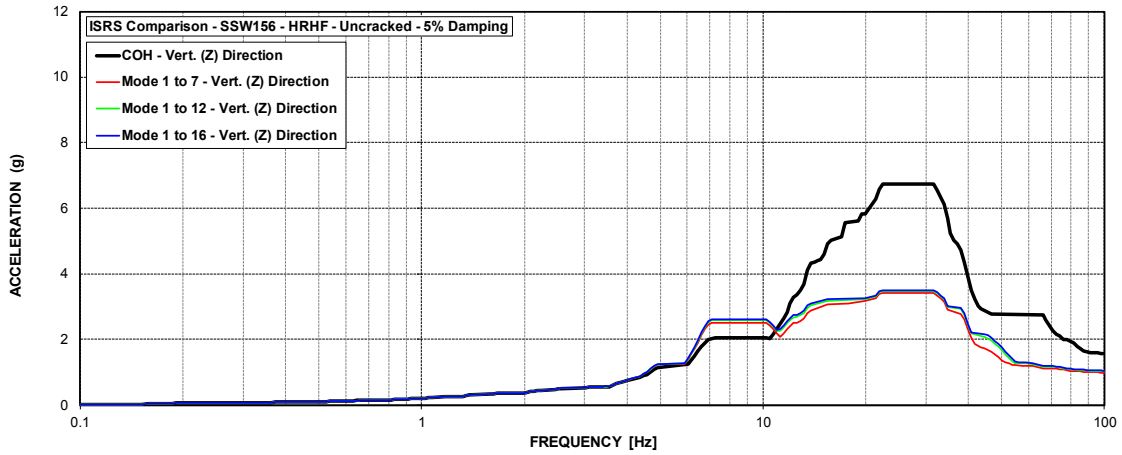

Figure 59 ISRS – Secondary Shield Wall (SSW156) at El. 156’ – HRHF – Uncracked

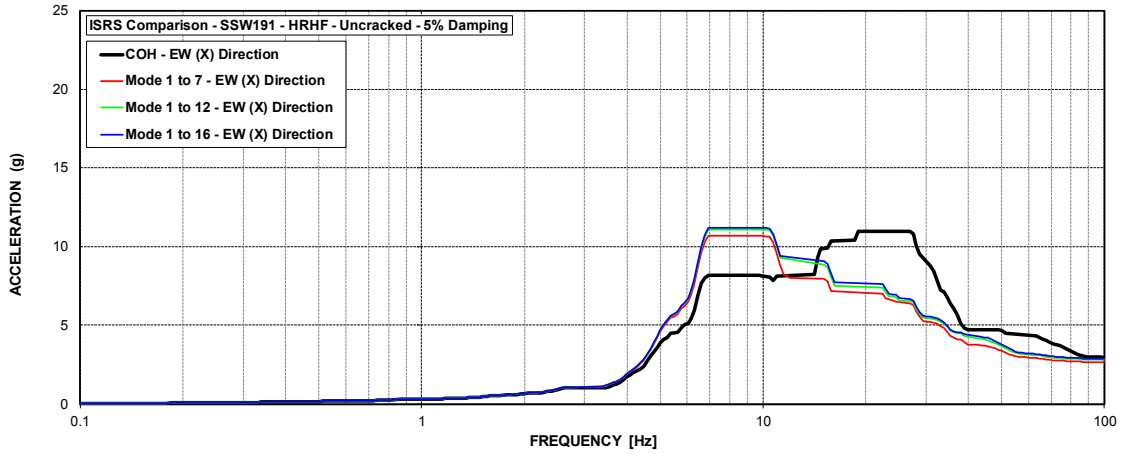

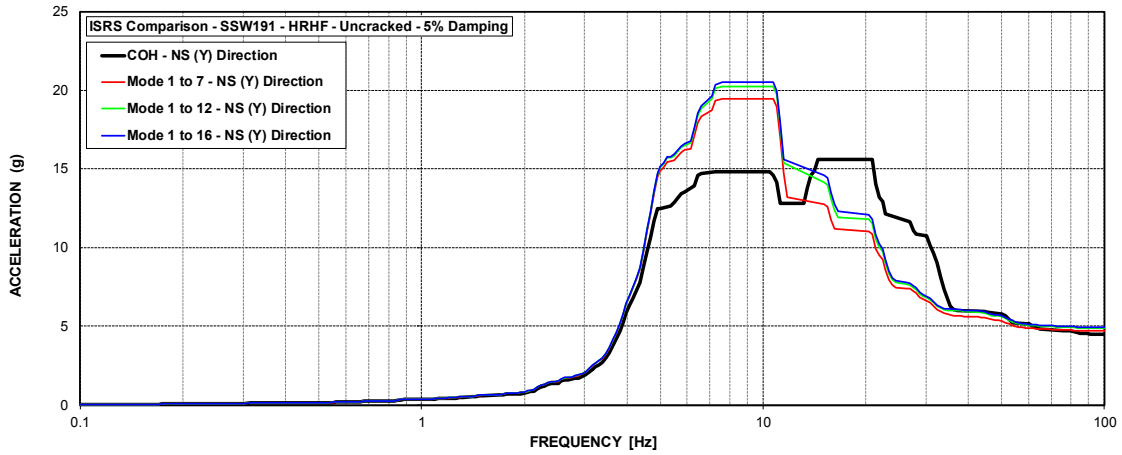

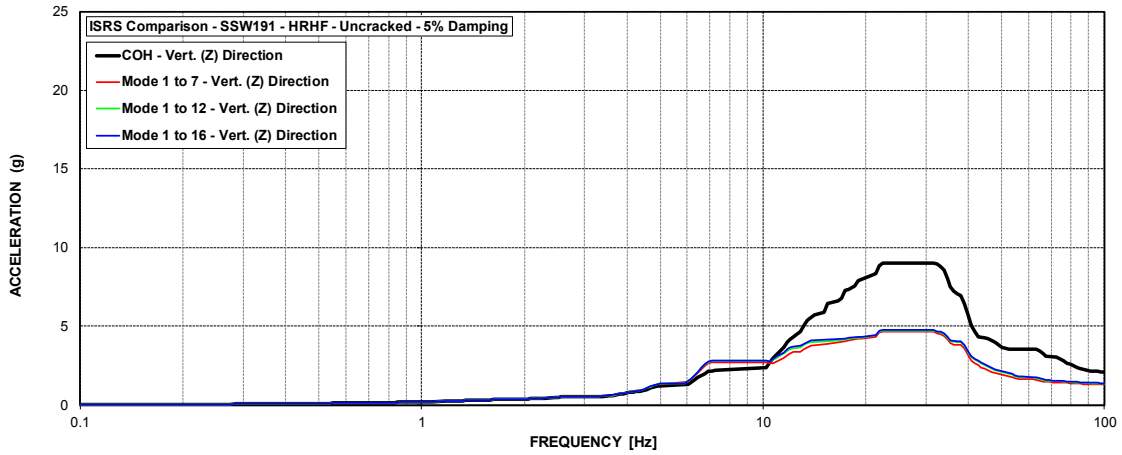

Figure 60 ISRS – Secondary Shield Wall (SSW191) at El. 191’ – HRHF – Uncracked

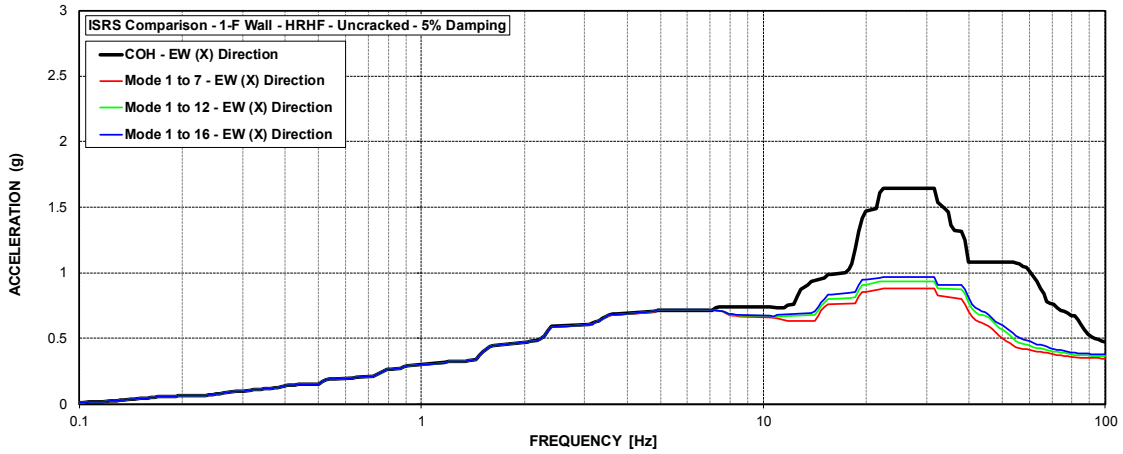

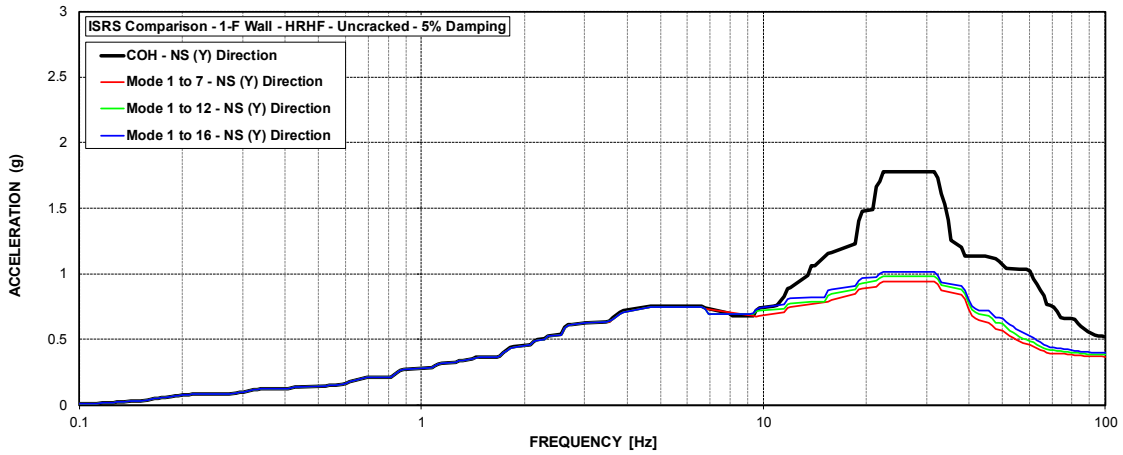

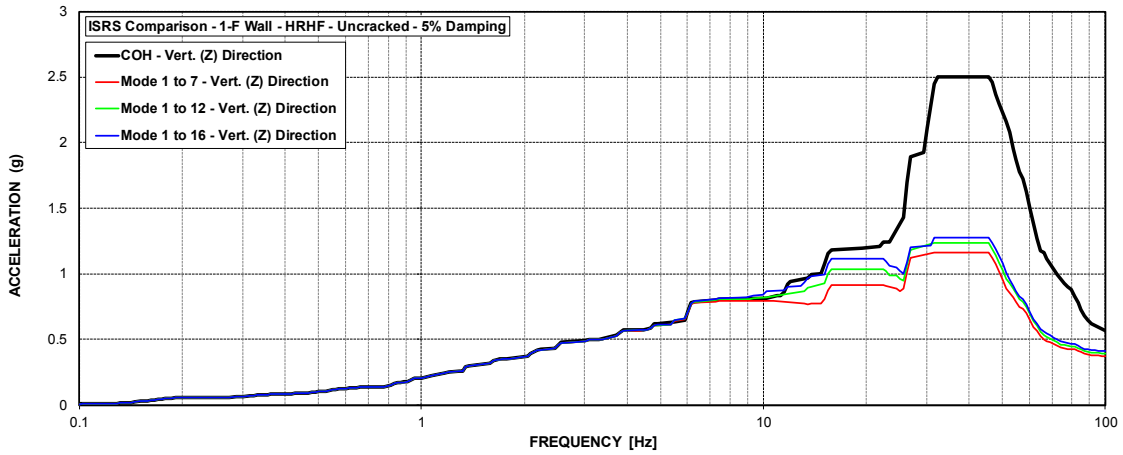

Figure 61 ISRS – AB Shear Walls (1-F) at El. 55’ – HRHF – Uncracked

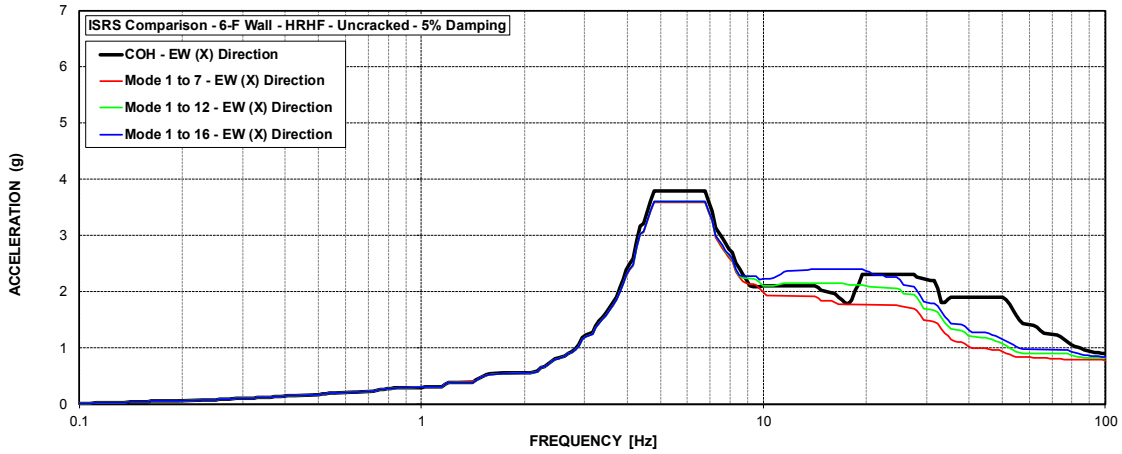

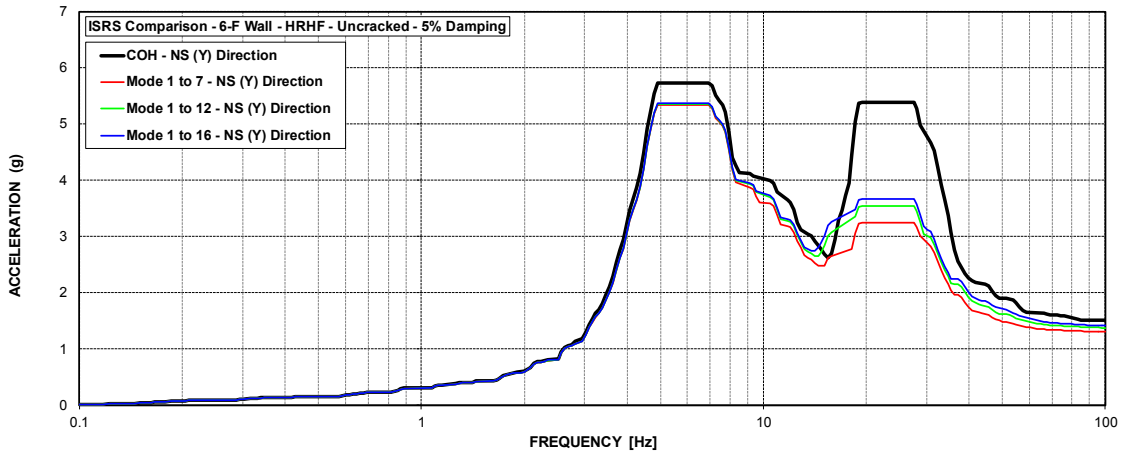

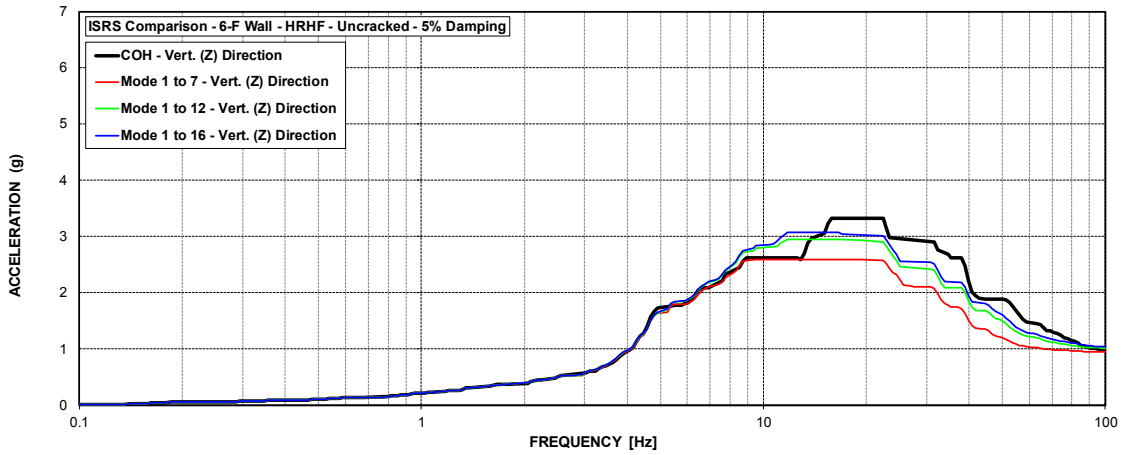

Figure 62 ISRS – AB Shear Walls (6-F) at El. 156’ – HRHF – Uncracked

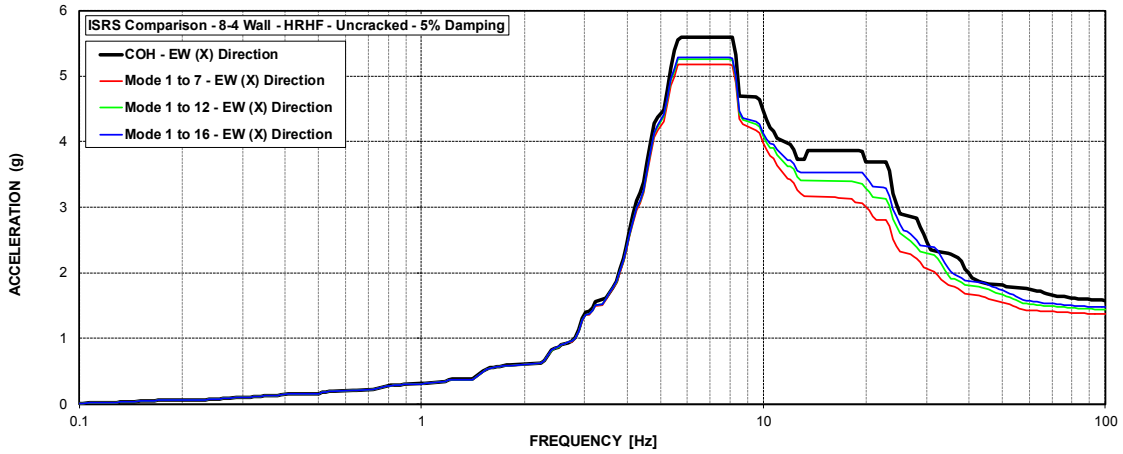

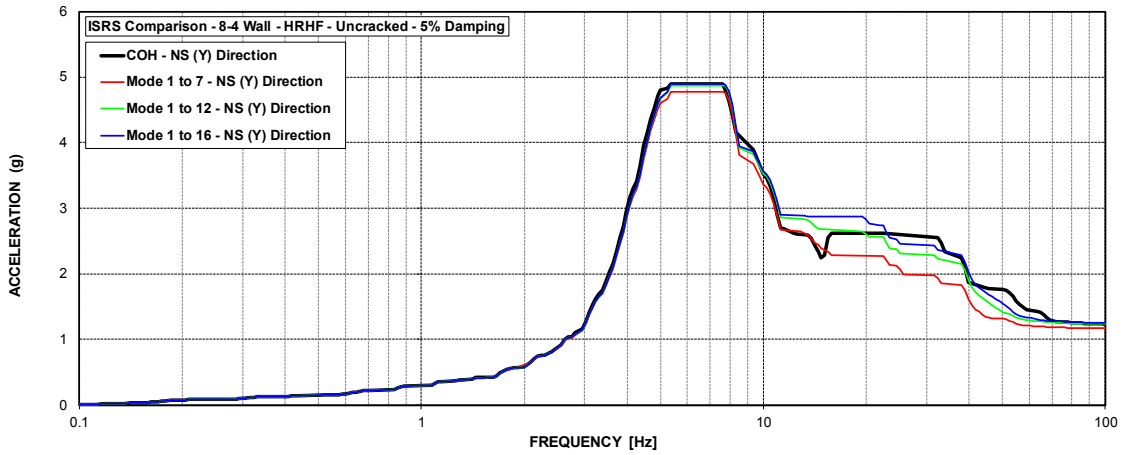

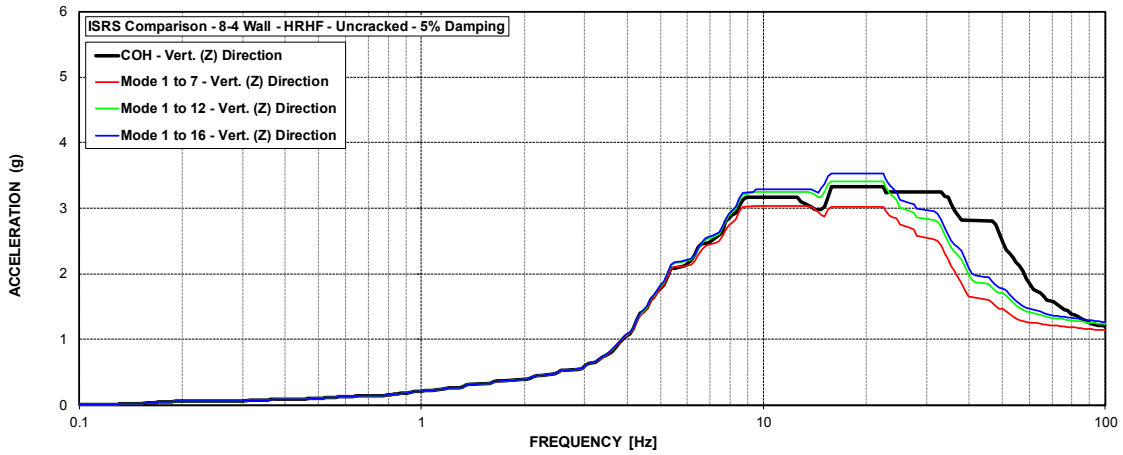

Figure 63 ISRS – AB Shear Walls (8-4) at El. 213.5’ – HRHF – Uncracked

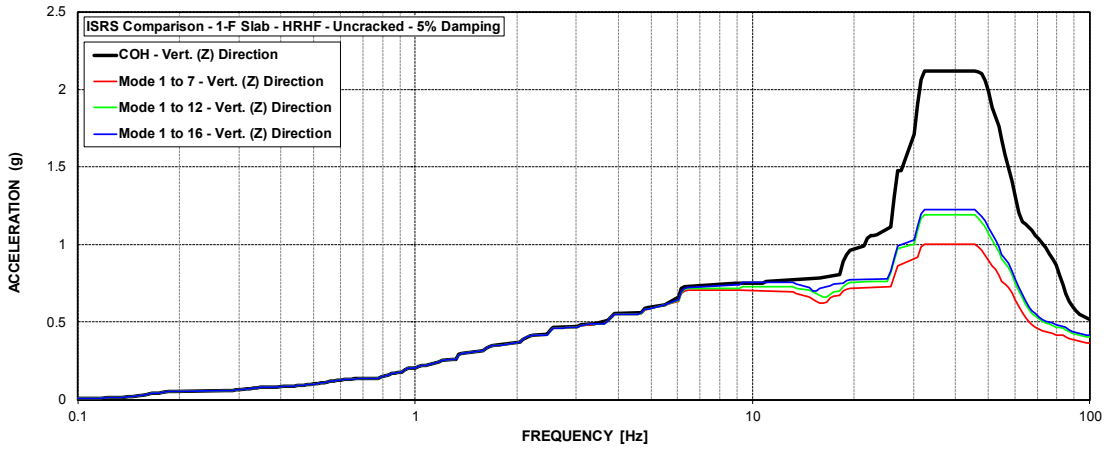

Figure 64 ISRS – AB Floor Slabs (1-F) at El. 55’ – HRHF – Uncracked

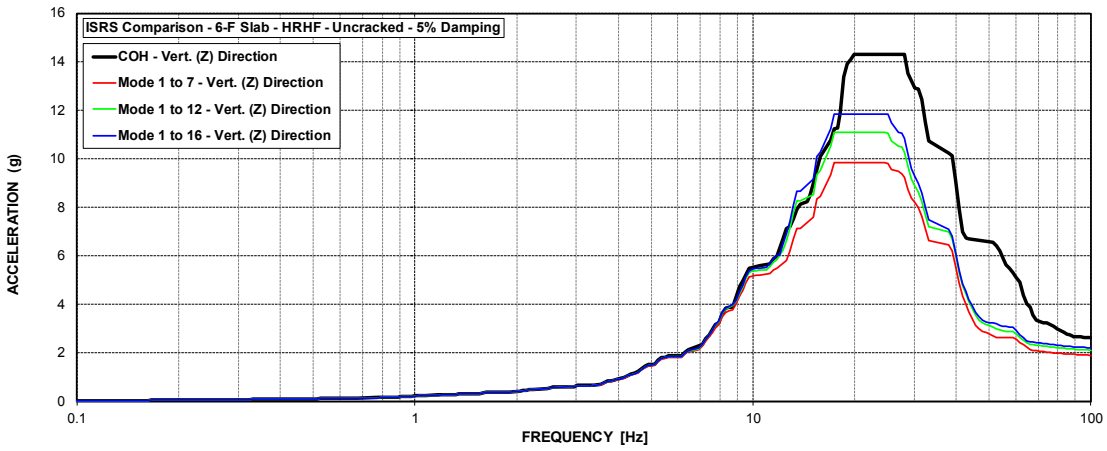

Figure 65 ISRS – AB Floor Slabs (6-F) at El. 156’ – HRHF – Uncracked

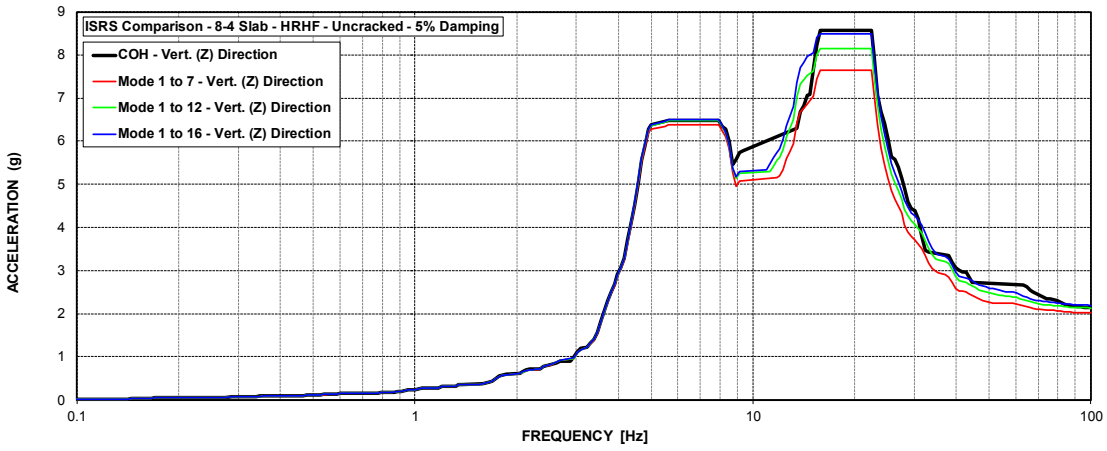

Figure 66 ISRS – AB Floor Slabs (8-4) at El. 213.5’ – HRHF – Uncracked

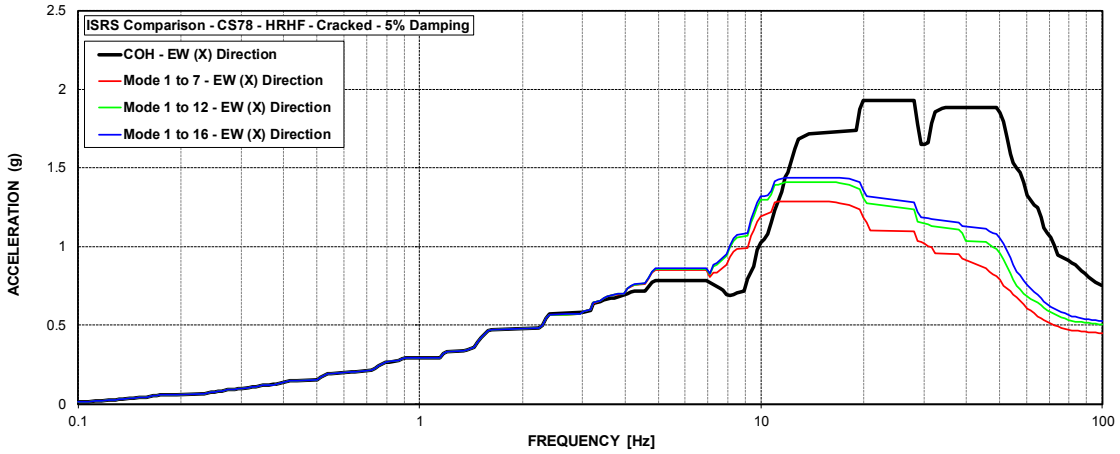

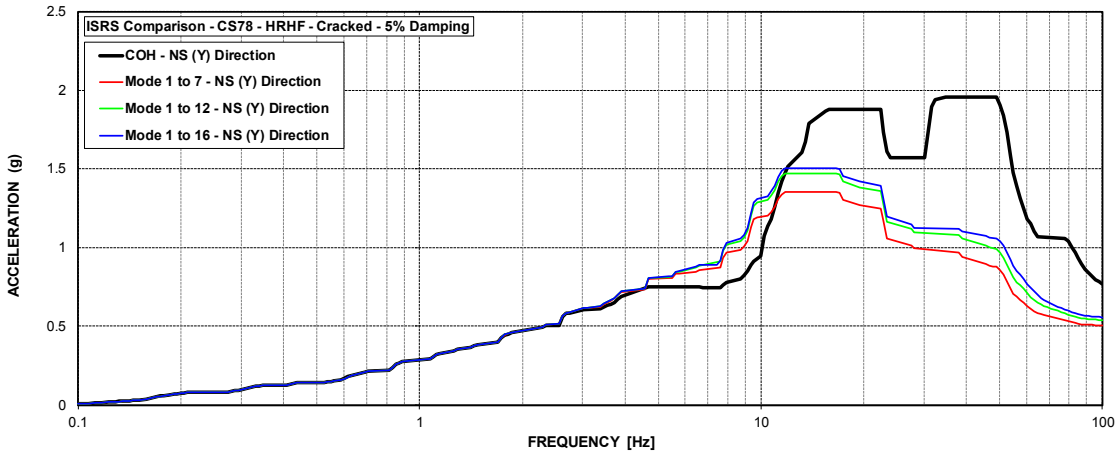

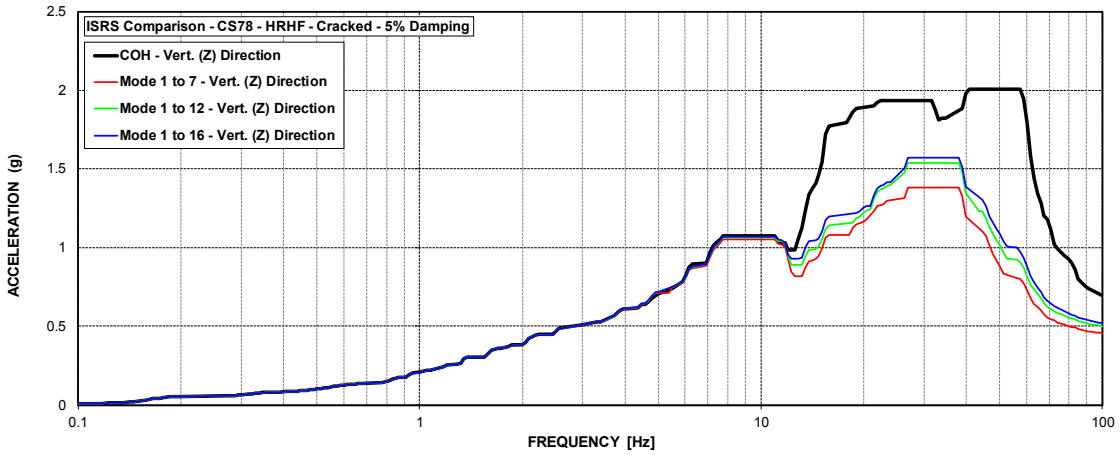

Figure 67 ISRS – Containment Structure (CS78) at El. 78’ – HRHF – Cracked

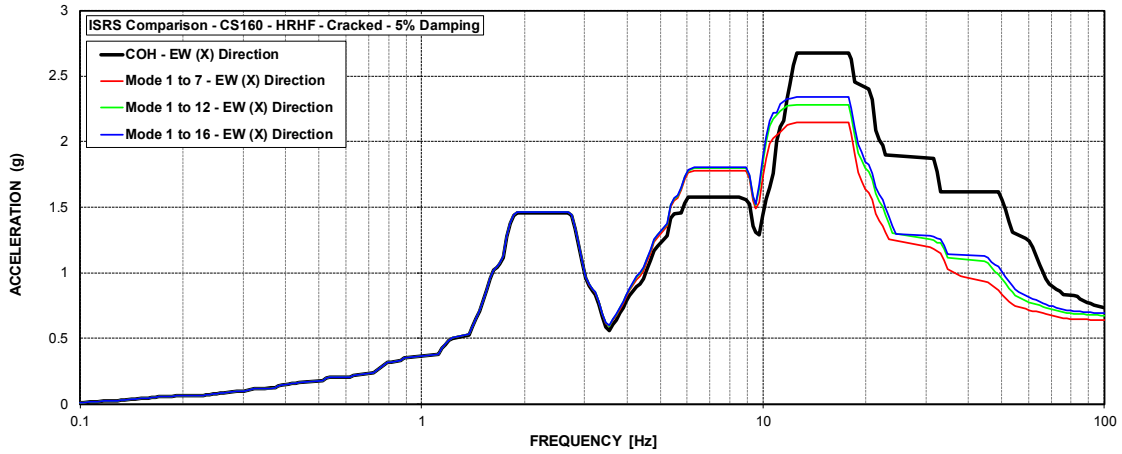

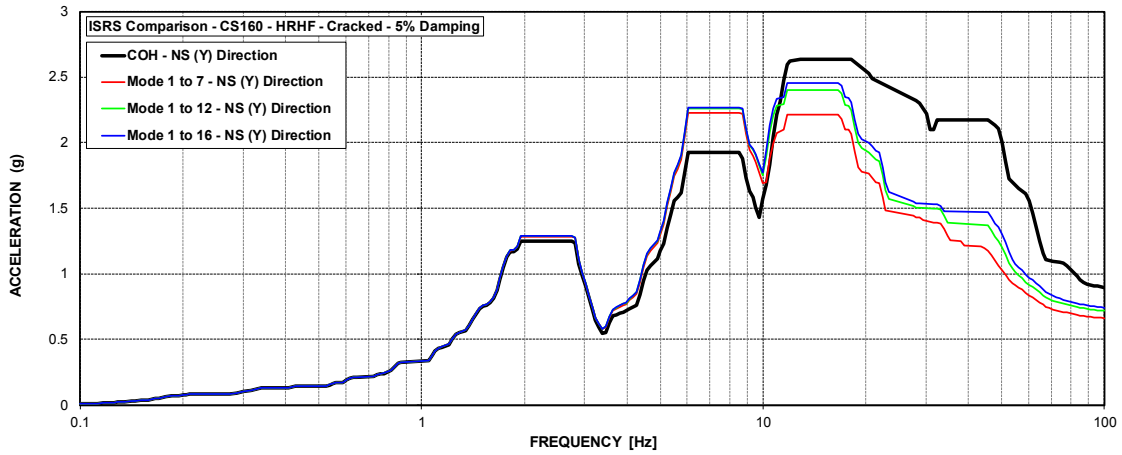

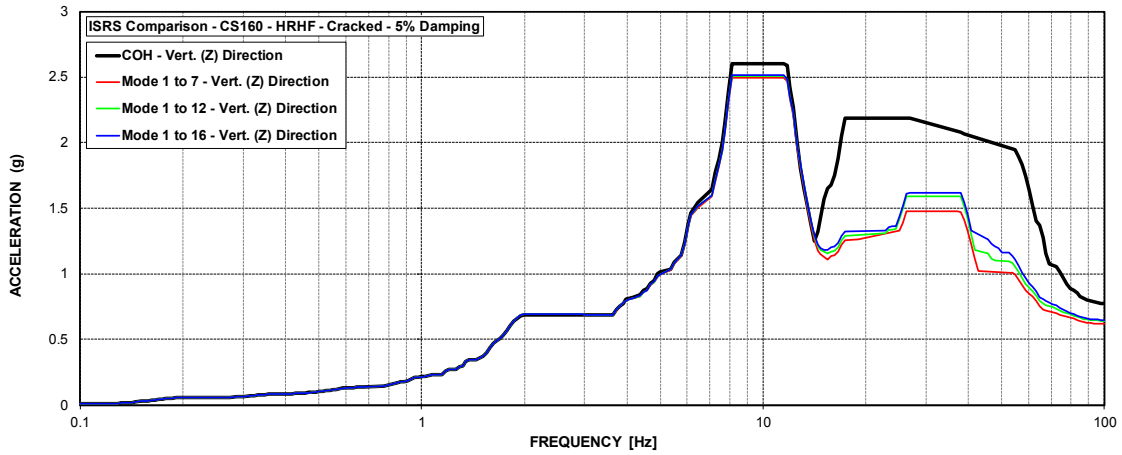

Figure 68 ISRS – Containment Structure (CS160) at El. 160’ – HRHF – Cracked

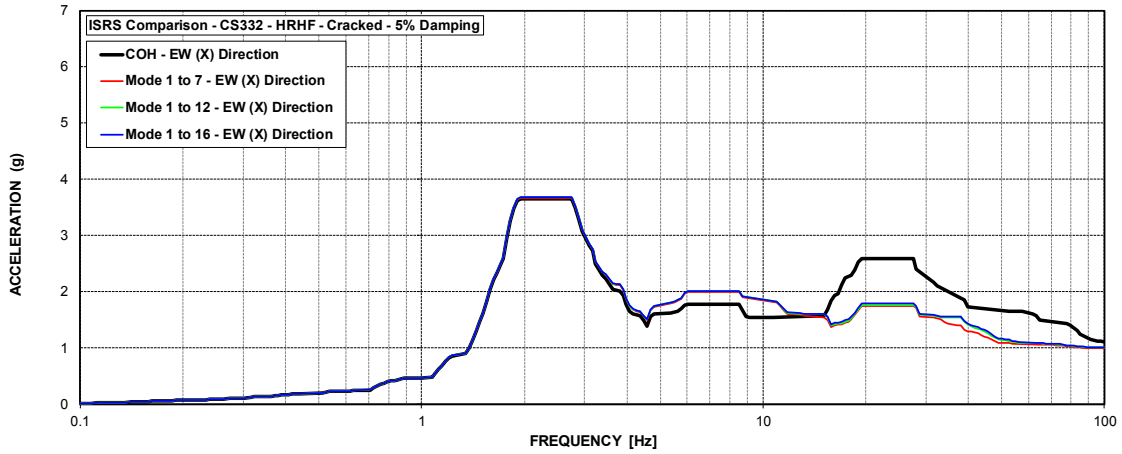

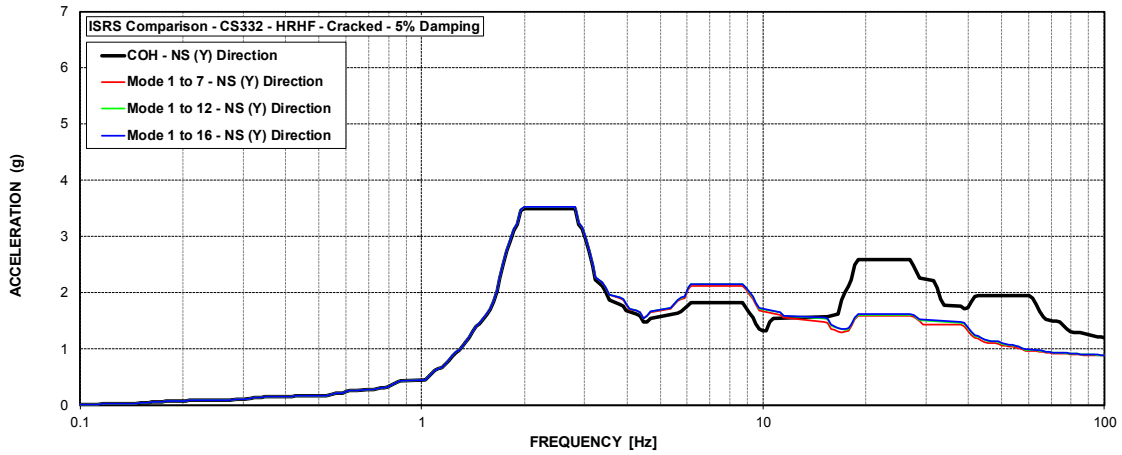

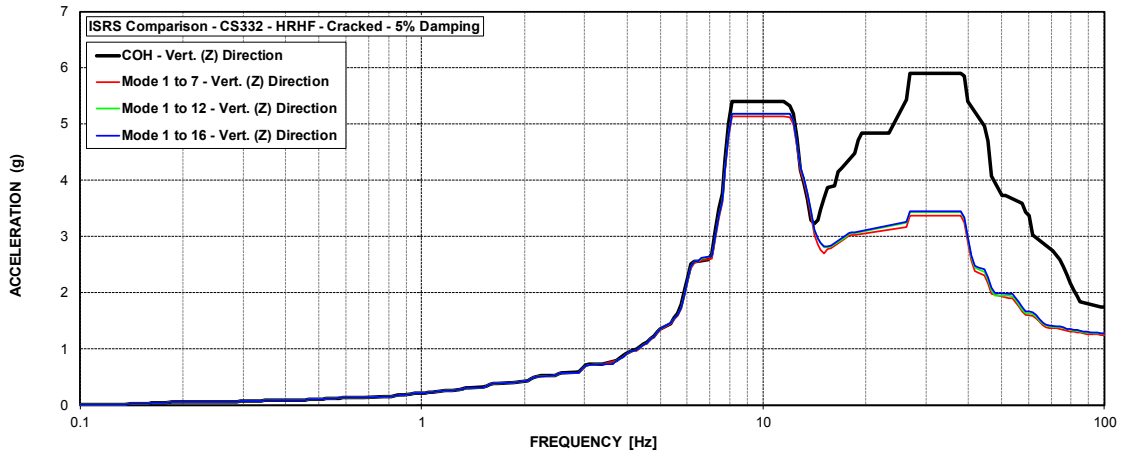

Figure 69 ISRS – Containment Structure (CS332) at El. 332’ – HRHF – Cracked

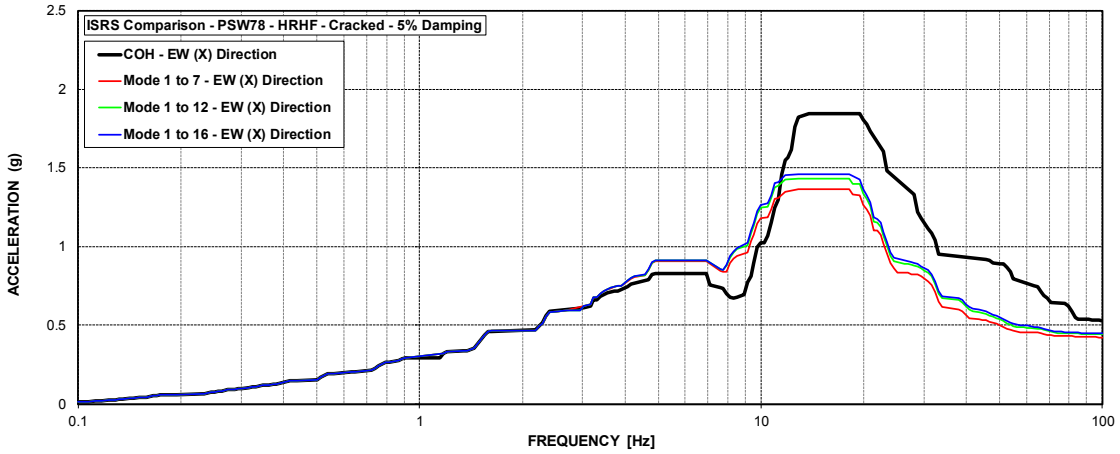

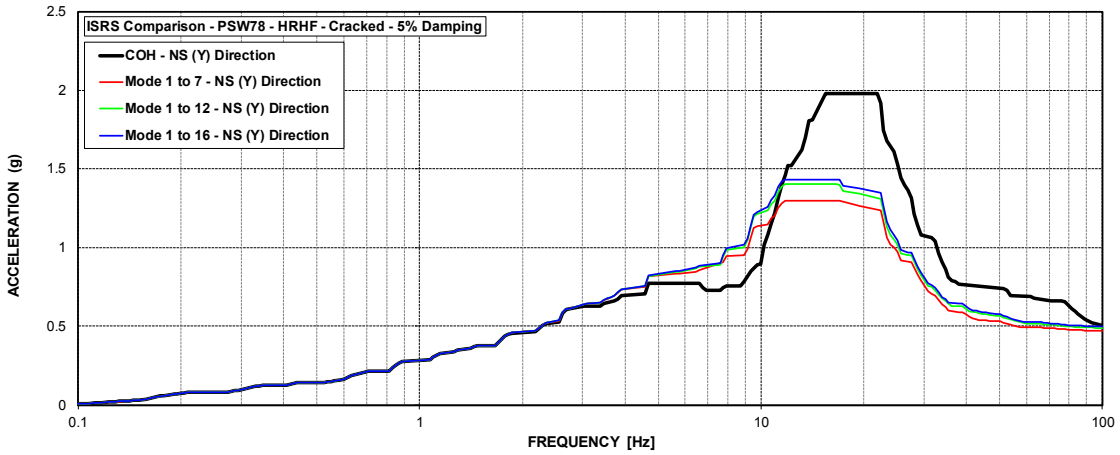

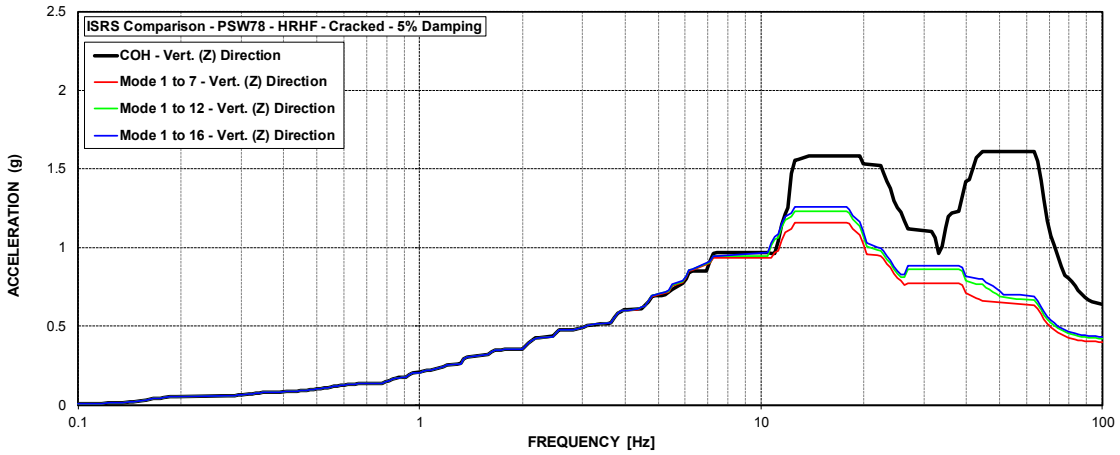

Figure 70 ISRS – Primary Shield Wall (PSW78) at El. 78’ – HRHF – Cracked

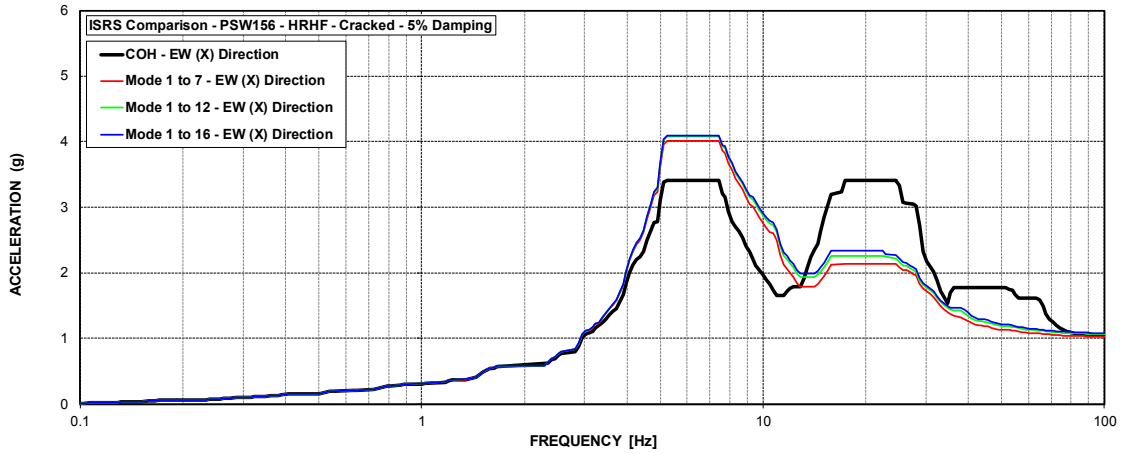

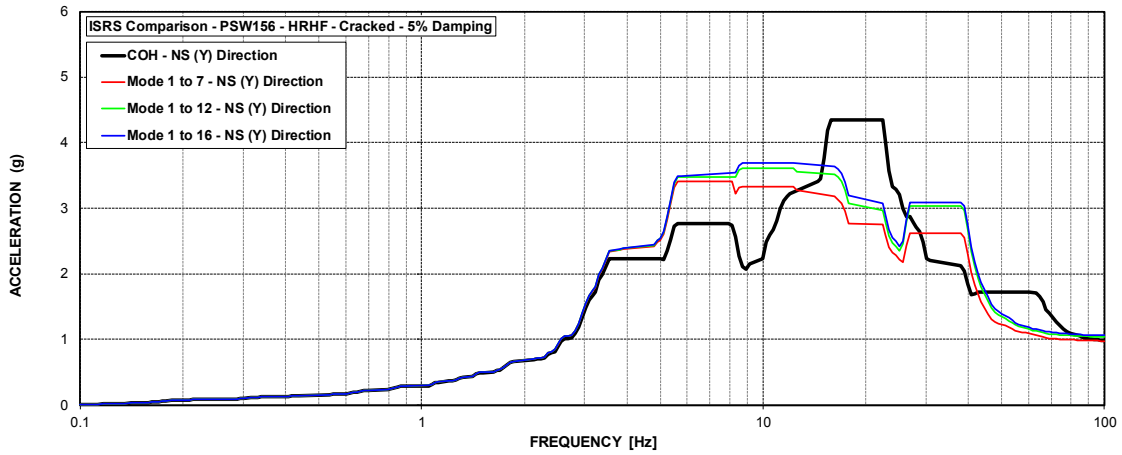

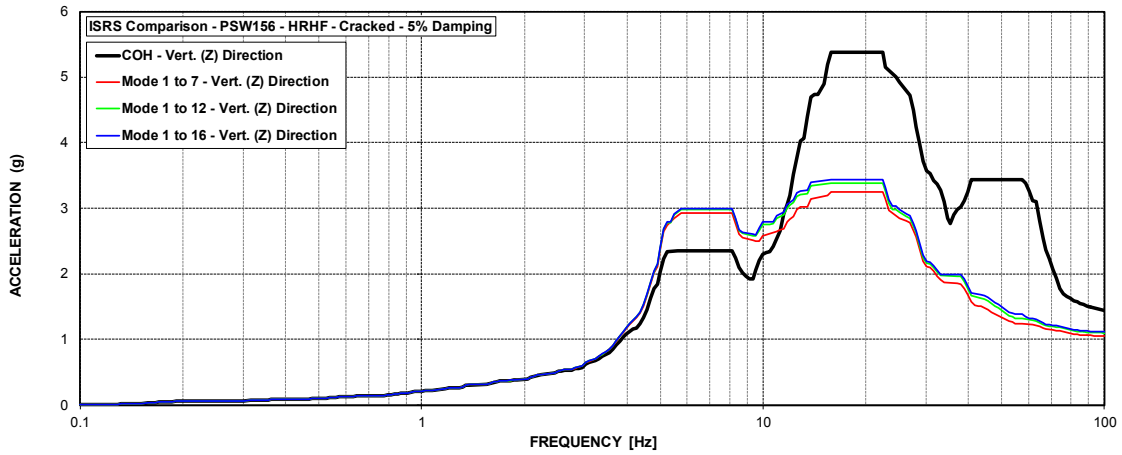

Figure 71 ISRS – Primary Shield Wall (PSW156) at El. 156’ – HRHF – Cracked

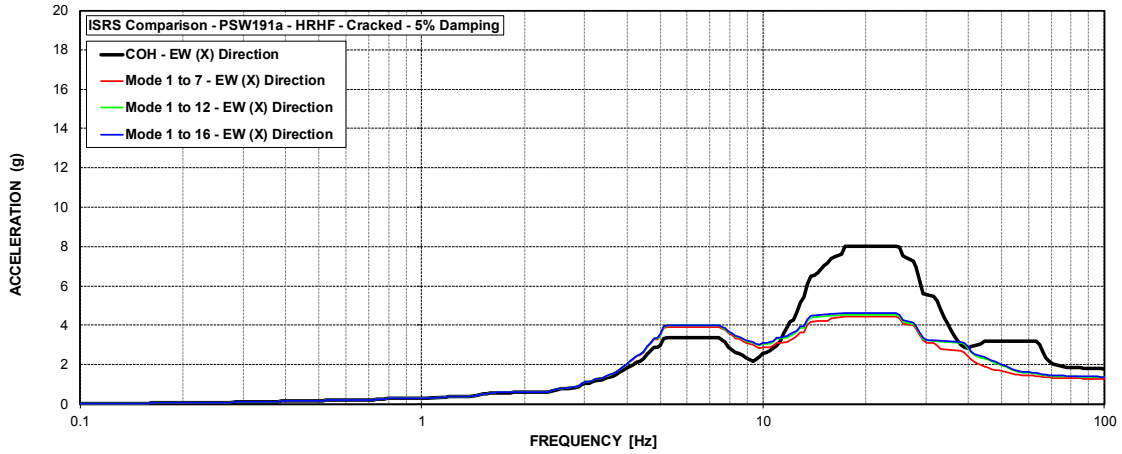

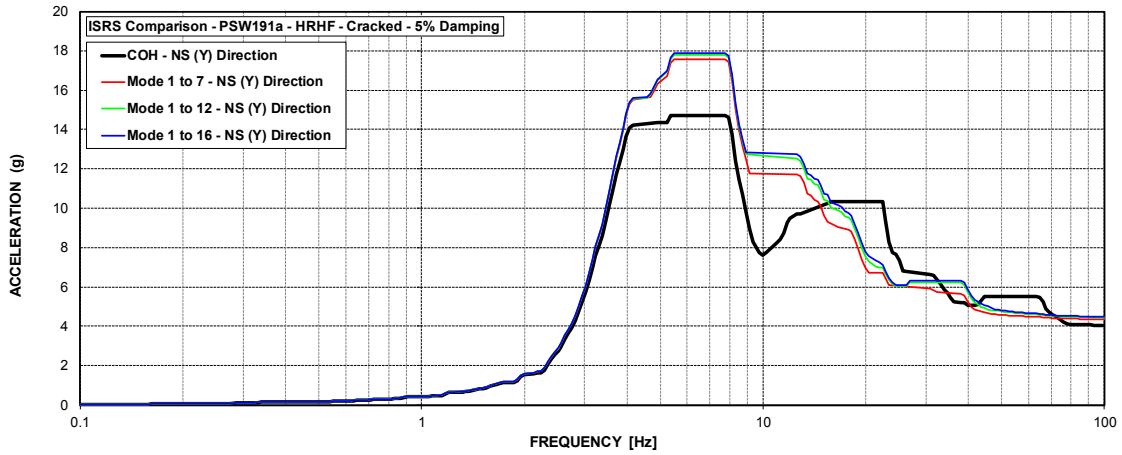

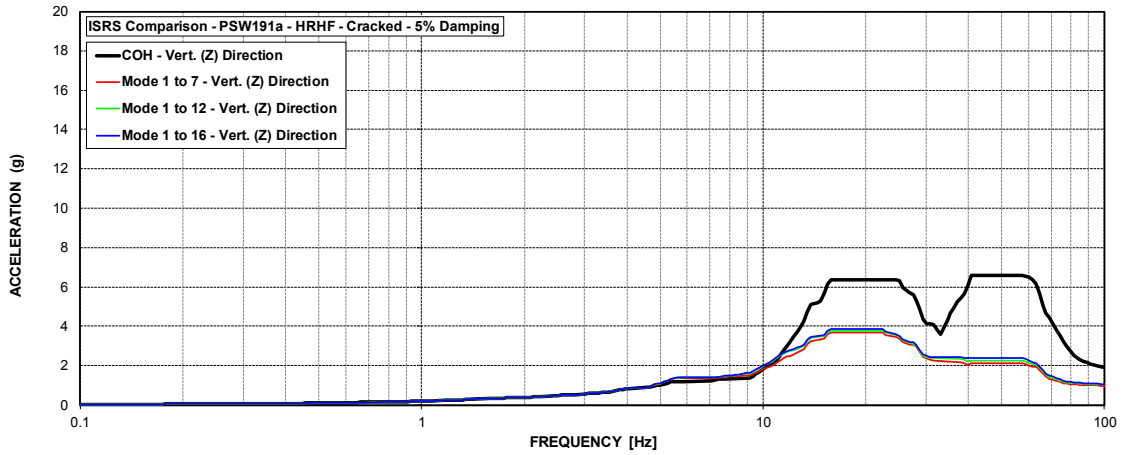

Figure 72 ISRS – Primary Shield Wall (PSW191a) at El. 191’ – HRHF – Cracked

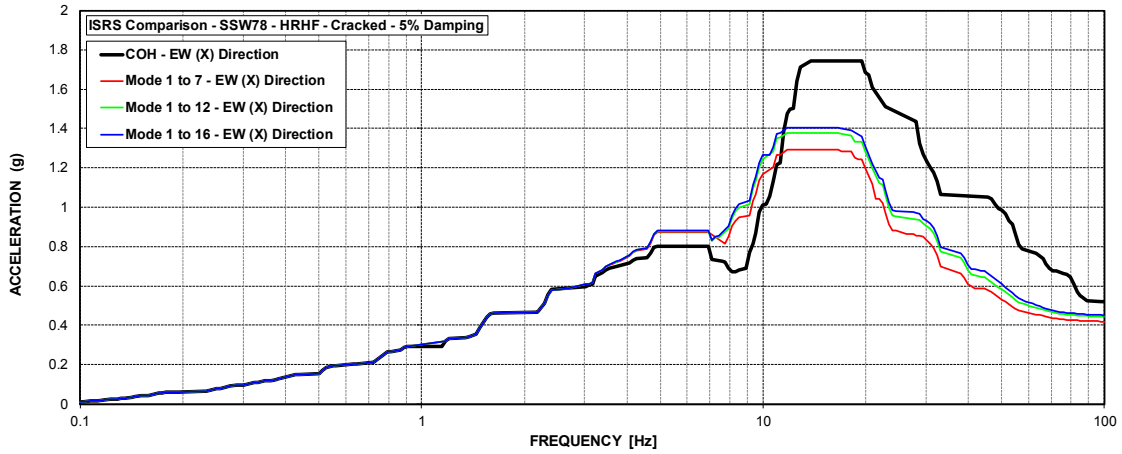

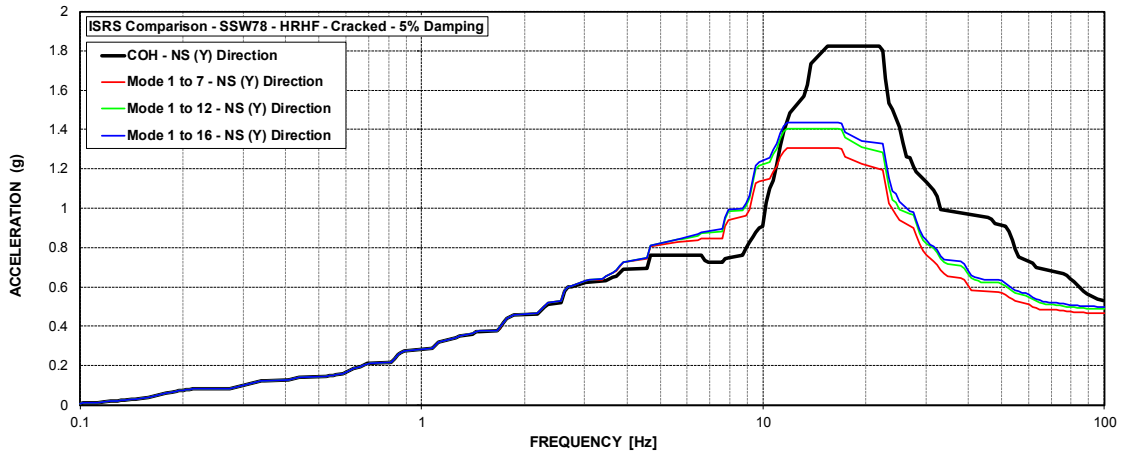

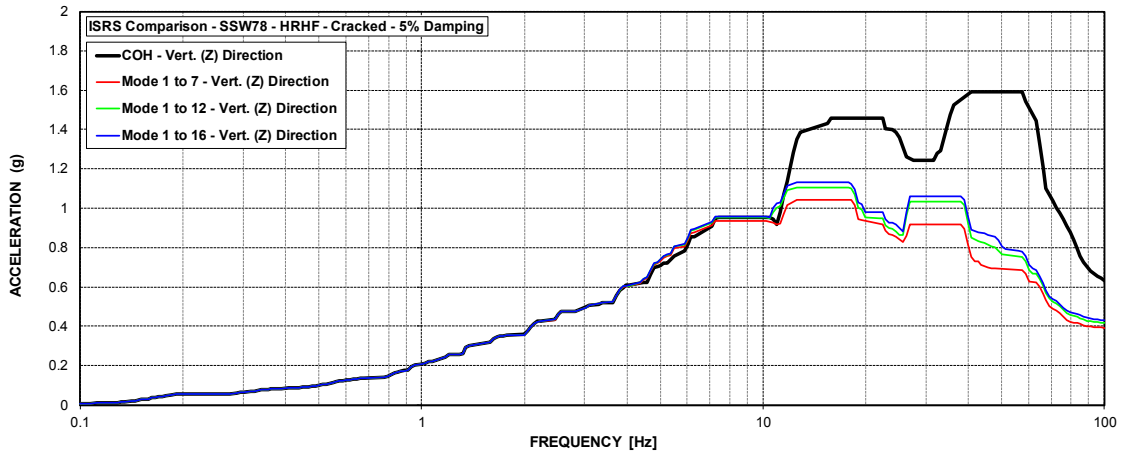

Figure 73 ISRS – Secondary Shield Wall (SSW78) at El. 78’ – HRHF – Cracked

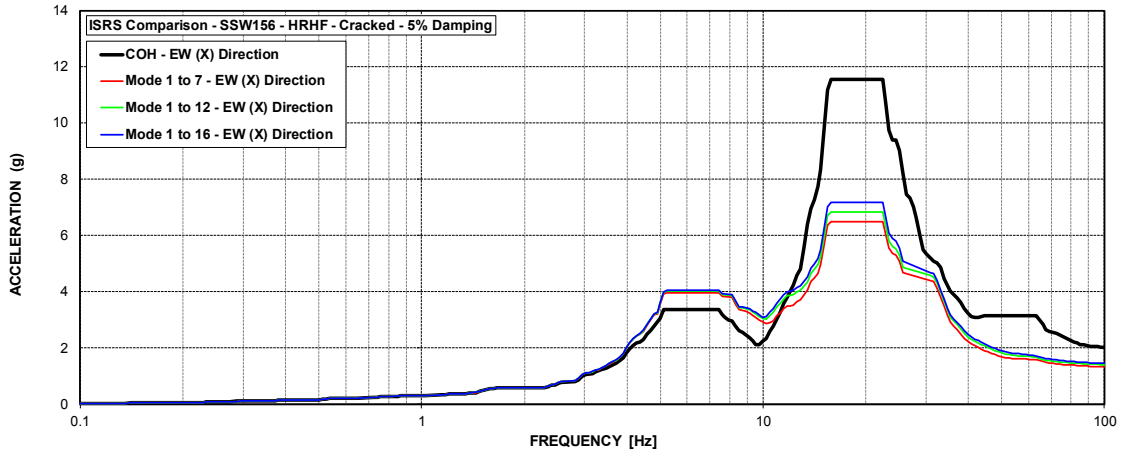

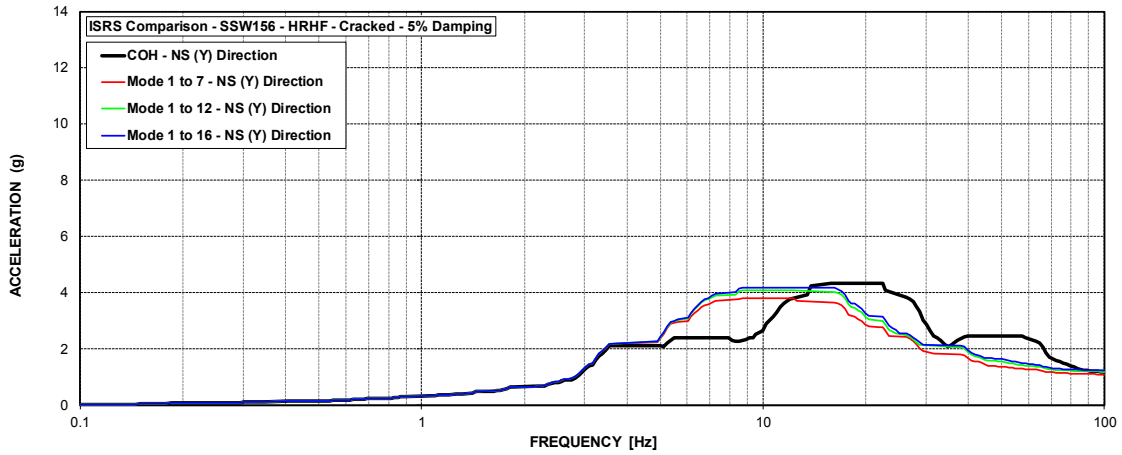

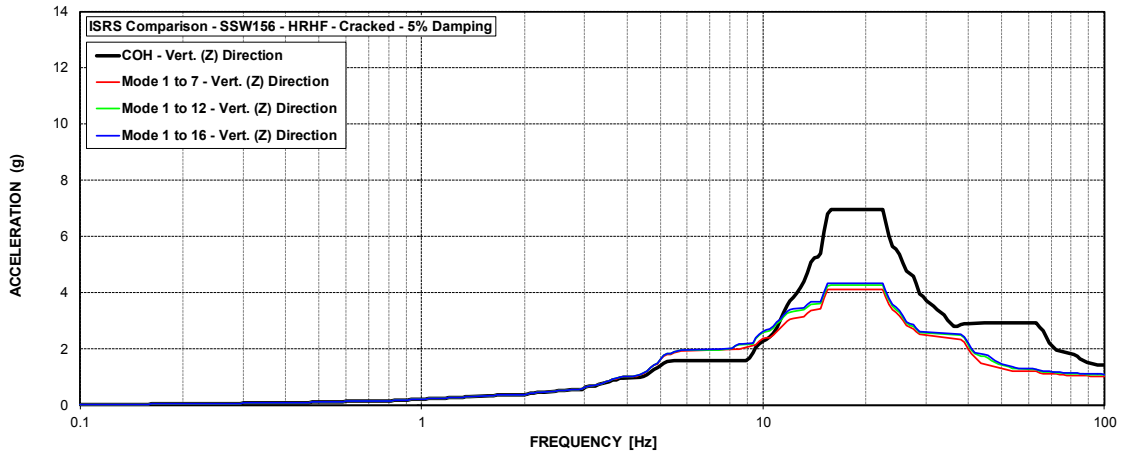

Figure 74 ISRS – Secondary Shield Wall (SSW156) at El. 156’ – HRHF – Cracked

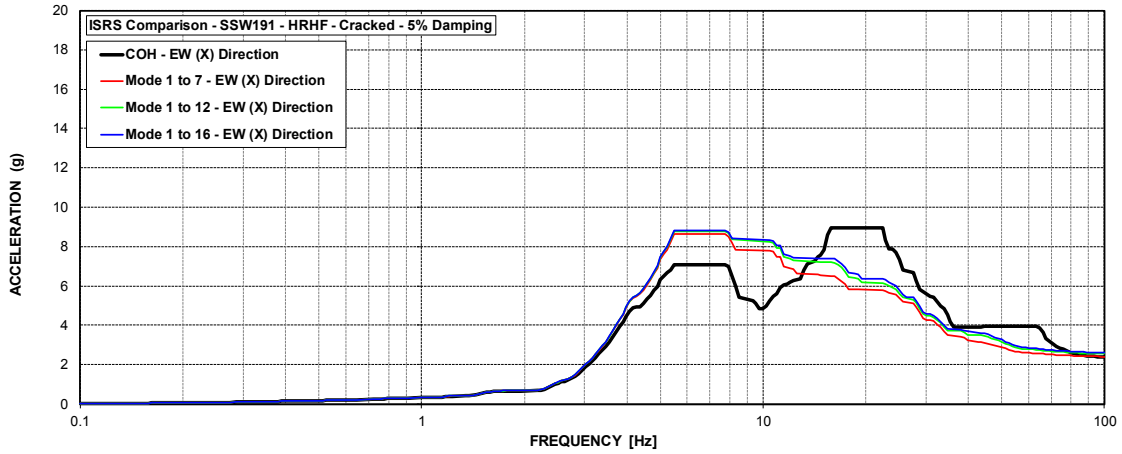

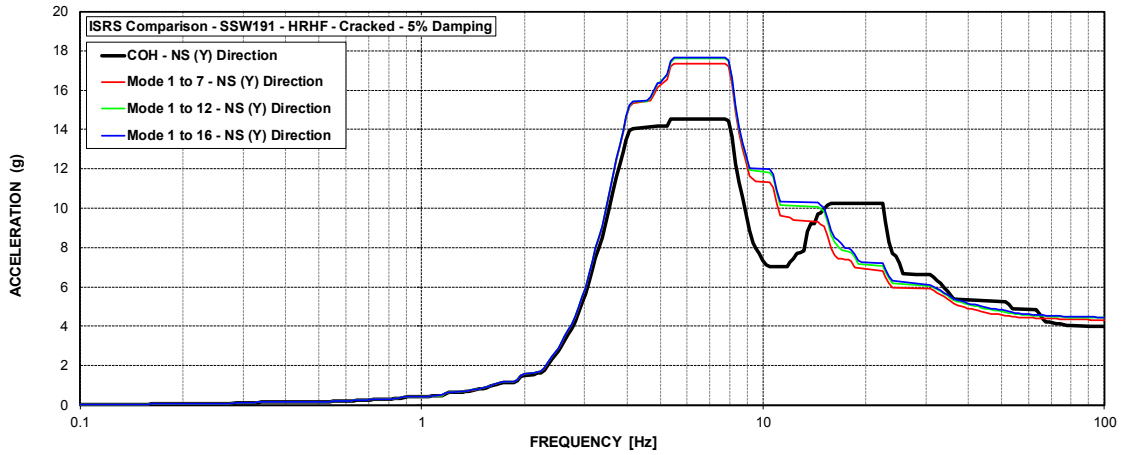

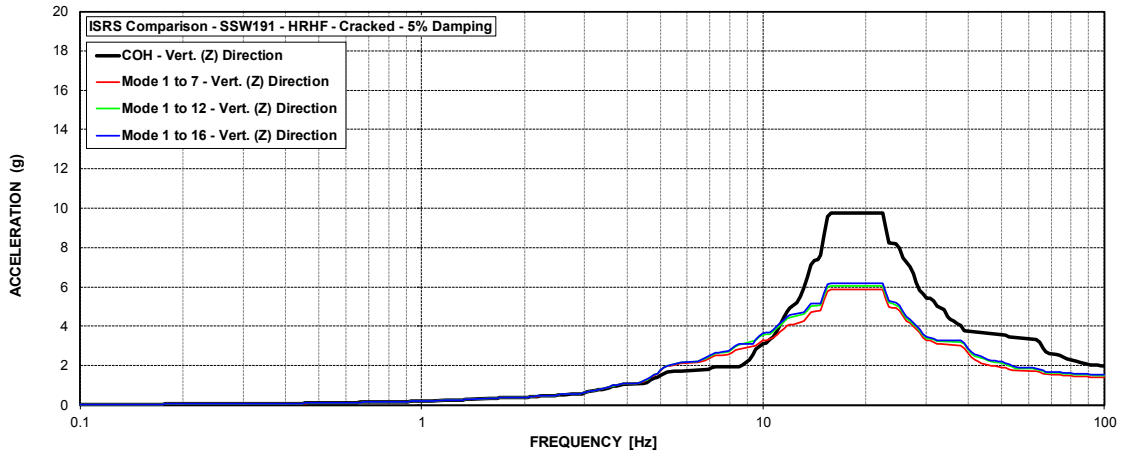

Figure 75 ISRS – Secondary Shield Wall (SSW191) at El. 191’ – HRHF – Cracked

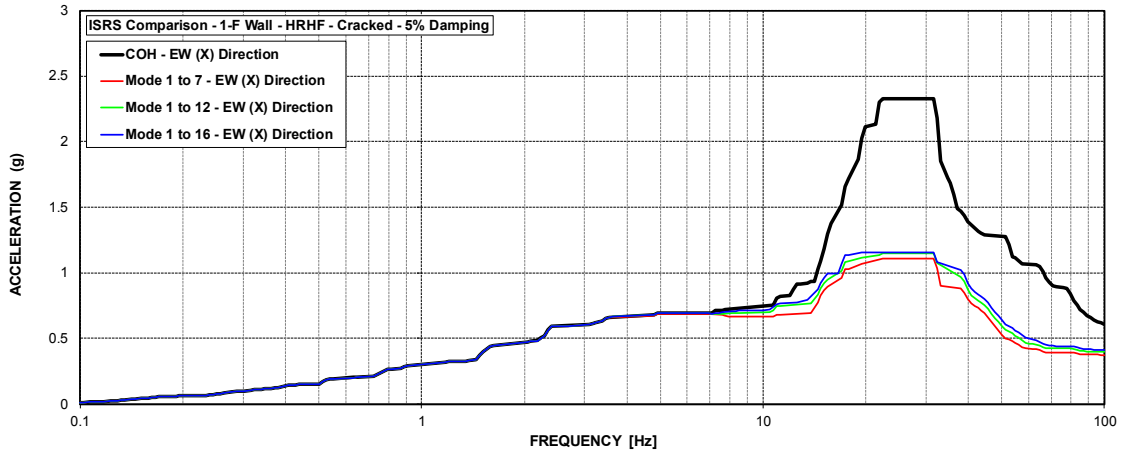

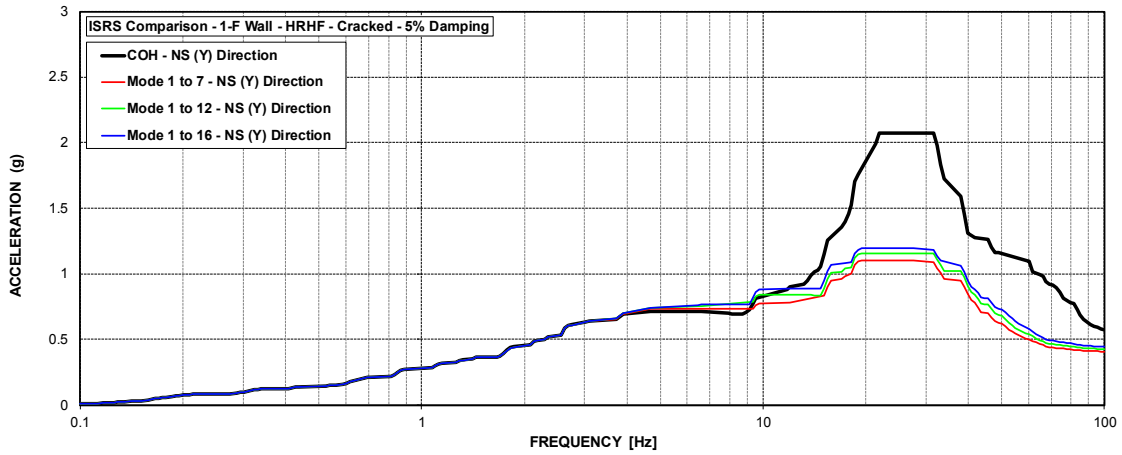

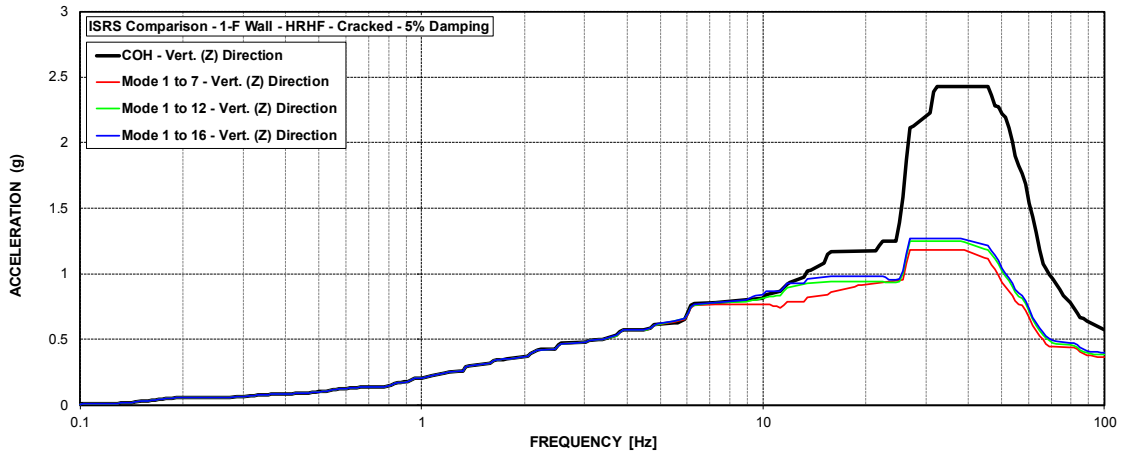

Figure 76 ISRS – AB Shear Walls (1-F) at El. 55’ – HRHF – Cracked

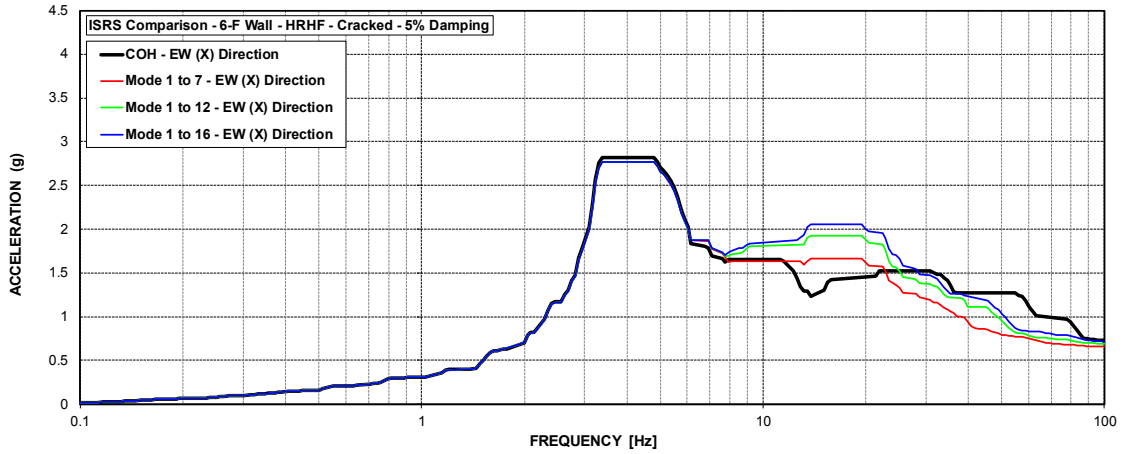

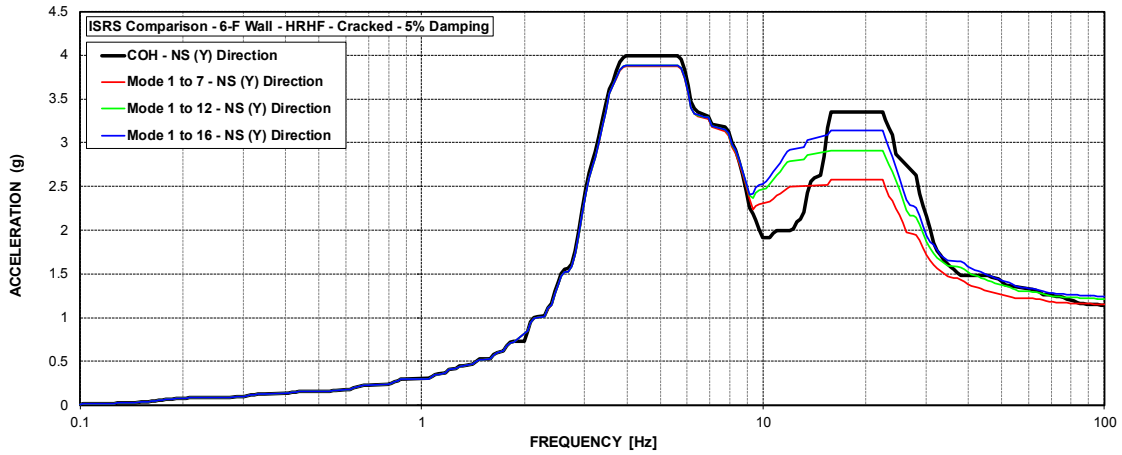

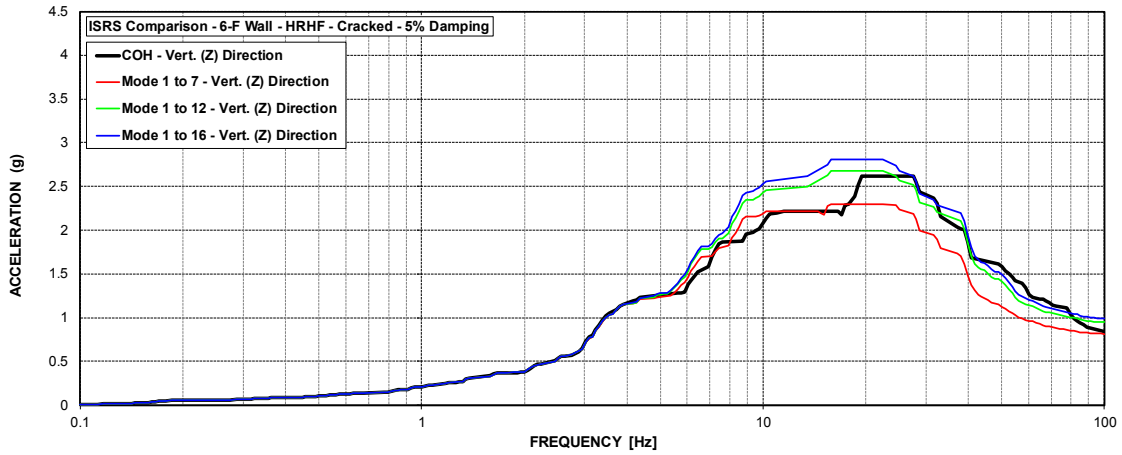

Figure 77 ISRS – AB Shear Walls (6-F) at El. 156’ – HRHF – Cracked

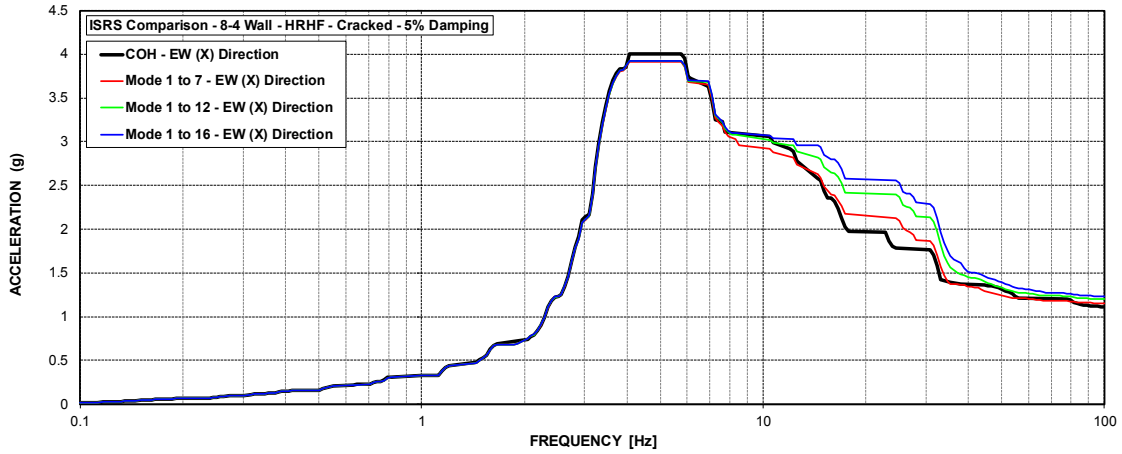

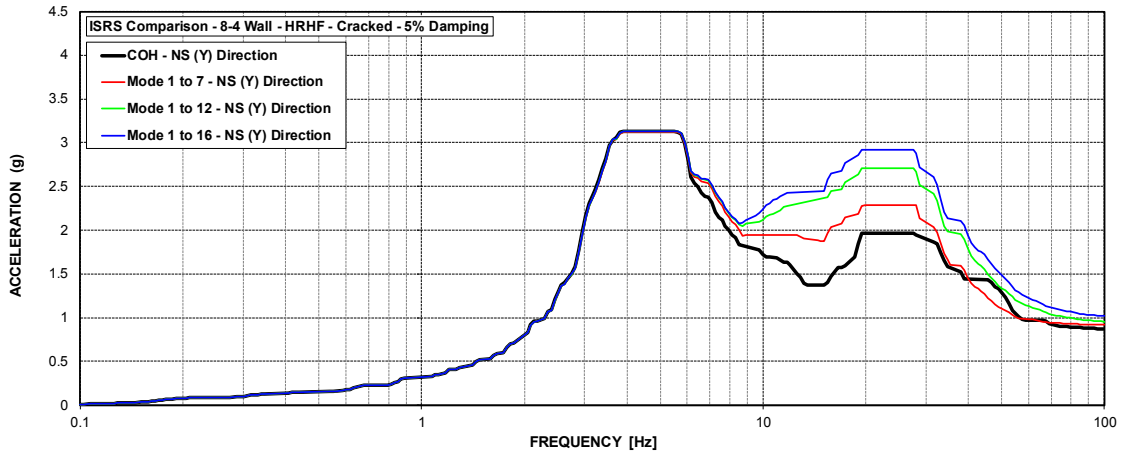

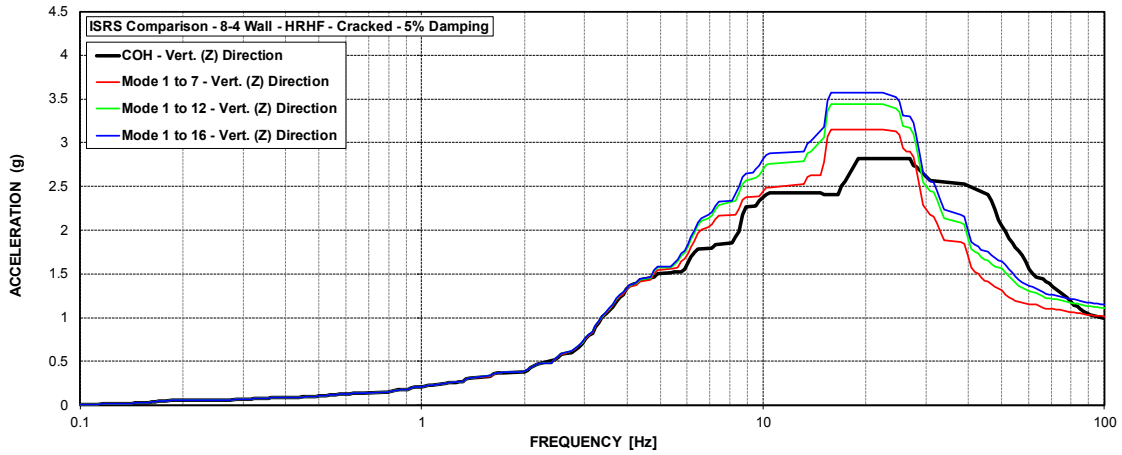

Figure 78 ISRS – AB Shear Walls (8-4) at El. 213.5’ – HRHF – Cracked

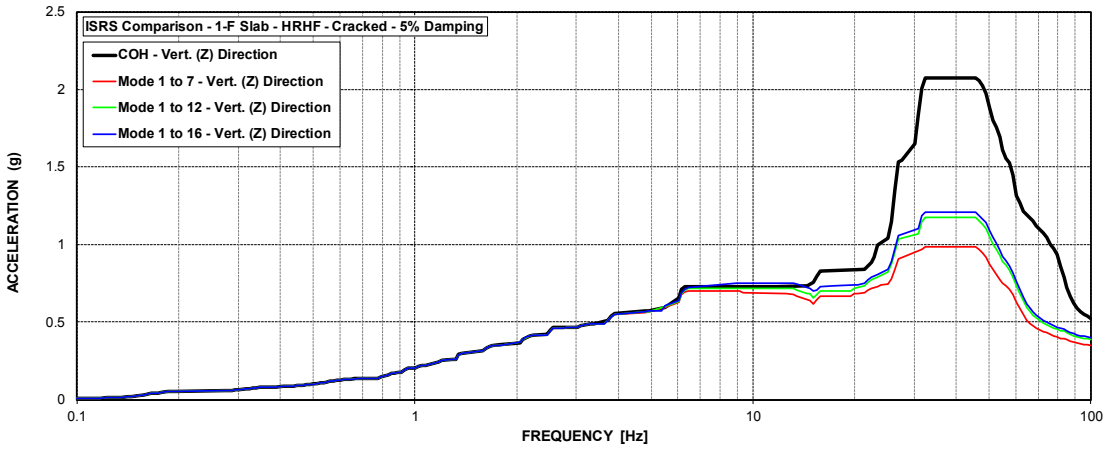

Figure 79 ISRS – AB Floor Slabs (1-F) at El. 55’ – HRHF – Cracked

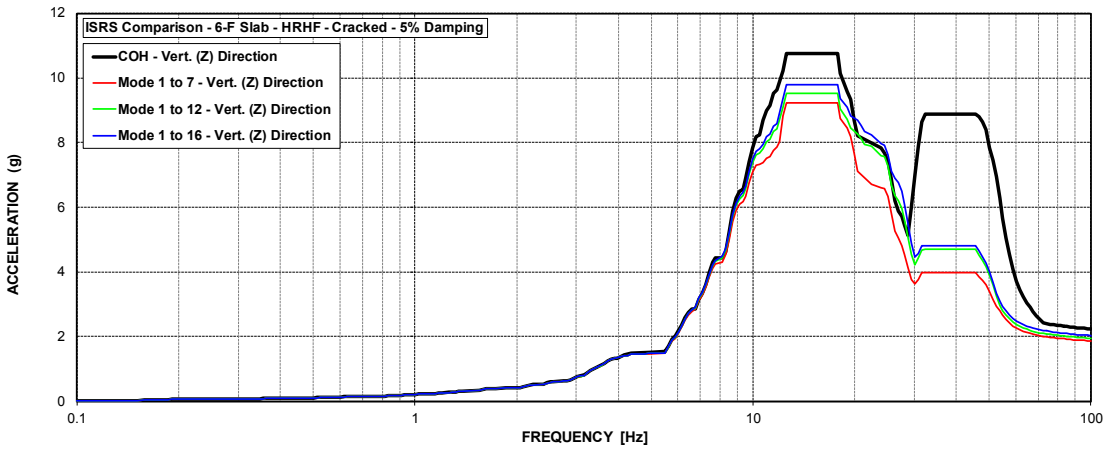

Figure 80 ISRS – AB Floor Slabs (6-F) at El. 156’ – HRHF – Cracked

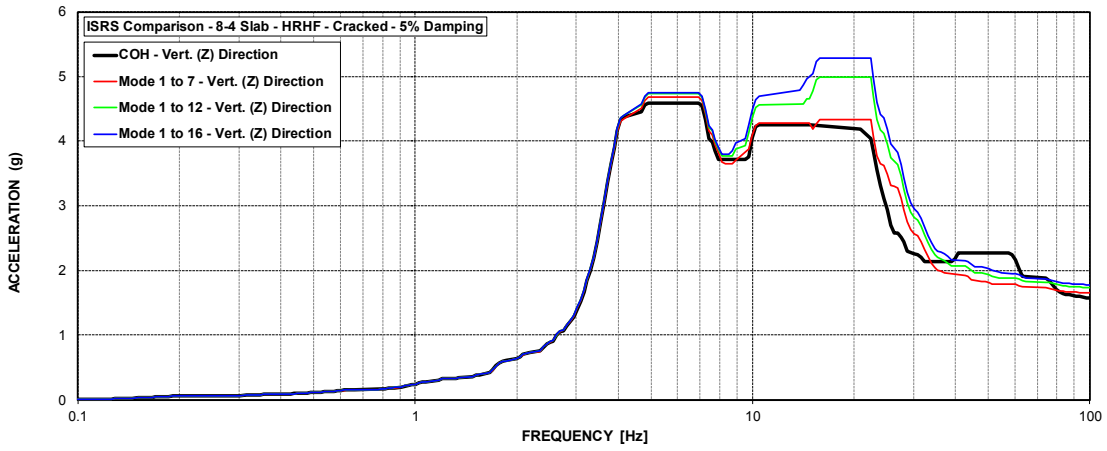

Figure 81 ISRS – AB Floor Slabs (8-4) at El. 213.5’ – HRHF – Cracked

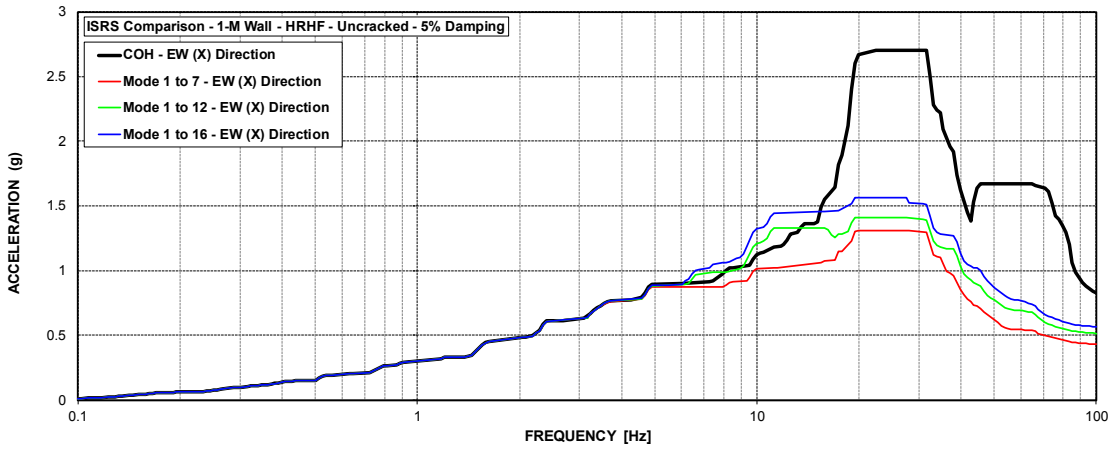

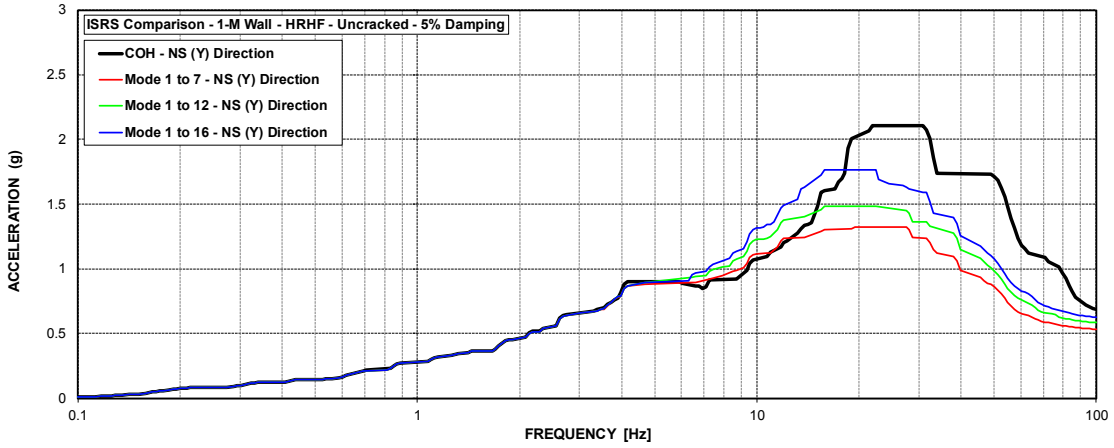

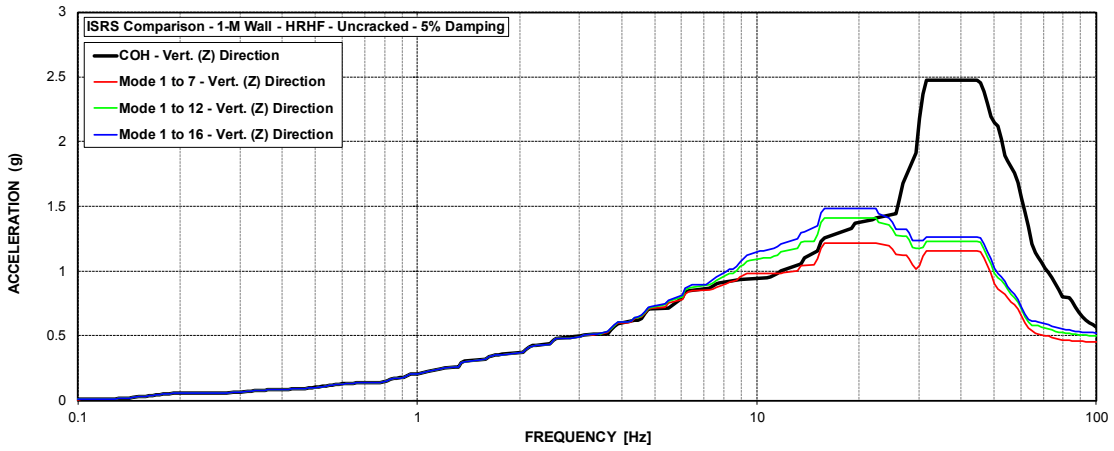

Figure 82 ISRS – AB Shear Walls (1-M) at El. 68’ – HRHF – Uncracked

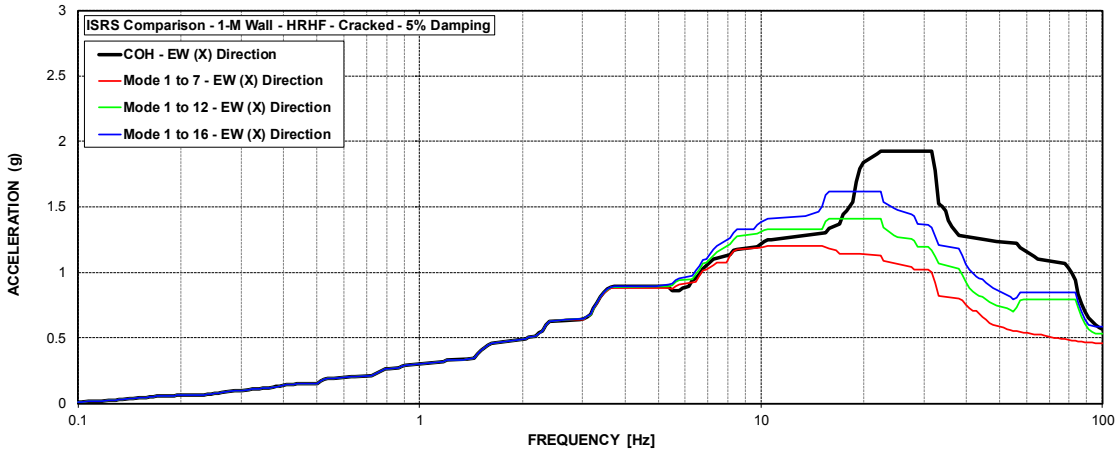

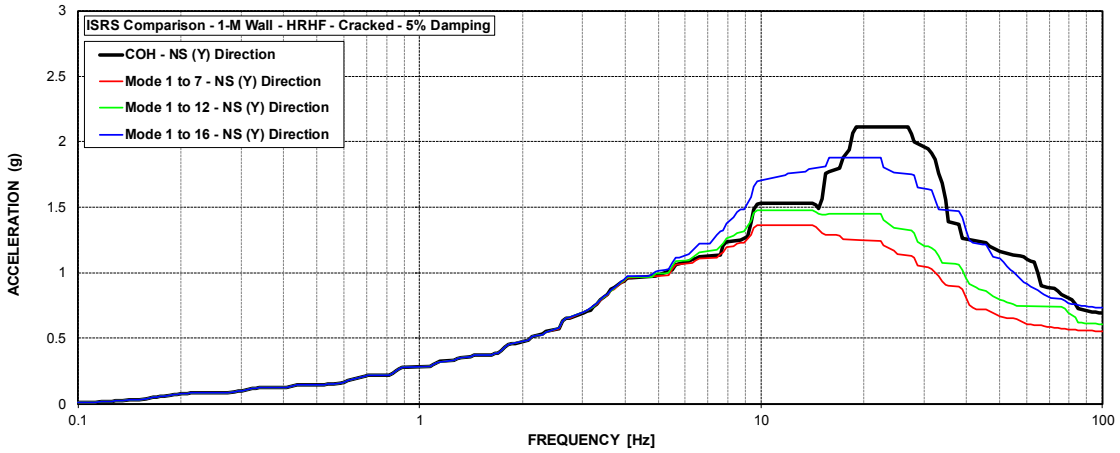

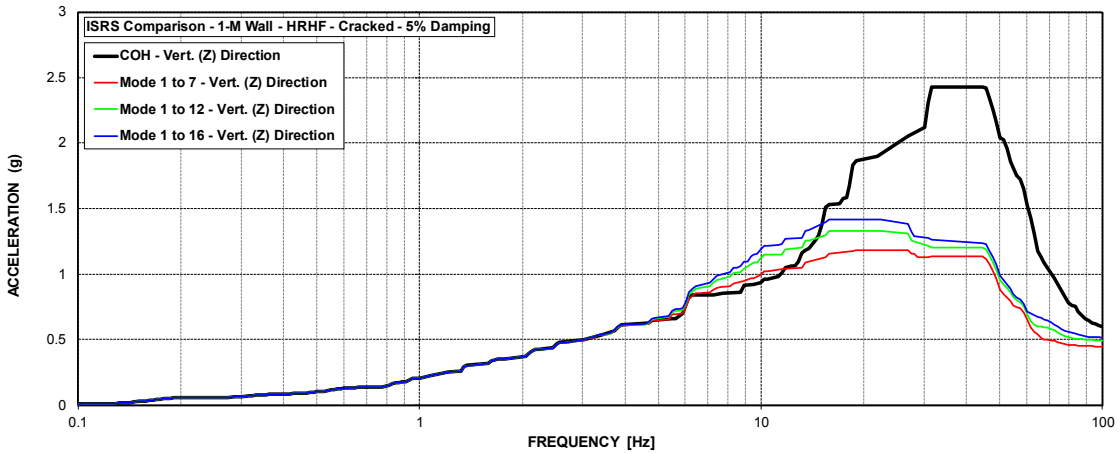

Figure 83 ISRS – AB Shear Walls (1-M) at El. 68’ – HRHF – Cracked

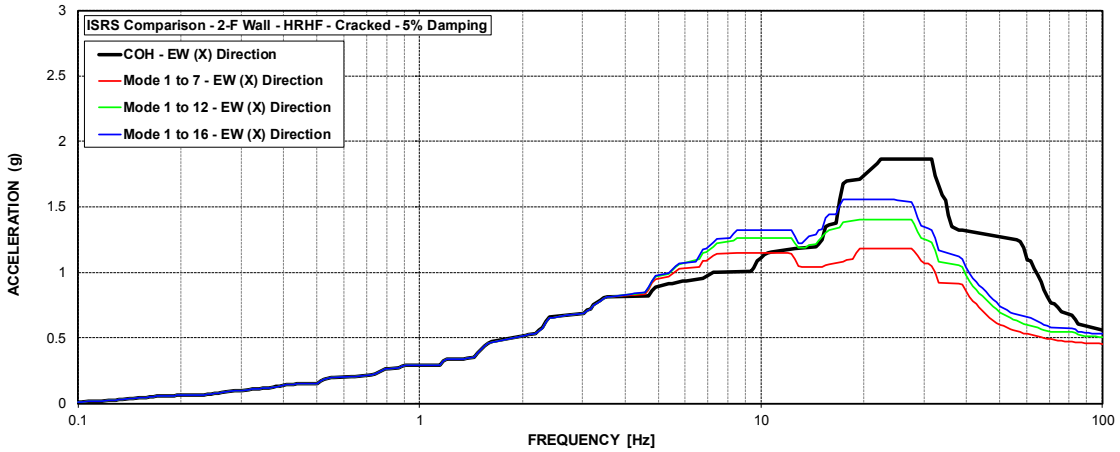

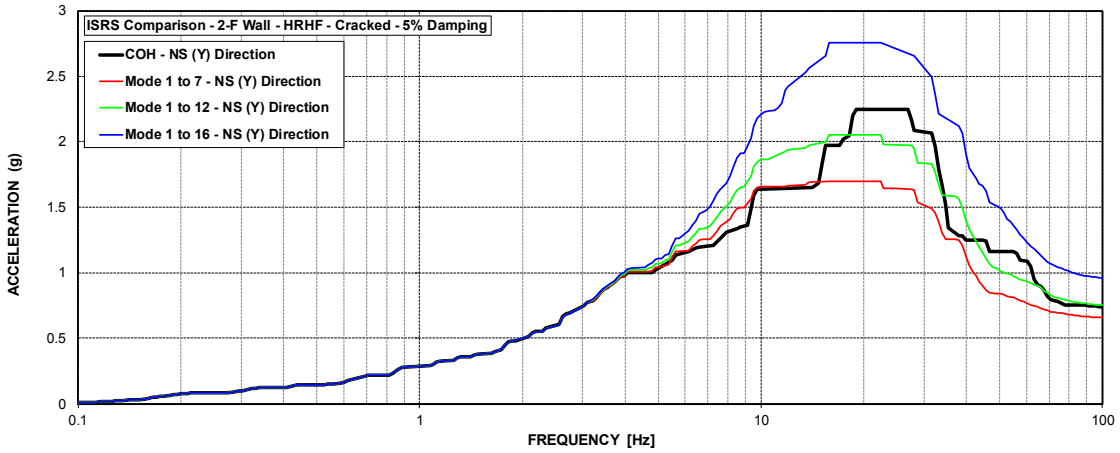

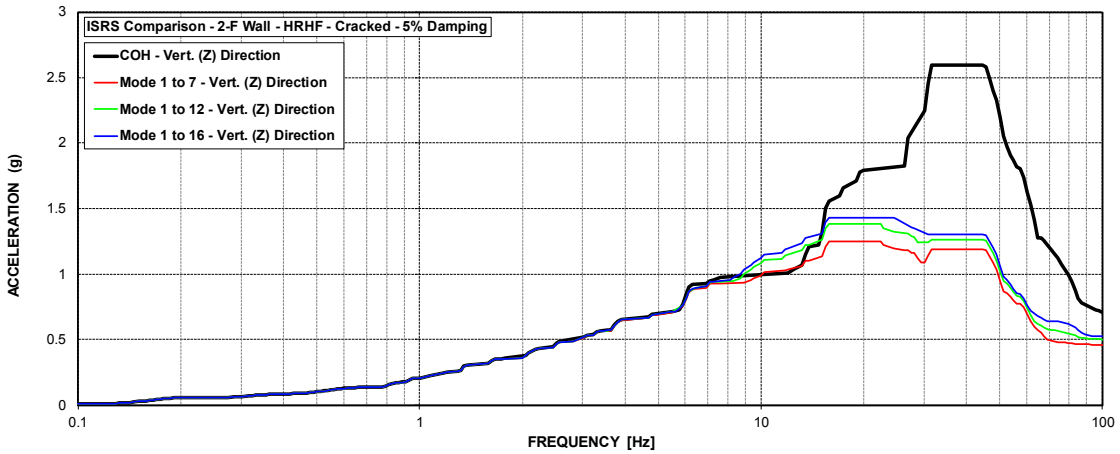

Figure 84 ISRS – AB Shear Walls (2-F) at El. 78’ – HRHF – Cracked

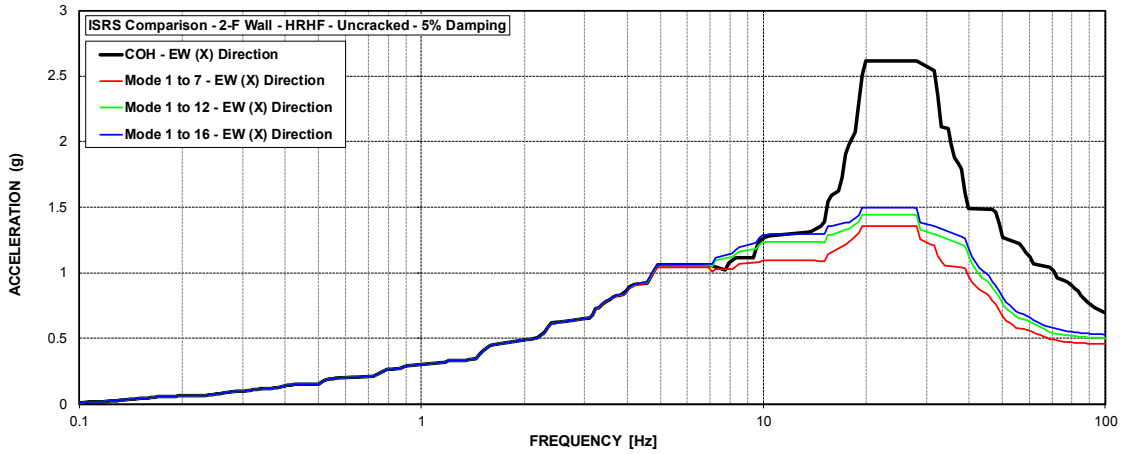

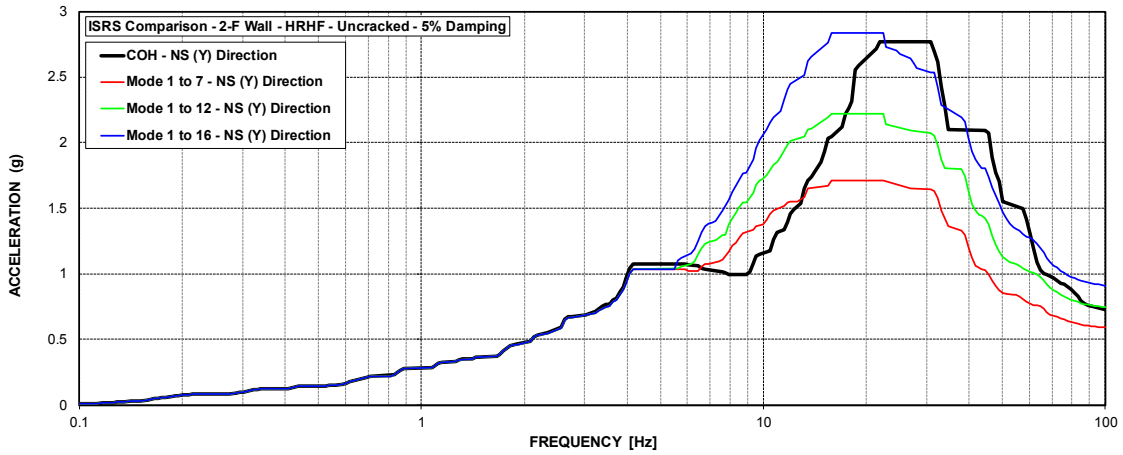

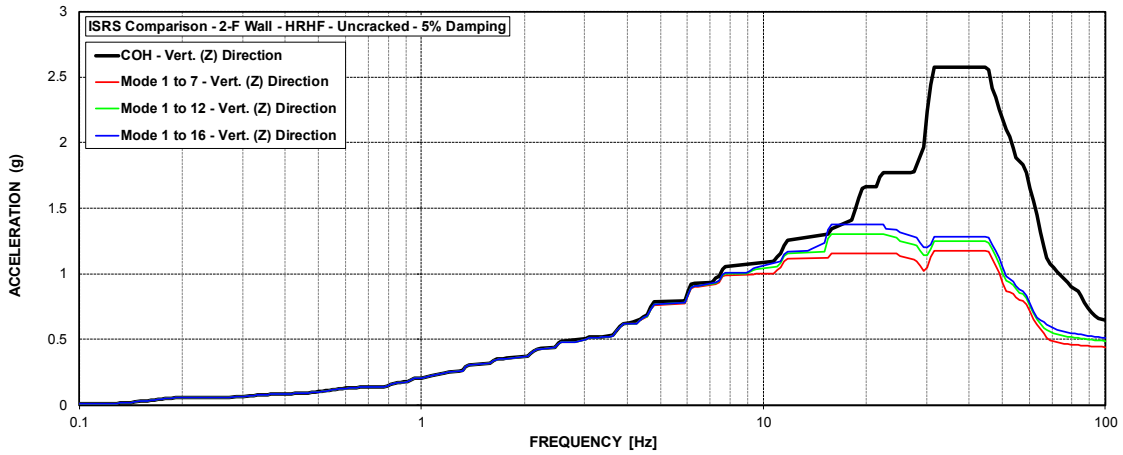

Figure 85 ISRS – AB Shear Walls (2-F) at El. 78’ – HRHF – Uncracked

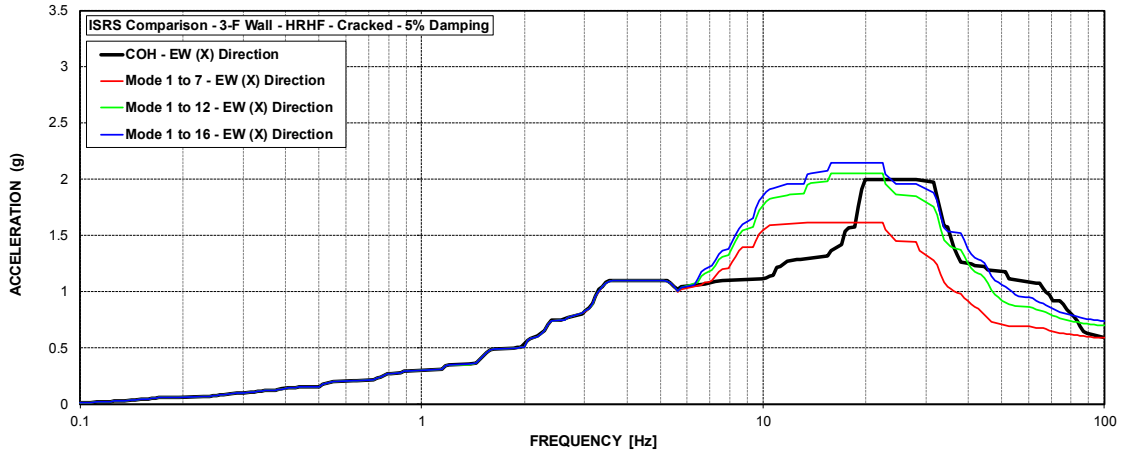

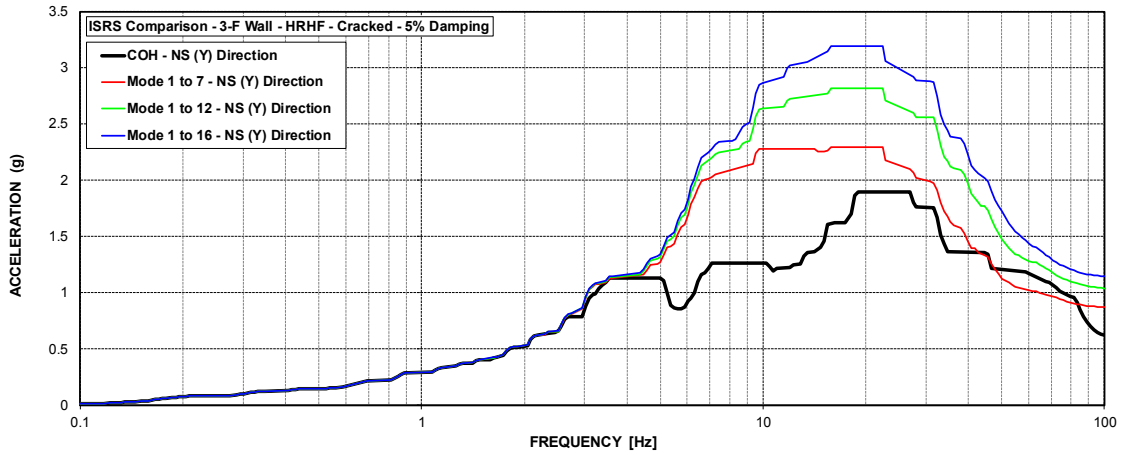

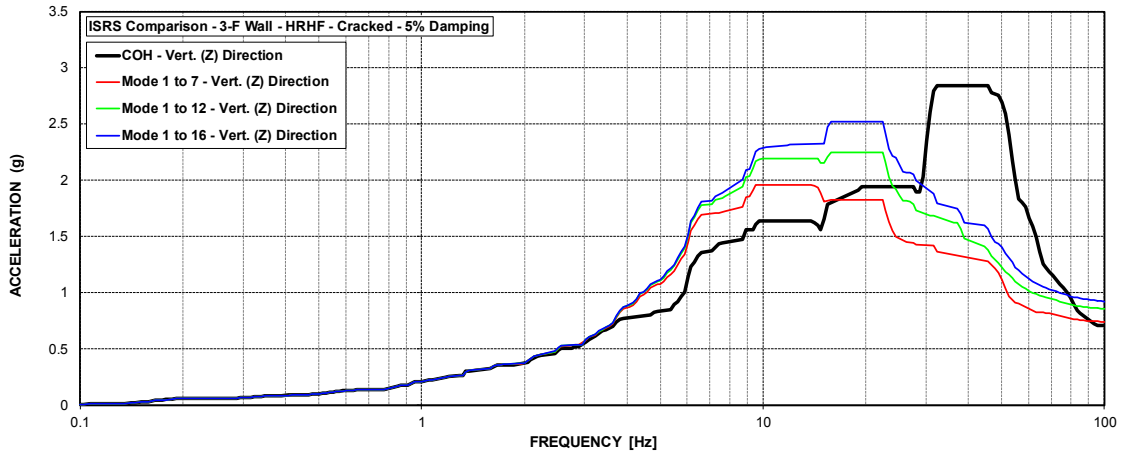

Figure 86 ISRS – AB Shear Walls (3-F) at El. 100’ – HRHF – Cracked

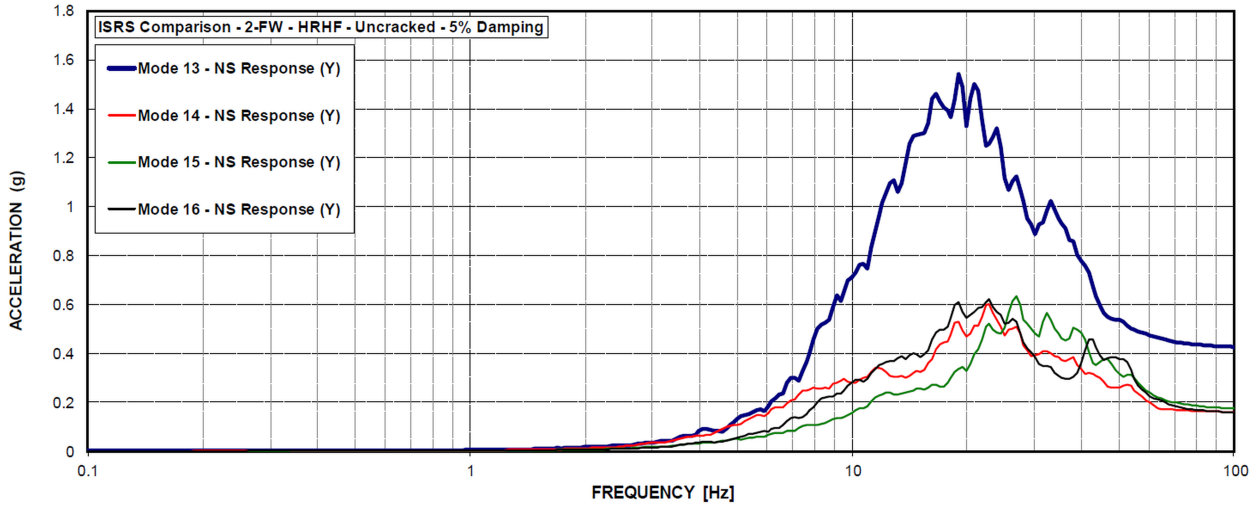

Figure 87 ISRS – AB Shear Walls (2-F) at El. 78’ – HRHF – Uncracked – Mode Comparison

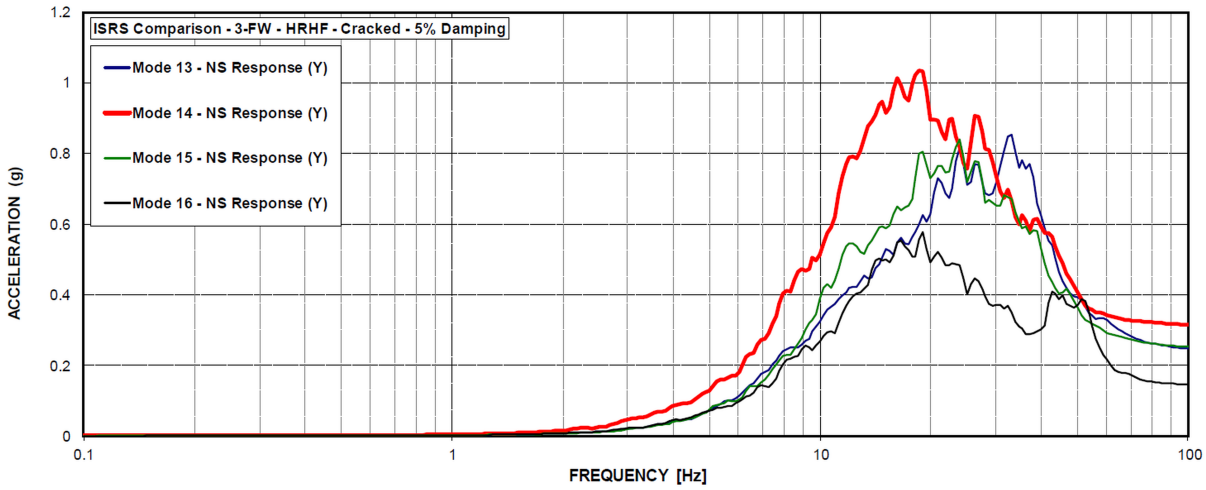

Figure 88 ISRS – AB Shear Walls (3-F) at El. 100’ – HRHF – Cracked – Mode Comparison

Impact on DCD

There is no impact on the DCD.

Impact on PRA

There is no impact on the PRA.

Impact on Technical Specifications

There is no impact on the Technical Specifications.

Impact on Technical/Topical/Environmental Reports

There is no impact on any Technical, Topical, or Environmental Report.